Quantum walks: background geometry and gauge invariance

Ivan Martin

UNIVERSITAT DE VALÈNCIA

Departament de Física Teórica de la facultat de Física
Instituto de física corpuscular (UVEG-CSIC)

AIX-MARSEILLE UNIVERSITÉ

Laboratoire d'Informatique et Systèmes (LIS) - UMR 7020

Quantum walks: background geometry and gauge invariance

Iván Márquez Martín

Tesis presentada por la Universidat de València. Programa de doctorat en Física

Thèse présentée pour obtenir le grade universitaire de docteur ED 184
Discipline: Mathematiques et informatique
Spécialité: Informatique

Bajo la dirección de:

Armando Pérez Cañellas
Giuseppe Di Molfetta
Pablo Arrighi

Octubre, 2019

VNIVERSITAT DE VALÈNCIA

Aix*Marseille université
Initiative d'excellence

Dr. Armando Pérez Cañellas, Catedrático de la Universidad de Valencia, en el departamento de física teórica; Dr. Giuseppe Di Molfetta, profesor de la Aix-Marseille Université y Dr. Pablo Arrighi, profesor de la Aix-Marseille Université

CERTIFICAN

que la presente memoria "Quantum walks: background geometry and gauge invariance", corresponde al trabajo realizado, bajo su supervisión, por el alumno **Iván Márquez Martín**, para su presentación como Tesis Doctoral en el programa de doctorado en **Física**, por la Universidad de Valencia y como Tesis Doctoral en el programa de doctorado de Matemáticas e Informática, con especialidad en **Informática**, por la Aix-Marseille Université.

Y para que conste, en cumplimiento con la legislación vigente, firman el presente certificado en Valencia, a 23 de octubre de 2019.

Armando Pérez Cañellas | Giuseppe Di Molfetta | Pablo Arrighi

Acknowledgment

Si tuviera que agradecer a cada una de las personas que, en cierto modo, han marcado esta etapa, podría escribir otra tesis, así que intentaré ser escueto (cosa que suele costarme)

En primer lugar, no podría haber realizado este largo camino sin la ayuda inestimable de mis directores Armando, Giuseppe y Pablo. Muchas gracias por haber confiado en mi, y haberme guiado por esta travesía que es una tesis doctoral. Sin duda, cada uno me aportó cosas distintas que me fueron de gran ayuda para poder crecer, tanto dentro como fuera del conocimiento científico. Ha sido un placer poder trabajar con vosotros.

También me gustaría agradecer a las personas con las que pude colaborar este tiempo: a Marcelo Forets, Alberto Verga, y en especial a Alejandro Díaz-Caro, que me dio la oportunidad de conocer un lindo lugar como es Buenos Aires. Incluyo también a Jose Luis Vilchis, por todas las horas que hemos pensado en el *cochecito* autónomo. También te agradezco por haber sido un amigo, haberme escuchado y aconsejado.

A Pablo Arnault, colaborador, pero sobretodo un gran amigo. Gracias por todas y cada una de las conversaciones que hemos tenido. Por haberme hablado siempre desde el corazón.

Este camino empezó construyéndose desde el grado en física, y por ello no puedo olvidarme de los grandes momentos que he vivido especialmente con Miguel, Alberto y Bart, mis guapos. También con Antonio, *el Gallego*, con el que he podido compartir cada una de las etapas de nuestro crecimiento académico y personal.

Fuera de la universidad, no puedo olvidarme de mis amigos (y casi hermanos), con los que he compartido prácticamente una vida entera, Álvari, *Barón* y Gordi. Tenemos un vínculo que espero que trascienda siempre.

También debo agradecer a Andoni, por tu horribilidad. Al bueno de Leo, por aportarme ese equilibrio racional que necesito en muchas ocasiones. A Julia, que has significado mucho en esta recta final. A mi querida Ana, por esa conexión y esa forma de ver el mundo tan especial.

Mi más sincera gratitud a Vicky, parte de esta tesis es tuya. Siempre recordaré el tiempo que vivimos juntos, y el aprendizaje personal que experimenté a tu lado. Una parte de mi siempre será uruguaya.

A Carolina, a pesar de nuestras idas y venidas, somos dos seres peculiares, y dentro de nuestra peculiaridad, nos queremos. Gracias por estar ahí.

A Concha, por la enorme y significante ayuda emocional que me has proporcionado.

Por último, y no menos importante, he de agradecer a mi familia. Sin vosotros no sería lo que soy ahora. A mis padres, Alfonso e Inés, por rescatarme, acogerme y educarme. A mis hermanas, Paloma y Patricia, por recibirme desde un primer momento con los brazos abiertos, y sobretodo, por vuestro cariño y amor infinito. A David y Diego, no se me ocurren mejores personas para añadir a la familia. A Alma, que tu alegría no tenga límites y sigas iluminando con tu inocencia cada uno de los rincones.

En definitiva, me considero afortunado por la gente que tengo a mi alrededor, ¡Va por vosotros!

Mientras tememos conscientemente no ser amados, el temor real, aunque habitualmente inconsciente, es el de amar.

El arte de amar
Erich Fromm

Resumen

Ciertos tipos de problemas no pueden resolverse usando los actuales ordenadores clásicos. Una forma de encontrar una solución, es mediante el uso de ordenadores cuánticos. Sin embargo, construir un ordenador cuántico es realmente complicado actualmente, debido a las limitaciones tecnológicas. Mientras tanto, los simuladores cuánticos han sido capaces de resolver algunos de estos problemas, ya que los simuladores cuánticos son más accesibles experimentalmente.

Las llamadas caminatas cuánticas, en su versión discreta, son una herramienta muy útil para simular ciertos sistemas físicos. En el límite al continuo, se puede obtener una serie de ecuaciones diferenciales, particularmente, la ecuación de Dirac entre ellas. En la presente tesis, se seguirán estudiando las propiedades de las caminatas cuánticas, como posibles simuladores cuánticos. Podemos resumir los resultados en: i) Se introduce un modelo de caminata cuántica, en el que se simula, en el continuo, la dinámica de fermiones en una teoría de branas. Eso abre la posibilidad de estudiar diferentes modelos de teorías de Kaluza-Klein; ii) Se discute la invariancia gauge en caminatas cuánticas, acopladas a campos electromagnéticos, donde se exhiben similitudes y diferencias con modelos previos. Este modelo presenta conexiones con la invariancia gauge realizada en "lattice gauge theories"; iii) Se introducen caminatas cuánticas sobre redes no rectangulares, como la red triangular o hexagonal, con el propósito de simular la ecuación de Dirac en el límite al continuo. Estos modelos se pueden extender, por medio de operadores locales unitarios, que permiten reproducir la dinámica de fermiones en espacio tiempo curvo.

Palabras claves: Caminatas cuánticas a tiempo discreto, Simulación cuántica, Invariancia Gauge discreta, Redes no rectangulares.

Résumé

Certains problèmes ne peuvent être résolus efficacement avec les ordinateurs actuels, dits “classiques”. Certains algorithmes quantiques apportent des solutions théoriques à ces problèmes, qui pourraient être résolus efficacement si un ordinateur quantique, sous-entendu, universel, pouvait implémenter ces algorithmes. Il se trouve que la construction d'un tel ordinateur quantique s'avère une tâche très compliquée, limitée aujourd'hui fortement par les technologies à notre disposition. Ceci étant dit, les recherches précédemment citées durant, des simulateurs quantiques specialisés ont déjà été capables de résoudre certaines versions modestes de ces problèmes. Les simulateurs quantiques actuels sont en effet, soit des ordinateurs quantiques effectuant une tâche spécifique, soit des machines quantiques analogiques mimant le phénomène physique d'intérêt.

Les dénommées marches quantiques, évolutions quantiques locales sur graphes discrets, sont un outil très pratique pour simuler certains systèmes physiques. Nous nous limiterons à leur version à temps discret, les marches quantiques à temps discret (MQTD). Dans certaines limites en espace-temps continu, ces marches quantiques coincident avec des équations d'onde pour fermions relativistes, dont l'archétype et pilier est l'équation de Dirac. Dans la présente thèse, nous poursuivons l'étude des propriétés des MQTD comme possibles schémas de simulation quantique. Nous pouvons résumer nos résultats en trois parties: i) Nous introduisons un schéma MQTD permettant de simuler, dans la limite au continu, la dynamique de fermions relativistes dans une théorie de branes; ceci ouvre la possibilité d'étudier différents modèles de théories Kaluza-Klein; ii) Nous discutons l'invariance de jauge U(1), i.e., électromagnétique, des MQTD, nous comparons notre modèle aux invariances précédemment introduites dans la littérature; notre invariance de jauge présente de fortes similitudes avec celle des théories de jauge sur réseau; iii) Nous introduisons des MQTD sur grilles non-rectangulaires, plus précisément, triangulaires et hexagonales, avec toujours comme condition de retrouver l'équation de Dirac au continuum; ces modèles peuvent être étendus au moyen d'opérateurs unitaires locaux spatiotemporellement inhomogènes et n'agissant que sur l'espace interne du marcheur, afin de générer dans la limite au continu l'equation de Dirac en espace-temps courbe.

Mots clés: Marches quantiques à temps discret, Simulation quantique

Abstract

There are many problems that cannot be solved using current *classical* computers. One manner to approach a solution of these systems is by using *quantum* computers. However, building a quantum computer is really challenging from the experimental side. Quantum simulators have been capable to solve some of these problems, as they are realizable experimentally.

Discrete Time Quantum Walks (DTQWs) have been proved to be an useful tool to quantum simulate physical systems. In the continuous limit, a family of differential equations can be achieved, in particular, the Dirac equation can be recovered. In this thesis we study QWs as possible schemes for quantum simulation. Specifically, we can summarize our results in: i) We introduce a QW-based model in which a brane theory can be simulated in the continuum, opening the possibility to study more general theories with extra dimensions; ii) Electromagnetic gauge invariance in QWs is discussed, presenting some similarities and differences to previous models. This QW model also makes a connection to gauge invariance in lattice gauge theories (LGT); iii) We introduce QWs over non-rectangular lattices, such a triangular or honeycomb structures, for the purpose of simulating the Dirac equation in the continuum. We also extent these models, by introducing local coin operators, that allow us to reproduce the dynamics of quantum particles under a curved space time.

Keywords: Discrete Time Quantum walks, Quantum simulations, Discrete Gauge invariance, Non-rectangular lattices.

Contents

List of Figures

Introduction

Quantum Walks (QWs), from a computer science perspective, are the quantum analogue of *classical random walks*. Instead of using probabilities, which are transformed by stochastic matrices, QWs involve probability amplitudes, which are transformed by unitary transformations. Among the interesting properties that appear in QWs one can mention interference effects or quantum entanglement.

Because of their quantum properties, we can define also QWs from a physical perspective. QWs can be seen as the dynamics of an excitation, in a quantum-mechanical spin system ruled by an unitary operator. Therefore, after some iterations, the location of the particle is a probability distribution, whose probabilities of being in a specific site, that can be calculated using the rules of quantum mechanics.

Quantum walks constitute an interdisciplinary scientific field, related to computer science and physics. Motivated by the algorithmic applications of classical random walks, there is a huge range of quantum algorithms based on quantum walks, specially since their computational universality has been proved [36, 86], such the Grover algorithm [121] or element distinctness problems [5]. On the other hand, due to the quantum properties of QWs, it is natural to consider their applications in physics: in particular, we are going to focus on their applications in *quantum simulation*.

First, in Chapter (2), we introduce the definition of QWs, in particular its discrete version, and their basic properties. Then, we study their applications in quantum simulations, and how they can simulate certain differential equations when the continuous limit is recovered. Specifically, we introduce a discrete-time quantum walk model which reproduces in the continuum a brane-world model proposed by Rubakov [114].

In Chapter (3) an important concept is studied in the context of DTQW, *gauge invariance*. Discrete gauge invariance is introduced in an alternative manner with respect to previous works. Indeed, we use a similar approach analogous to that of *lattice gauge theories*, which could be beneficial for both fields.

Later, in Chapter (4) , quantum walks are defined over some non-rectangular lattices. We introduce a DTQW on the honeycomb and triangular lattices, which allow us to recover the Dirac equation in the continuum. This represents one of our main results, since QWs on the honeycomb and triangular lattices have been only used for quantum algorithmic purposes, and it remained an open-question whether the Dirac equation could be reproduced by DTQW defined on

non-rectangular lattices [42].

In Chapter (5) we extend the QW-based model on the honeycomb and triangular lattice, by introducing local unitaries that allow us to reproduce the dynamics of the Dirac equation in curved space-time.

Finally, we discuss the possibility of extending these results to a higher dimensional space, specifically, how we can define a QW over a discretized 3D space using tetrahedrons.

1 Quantum walks: an introduction

Summary

In this chapter we introduce the definition of quantum walks, specifically its discrete time version. In order to understand better the quantum version, we introduce first the well-known classical random walk. Then, we define the quantum version of the random walk on a line, highlighting some of its basic properties. Finally, we show how quantum walks can be studied analytically in momentum space.

1.1 Classical random walk

Classical random walks (CRWs) are a subset of stochastic processes which are a powerful technique for the development of stochastic algorithms [98, 71]. References [102, 85] are recommended to obtain a deeper knowledge in algorithms based on CRWs. Moreover, apart from their importance in algorithmic, CRWs have been extensively used in many areas of scientific research as physics, biology, finances, etc [52, 72, 93, 25].

Let us introduce the simplest case of a classical random walk. It consists on a particle (called 'the walker'), that moves on a discrete line. At every time step j, it can jump either to left or to right, depending on the result of a probability device with, in this case, two mutually exclusive results[1]. Generally, the walker can move to the right with probability p or to the left with probability $q = 1 - p$, Fig.(1.1).

[1] In the case where the particle has the same probability to move left and right, we can use the analogy of tossing an unbiased coin at every step

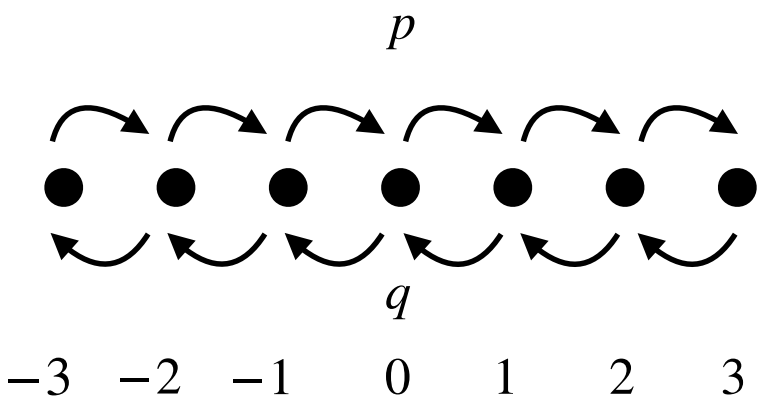

Figure 1.1: A classical discrete random walk. The probability of moving right is p and the probability of moving left is $q = 1 - p$.

The probability distribution of finding the particle at position x, after j time step, is given by the Bernoulli-distributed random variable, x. We can write the probability distribution, with initial condition localized at $x_0 = 0$, as:

$$P(x,j) = \begin{cases} \binom{j}{\frac{1}{2}(x+j)} p^{\frac{1}{2}(x+j)} p^{\frac{1}{2}(x-j)}, & \frac{1}{2}(x+n) \in \mathcal{N}; \\ 0, & \text{otherwise.} \end{cases} \tag{1.1}$$

In the limit in which j is large, we can approximate the probability distribution, Eq.(1.1), by a Gaussian distribution [112]. In the symmetric case, $q = p = \frac{1}{2}$, the probability is given, for j large, by:

$$P(x,j) \approx \frac{1 + (-1)^{j-x}}{\sqrt{2\pi n}} \exp\left(-\frac{x^2}{2j}\right). \tag{1.2}$$

In order to compare with the quantum case, we can study one of the most important properties, the standard deviation σ. This magnitude indicates how far the probability distribution has spread, after a certain time step, from the mean value, $\langle x \rangle = 0$. In Fig.(1.2), it is represented the standard deviation as a function of the time step, $\sigma(j)$. In the case of the CRW, σ is proportional to the square root of the evolution time.

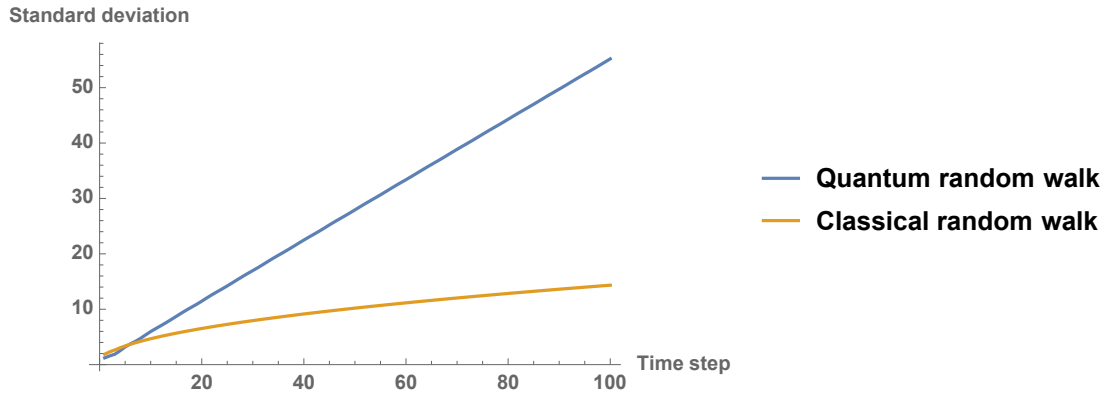

Figure 1.2: Comparison of the evolution of the standard deviation as a function of the time step for the QW and the CRW. The initial condition in the QW is $\psi_0 = \frac{1}{\sqrt{2}} |0\rangle \otimes (|\uparrow\rangle + i |\downarrow\rangle)$, whereas in the CRW the initial condition is localized around x_0. The total number of time steps is $J = 100$.

1.2 Discrete time quantum walk

To illustrate what a quantum random walk is, we introduce the simplest, and most studied model of quantum walk, i.e the discrete-time quantum walk (DTQW) on a infinite line. Of course, DTQWs can be defined in more sophisticated structures like cycles or higher dimensional lattices. However, as the QW on the line is a simple model, it helps us to understand the most relevant properties.

Let us consider the dynamical evolution of the DTQW described by the Hilbert space $\mathcal{H} = \mathcal{H}_p \otimes \mathcal{H}_c$. $\mathcal{H}_p$ is the Hilbert space spanned by the positions of the particle. In the case of the discrete line, it is spanned by the basis $\{|p\rangle\}_{p\in\mathbf{Z}}$. $\mathcal{H}_c$ is the internal degree of freedom, which is referred as the 'coin'-space. In the simplest case, the coin space is spanned by the two basis states $\{|\uparrow\rangle, |\downarrow\rangle\}$, which play the role of the spin-$\frac{1}{2}$ of the particle.

The evolution of the system is determined by the application of a unitary operator, instead of a stochastic matrix as in the CRW. The unitary operator which acts on the total Hilbert space is given by:

$$U = T\left(\mathbf{I}_P \otimes C\right). \tag{1.3}$$

Therefore, the evolution of the DTQW after j time steps is written as:

$$|\psi(j)\rangle = U^j |\psi(0)\rangle, \tag{1.4}$$

where $\mathbf{I}_P$ is the identity operator in $\mathcal{H}_P$. C is the coin operator, which only acts on $\mathcal{H}_C$, whereas T is the conditional shift operator, which involves the whole Hilbert space $\mathcal{H}$.

The conditional shift operator T allows the particle to move one step forward/backward, depending on the internal degree of freedom, e.g the walker goes forward if it has spin up $|\uparrow\rangle$) , and goes backwards in case of spin down $|\downarrow\rangle$. This is represented by:

$$T = \sum_{p\in\mathbf{Z}} |p+1\rangle \langle p| \otimes |\uparrow\rangle \langle\uparrow| + |p-1\rangle \langle p| \otimes |\downarrow\rangle \langle\downarrow| . \tag{1.5}$$

On the other hand, $\mathbf{I}_P \otimes C$ acts only on the coin space, playing the role of 'tossing' the quantum coin. C rotates the internal degree of freedom of the walker. Since a unitary transformation is quite arbitrary, we can define a family of walk with different behaviors. The most general unitary rotation can be chosen as:

$$C(\alpha,\theta,\gamma,\phi) = e^{i\alpha} \begin{pmatrix} e^{i\gamma}\cos\theta & e^{i\phi}\sin\theta \\ -e^{-i\phi}\sin\theta & e^{-i\gamma}\cos\theta \end{pmatrix} \tag{1.6}$$

where the four parameters $(\alpha,\theta,\gamma,\phi)$ are real. In the case where $\theta = \frac{\pi}{4}$, $\alpha = -\gamma = \frac{\pi}{2}$ and $\phi = -\frac{\pi}{2}$, the quantum coin becomes the so-called Hadamard coin:

$$C_H = \frac{1}{\sqrt{2}} \begin{pmatrix} 1 & 1 \\ 1 & -1 \end{pmatrix} . \tag{1.7}$$

The Hadamard coin C_H is said to be balanced, which means that applying the evolution operator U:

$$\begin{aligned} |\uparrow\rangle \otimes |0\rangle &\to \frac{1}{\sqrt{2}}(|\uparrow\rangle + |\downarrow\rangle) \otimes |0\rangle \\ &\to \frac{1}{\sqrt{2}} \left(|\uparrow\rangle \otimes |1\rangle + |\downarrow\rangle \otimes |-1\rangle\right) , \end{aligned} \tag{1.8}$$

the probability of finding the particle in the basis $\{|\uparrow\rangle \otimes |1\rangle , |\downarrow\rangle \otimes |-1\rangle\}$ is $p = \frac{1}{2}$ for each state. Note that if we continue the quantum walk by performing a measurement after each step, we recover the behavior of the classical random walk. Obviously, in the case of the quantum case, we do not measure at each time step, otherwise we destroy its quantum nature.

By "quantum nature", we mean that in the quantum walk we find: *interference* of the state and *entanglement* between coin and position space. To illustrate how the probability distribution differs from the classical one, let us evolve the walker a few steps, using as an initial condition $|\psi\rangle_0 = |\uparrow\rangle \otimes |0\rangle$. The evolved state reads

as:

$$
\begin{aligned}
|\psi\rangle_0 &\xrightarrow{U} \frac{1}{\sqrt{2}}\left(|\uparrow\rangle \otimes |1\rangle - |\downarrow\rangle \otimes |-1\rangle\right) \\
&\xrightarrow{U} \frac{1}{2}\left(|\uparrow\rangle \otimes |2\rangle - (|\uparrow\rangle - |\downarrow\rangle) \otimes |0\rangle + |\downarrow\rangle\, |-2\rangle\right) \\
&\xrightarrow{U} \frac{1}{2\sqrt{2}}\left(|\uparrow\rangle \otimes |3\rangle + |\downarrow\rangle \otimes |1\rangle + |\uparrow\rangle \otimes |-1\rangle\right. \\
&\left. -2\,|\downarrow\rangle \otimes |-1\rangle - |\downarrow\rangle \otimes |-3\rangle\right). \qquad (1.9)
\end{aligned}
$$

It is possible to observe, after some iterations, that the quantum walk probability distribution is different from the classical probability distribution. In Fig.(1.3), we make a comparison between the quantum and the classical case.

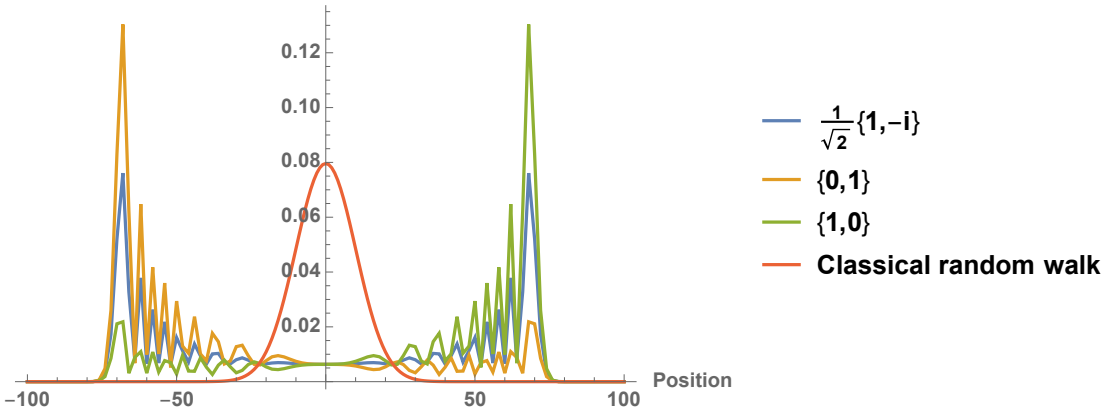

Figure 1.3: Probability density of a Hadamard walk on a line for $J = 100$ steps, compared with the probability distribution of a classical random walk. The initial condition is localized in $x = 0$, and different initial spin conditions are considered.

Some features that we can observe, from Fig.(1.3) and from Eq.(1.9), is that the probability distribution can be asymmetric or symmetric, depending on the initial condition. This is due to basic property of quantum mechanics, such as interference. For instance, the initial condition $|\psi\rangle_0 = |\uparrow\rangle \otimes |0\rangle$, induces more cancellations from the right path, whereas constructive interference appears from the left. To obtain a symmetric distribution, we can use as an initial condition a superposition of $|\uparrow\rangle$ and $|\downarrow\rangle$ state, such a:

$$
|\psi\rangle_0 = \frac{1}{\sqrt{2}}(|\uparrow\rangle + i\,|\downarrow\rangle) \otimes |0\rangle\,. \qquad (1.10)
$$

Since the Hadamard coin does not introduce complex amplitudes, the $|\uparrow\rangle$ amplitude will remain real, whereas $|\downarrow\rangle$ will be purely imaginary. Therefore they will

not interfere, leaving the probability distribution symmetric. Another possibility to obtain a symmetric probability distribution consists in changing the coin. Choosing:

$$C = \frac{1}{\sqrt{2}} \begin{pmatrix} 1 & i \\ i & 1 \end{pmatrix}, \tag{1.11}$$

both components $|\uparrow\rangle$ and $|\downarrow\rangle$ are treated in the same way. Thus, the walk is not biased, independently of its initial condition.

On the other hand, we also observe that, in the case of the quantum walk, the probability distribution spreads over the interval $\left[-\frac{j}{\sqrt{2}}, \frac{j}{\sqrt{2}}\right]$, where j is the number of steps. This differs from the classical case, in which the distribution is peaked around the initial position, Fig.(1.3).

As mentioned before, the standard deviation on the classical random walk scales as $\sigma \sim \sqrt{j}$, whereas it can be shown that in the quantum walk the variance scales as $\sigma \sim j$, as proved in [4], and showed numerically in Fig.(1.2). This result confirms the quadratic speedup of the probability density spreading, being able to scan significantly faster a graph than the classical walker. This is one of the reasons why quantum walks are interesting for developing quantum algorithms.

1.2.1 Quantum walk in momentum space

The analytical study of the discrete time quantum walk using the Discrete Time Fourier Transform (DTFT) was introduced first by Nayak and Vishwanath [101]. For simplicity, we will consider the Hadamard coin, which due to its translational invariance, permits a simple description in the Fourier domain. Let us describe the position of the walker as a two component spinor, being at position p at time-step j, described by:

$$\psi(p, j) = \begin{pmatrix} \psi_R(p, j) \\ \psi_L(p, j) \end{pmatrix}. \tag{1.12}$$

Upon identifying this notation with the notation in operator terms, we can write the spinor as:

$$|\psi(p, j)\rangle = \psi_R(p, j) |\uparrow\rangle + \psi_L(p, j) |\downarrow\rangle . \tag{1.13}$$

Applying the unitary evolution operator, Eq.(1.3), to a state at time j, it is possible to relate it to the state at time $j + 1$. Thus, the dynamics in matrix notation is written as:

$$\psi(p, j + 1) = M_+ \psi(p + 1, j) + M_- \psi(p - 1, j). \tag{1.14}$$

using the notation:

$$M_+ = \frac{1}{\sqrt{2}} \begin{pmatrix} 1 & 1 \\ 0 & 0 \end{pmatrix} \qquad M_- = \frac{1}{\sqrt{2}} \begin{pmatrix} 0 & 0 \\ 1 & -1 \end{pmatrix}. \tag{1.15}$$

Therefore, the finite difference equations after one iteration of the unitary evolution operator U, for each amplitude $\psi_R(p,j)$ and $\psi_L(j,p)$ are given by:

$$\begin{aligned}\psi_R(p,j+1) &= \frac{1}{\sqrt{2}}\left(\psi_R(p+1,j)+\psi_L(p+1,j)\right)\\ \psi_L(p,j+1) &= \frac{1}{\sqrt{2}}\left(\psi_R(p-1,j)-\psi_L(p-1,j)\right).\end{aligned} \tag{1.16}$$

In this way, the analysis of the QW on the line, for the Hadamard coin, reduces to solving a two dimensional linear recurrence system.

The discrete Fourier transform of the wave function $\psi(p,j)$, over $\mathbf{Z}$ is defined by:

$$\tilde{\psi}(k,t) = \sum_p \psi(p,j)e^{ikp} \tag{1.17}$$

where $k \in [-\pi,\pi]$ is the quasi-momentum. The inverse Fourier transform is given by:

$$\psi(p,j) = \frac{1}{2\pi}\int_{-\pi}^{\pi} \tilde{\psi}(k,j)e^{-ikp}dk \tag{1.18}$$

Using the definition of the discrete Fourier transform, Eq.(1.14), can be transformed as:

$$\begin{aligned}\tilde{\psi}(k,t+1) &= \sum_p \left(M_+\psi(p+1,j)+M_-\psi(p-1,j)\right)e^{ikp}\\ &= e^{ik}M_+\sum_p \psi(p-1,j)e^{ik(p-1)} + e^{-ik}M_-\sum_p \psi(p+1,j)e^{ik(p+1)}\\ &= \left(e^{ik}M_+ + e^{-ik}M_-\right)\tilde{\psi}(k,j)\end{aligned} \tag{1.19}$$

Therefore, we have

$$\tilde{\psi}(k,j+1) = M_k\tilde{\psi}(k,j), \tag{1.20}$$

where

$$M_k = e^{-ik}M_+ + e^{ik}M_- = \frac{1}{\sqrt{2}}\begin{pmatrix} e^{-ik} & e^{-ik}\\ e^{ik} & -e^{-ik}\end{pmatrix}. \tag{1.21}$$

The recurrence in Fourier since can be written in the following simple form:

$$\tilde{\psi}(k,j) = M_k^j\tilde{\psi}(k,0), \tag{1.22}$$

noticing that we have a local operator. We can compute M_k^t by diagonalizing the matrix M_k:

$$M_k = \lambda_k^1 \left|\phi_k^1\right\rangle\left\langle\phi_k^1\right| + \lambda_k^2\left|\phi_k^2\right\rangle\left\langle\phi_k^2\right|, \tag{1.23}$$

where λ_k^i are the eigenvalues, and $\left|\phi_k^i\right\rangle$ are the eigenvectors of M_k. Hence, we obtain the time evolution matrix as:

$$M_k^t = \left(\lambda_k^1\right)^j\left|\phi_k^1\right\rangle\left\langle\phi_k^1\right| + \left(\lambda_k^2\right)^j\left|\phi_k^2\right\rangle\left\langle\phi_k^2\right|. \tag{1.24}$$

The eigenvalues of M_k are $\lambda_k^1 = e^{i\omega_k}$ and $\lambda_k^2 = e^{i(\pi-\omega_k)}$, where $\omega_k \in \left[-\frac{\pi}{2}, \frac{\pi}{2}\right]$ satisfies $\sin(\omega_k) = \frac{\sin k}{\sqrt{2}}$. The eigenvectors are given by:

$$\begin{aligned}\phi_k^1 &= \frac{1}{\sqrt{2N(k)}}\begin{pmatrix} e^{-ik} \\ \sqrt{2}e^{i\omega_k} + e^{-ik}\end{pmatrix} \\ \phi_k^2 &= \frac{1}{\sqrt{2N(\pi-k)}}\begin{pmatrix} e^{-ik} \\ -\sqrt{2}e^{-i\omega_k} + e^{-ik}\end{pmatrix}\end{aligned} \tag{1.25}$$

with the normalization factor

$$N(k) = (1+\cos^2 k) + \cos k\sqrt{1+\cos^2 k}. \tag{1.26}$$

If the initial state is represented by $\tilde{\psi}(k,0) = (0,1)^T$ for all k. The wave functions for any time, in Fourier space is written as:

$$\begin{aligned}\tilde{\psi}_R(k,j) &= \frac{1}{2}\left(1 + \frac{\cos k}{\sqrt{1+\cos^2 k}}\right)e^{i\omega_k j} + \frac{(-1)^j}{2}\left(1 - \frac{\cos k}{\sqrt{1+\cos^2 k}}\right)e^{-i\omega_k j} \\ \tilde{\psi}_L(k,j) &= \frac{e^{-ik}}{2\sqrt{1+\cos^2 k}}\left(e^{i\omega_k j} - (-1)^j e^{-i\omega_k j}\right)\end{aligned} \tag{1.27}$$

Using the inverse of the Fourier transform, we can transform the amplitudes into real space:

$$\tilde{\psi}_R(p,j) = \frac{1+(-1)^{p+j}}{2}\int_{-\pi}^{\pi}\frac{dk}{2\pi}\left(1 + \frac{\cos k}{\sqrt{1+\cos^2 k}}\right)e^{-i(kp+\omega_k j)} \tag{1.28}$$

$$\tilde{\psi}_L(p,j) = \frac{1+(-1)^{p+j}}{2}\int_{-\pi}^{\pi}\frac{dk}{2\pi}\left(\frac{e^{ik}}{\sqrt{1+\cos^2 k}}\right)e^{-i(kp+\omega_k j)} \tag{1.29}$$

Notice that the amplitudes vanish for even p (respectively, odd p) at odd t (even t), as we would expect from the definition of the walk. There is not analytical solution to these integrals, however they can be resolved numerically.

1.2.2 The asymptotic probability distribution in the long time limit

It is possible to obtain the analytical solution of Eq.(1.28), at large times. In fact, there are several methods to study the asymptotic distribution of the DTQW.

One of them is called the stationary phase method [33],in which the asymptotic behavior of the wavefunction can be studied analytically. This method is useful to solve integrals of the form:

$$I(\alpha) = \frac{1}{2\pi}\int_{-\pi}^{\pi} g(k)e^{i\phi(k,\alpha)t}dk \tag{1.30}$$

where $\alpha = \frac{n}{t}$. The method of stationary phase was introduced by [101], to find the asymptotic probability distribution, using the Hadamard coin and using an initial state given by $|\psi(0,0)\rangle = (0,1)^T \otimes |0\rangle$.

The probability distribution of the quantum walk, in the long time limit for points $\alpha = \frac{p}{j}$, between $-\frac{1}{\sqrt{2}} + \epsilon$ and $\frac{1}{\sqrt{2}} - \epsilon$ where ϵ is an arbitrarily small constant $\epsilon > 0$, is given by:

$$\begin{aligned} P(\alpha, j) &= |\psi_R(\alpha j, j)|^2 + |\psi_L(\alpha j, j)|^2 \\ &= \frac{2}{\pi\sqrt{1-2\alpha^2 j}} \cos^2(-\omega j + \frac{\pi}{4} - \rho) + \frac{2(1+\alpha)}{\pi(1-\alpha\sqrt{1-2\alpha^2 j})} \cos^2(-\omega j + \frac{\pi}{4}) \end{aligned} \tag{1.31}$$

where $\omega = \alpha\rho + \theta$,$\rho = \arg(-B + \sqrt{\Delta})$,$\theta = \arg(B + 2 + \sqrt{\Delta})$,$B = \frac{2\alpha}{1-\alpha}$, and $\Delta = B^2 - 4(B+1)$. The exact calculation can found in [101].

Another method to derive the long-term behavior of the probability distribution is given by [61], called *weak limit*.

On the other hand, an other approach to compute the asymptotic probability distribution of the DTQW, was developed by [79], based on combinatorial methods.

2 Quantum walks as a quantum simulators

Summary

2.1 Quantum simulation

Many quantum systems, due to the number of particles they involve, are very inefficient to simulate in classical devices, i.e the time and memory resources that takes the simulation grows exponentially with the size of the system. Feynman in 1982 [54] suggested that quantum devices would perform more efficient simulations of quantum systems, due to the quantum nature, than classical devices. It does not mean that classical devices are not useful in the task of simulating quantum models, for instance tensor network [37, 129], quantum monte carlo algorithms [132], density functional theory [110], etc. are classical simulations of physical systems that are quite useful, however all have their limitations.

Quantum computers are expected to overtake the efficiency in simulating quantum models, specially when the size of the system is large enough. The principal benefit of these devices is that they can storage and manipulate an exponentially amount of information using the basic properties of quantum mechanics, i.e superposition and entanglement.

Being specific, Lloyd [84] shows that a quantum computer (*i.e., an ensemble of well-defined qubits that can be initialized, measured, and on which universal quantum gates can be performed*) can be used as an universal quantum simulator, where *universal* means that the same device is able to solve a complete set of task.

However, because of the technical difficulties that are well known in the building of a quantum computer, quantum simulators have been a subject of interest

due to the applications in different fields: physics, chemistry or biology. Quantum simulators are just specific quantum systems that mimic other quantum models, while loosing the universality is the price to pay[1]. However, it is also true that experimental implementations of quantum simulators are easier than building an universal quantum computer with a sufficiently large number of qubits.

Experimental realization The most common designs of quantum simulators are focused on the study of condensed-matter physics with different physical implementations, such a:

Neutral atoms in optical lattices are flexible systems that are easily tunable and defect free, also they can be adjusted to simulate different geometries like kagome lattices [83] or triangular lattices [125]), but the individual control of the qubits and readout is the main difficulty, for a further study [82, 41, 27].

Superconducting circuits [140, 38, 90] Each qubit is an LC circuits, composed by an inductor and a capacitor. Manipulating the energy states of the circuits, it can be created a superposition of $|0\rangle$ and $|1\rangle$. Then, by using resonators, these circuits can be entangled, however connecting all these qubits is hard. In consequence, not all the qubits are entangled with each other in the current quantum devices, e.g in the 5 qubits IBM Q, there are 20 possible combinations, but only 6 are implemented. An extended review in the topic can be found [130].

Photons can also be used to implement quantum simulations, as they have long coherence times which make them useful in the task of carrying information at a long distance without decoherence or noise [20]. Although the flexibility and scalability of quantum simulators based in photons is a difficult task, there are some progress in the field which make this kind of simulators promising [64].

Some nice references in the topic of quantum simulations are [59]

Physical implementations of QWs Here we review the possible physical implementations of the QW. Most of the experimental proposals are focused in the realization of discrete-time quantum walks, thus this means that the physical system requires some common characteristics.

First, the system should exhibit addressable states to describe the position and also the coin states of the walk. Moreover the system needs to allow some interaction with the internal states to implement the so-called coin operators. Finally, it is indispensable to implement the translations operators depending on the internal state.

On the other hand, almost all the proposals are for one-particle quantum walks, and an inherently quantum system is not required strictly to implement a quantum walk. The dynamics of the single-particle quantum walk is governed by the interference features of the state in the discrete space. This phenomenon

[1] Quantum simulators are defined to solve specific problems

can be found in quantum systems but also in many classical systems involving waves.

Of course, there are new theoretical and experimental proposals of two particles and multi particle quantum walks [26, 111, 117, 12] which are not possible to implement using classical systems due to the new rich dynamics which can only be explained in terms of quantum systems and open up new perspectives for applications in quantum algorithms and in quantum simulations (i.e quantum field theory simulation). Although there is a huge number of proposals, it is possible to divide them into the following classes:

Linear optics. This approach is related with the, already mentioned, fact that a quantum system is not required to implement a one-particle quantum walk, and that it properties can be effectively reproduced using the interference of a classical field.

A proposal by Knight et al [77], based in an experiment in the context of the optical Galton board [29], implements a discrete quantum walk in a optical cavity just making use of the interference of light. In this scheme, the frequency modes of the light field implement the walker, and the polarization plays the role of the coin state. Also Knight et al [76] proposed a different design, a ring cavity, where now the coin state is not implemented using a polarization cebit[2], instead it is used a position cebit which requires two different paths of light inside the cavity.

It is possible to generalize this implementation for multi particle quantum walks if one adds more than two optical paths, using coin states with more than two components. It is interesting to mention that, in the context of cavity rings, the use of optical feedback loop provides great advantages since the amount of resources remains constant as the number of quantum walk steps increases.

There are other experimental realizations of coined quantum walks, using a set of modified Michelson interferometers [109], or even employing optical networks [141]

Cavity QED. There are some proposals to implement quantum walks using cavity quantum electrodynamics, based on the work of [3, 137]. It consists on injecting a highly excited atom (Rydberg atom) into a optical cavity, and then applying an external field. This atom is a two level system, which plays the role of coin states, whereas the position states are the cavity modes. Also, there are alternatives approach based in cavity QED [116, 49]

Neutral atoms Proposals based on neutral atoms traps have been studied by several authors [34, 51, 39, 92] to implement quantum walks. One type of traps used are the optical lattices [50], which consist in the interference of

[2] A cebit is a two-component complex vector representing the light-field, and can be used as a classical counterpart of the qubit. In the case of *polarization cebit*, the polarization of the field plays the role of the internal state of the walker, whereas in the *position cebit*, there are different direction of propagation of the field, and these different paths play the role of the walker's coin state

contra-propagating laser beams, producing a periodic trapping potential where the atoms remain. Therefore, the position basis is represented by the location at which the atom is in the 1D optical lattice, whereas the coin basis is played by the internal state of the atom. Laser pulses can be used to alter their internal state, then the conditional shift operators can be realized.

We mentioned some classes of physical implementations by which quantum walks can be realized, but there are also other proposals such an *ion traps* [126], where a single $^9Be^+$ ion is used which is laser-cooled and confined in a coaxial resonator radio frequency ion trap, thus the position states are encoded into the motional states of the ion, and the electronic states of the ion are used as a coin basis. There are also proposals based in solid state physics [91], using a 2D array of interacting quantum dots.

An interesting implementation of quantum walks consist in making use of quantum circuits, as the development of quantum computers is growing quite fast in the recent years. There are some proposals based in this architecture [57, 22] that could be interesting to extend.

2.2 QW continuous limit

It is already well-studied the connections between the DTQW and their continuous limit [45, 46], however it is necessary give an introduction to this topic because it constitutes the basic mathematical technique to prove that DTQW can be used for the purpose of quantum simulation.

Homogeneous QW In this basic example we consider a quantum walk defined on a discrete one-dimensional space and discrete time. The evolution of this QW is driven by a $U(2)$ coin, which acts on a walker represented by a two-component field ψ. The discrete space points are labeled by $p \in \mathbb{Z}$, and the time steps are labeled by $j \in \mathbb{N}$. The finite difference equation reads

$$\begin{pmatrix} \psi^{\uparrow}_{j+1,p} \\ \psi^{\downarrow}_{j+1,p} \end{pmatrix} = Q(\alpha,\theta,\xi,\zeta)T \begin{pmatrix} \psi^{\uparrow}_{j,p} \\ \psi^{\downarrow}_{j,p} \end{pmatrix} \tag{2.1}$$

where the operators T and Q are given by:

$$\begin{aligned} T\psi_{j,p} &= \begin{pmatrix} \psi^{\uparrow}_{j,p+1} \\ \psi^{\downarrow}_{j,p-1} \end{pmatrix} \\ Q(\theta,\xi,\zeta) &= e^{i\alpha} \begin{pmatrix} e^{i\xi}\cos\theta & e^{i\zeta}\sin\theta \\ -e^{-i\zeta}\sin\theta & e^{-i\xi}\cos\theta \end{pmatrix} \end{aligned} \tag{2.2}$$

We will consider the case with $\alpha = 0$,$\zeta = \pi/2$ and $\xi = 0$. In order to study the continuous limit, it is introduced a time step $\epsilon_t \in \mathbb{R}^+$ and a space-step $\epsilon_x \in \mathbb{R}^+$.

We assume that $\psi_{j,p}$ coincides with the continuous space-time field $\tilde{\psi}$ at space-time points ($t_j = j\epsilon_t$,$x_p = p\epsilon_x$), and let ϵ_t and ϵ_x go to zero. Therefore, Eq.(2.1) then reads as

$$\begin{pmatrix} \tilde{\psi}^{\uparrow}_{t_j+\epsilon_t,x_p} \\ \tilde{\psi}^{\downarrow}_{t_j+\epsilon_t,x_p} \end{pmatrix} = Q(0,\theta,0,\pi/2) \begin{pmatrix} \tilde{\psi}^{\uparrow}_{t_j,x_p+\epsilon_x} \\ \tilde{\psi}^{\downarrow}_{t_j,x_p-\epsilon_x} \end{pmatrix} \tag{2.3}$$

We also need some condition on the angle θ to have a sensible continuous limit. We therefore write θ as

$$\theta = \theta_0 + \bar{\theta}\epsilon_m, \tag{2.4}$$

where θ_0 is the value of θ at zero order, when ϵ_t and ϵ_x go to zero and also $\epsilon_m \in \mathbb{R}^+$ goes to zero. $\bar{\theta}$ is an arbitrary parameter, which will act like the mass of the particle. The wavefunction ψ has to be differentiable at least twice, in both space and time variables so that we can Taylor expand at first order, in ϵ_x,ϵ_t and ϵ_m, Eq.(2.3).

A requisite to the validity of the continuous limit is that the operator $Q(\theta,0,\pi/2)$ has to tend to unity as (ϵ_x,ϵ_t, ϵ_m) tend to zero, therefore the zero order terms at the left- and right- hand sides of Eq.(2.1) must be equal:

$$\begin{pmatrix} \tilde{\psi}^{\uparrow}_{t,x} \\ \tilde{\psi}^{\downarrow}_{t,x} \end{pmatrix} = \begin{pmatrix} \cos\theta_0 & i\sin\theta_0 \\ i\sin\theta_0 & \cos\theta_0 \end{pmatrix} \begin{pmatrix} \tilde{\psi}^{\uparrow}_{t,x} \\ \tilde{\psi}^{\downarrow}_{t,x} \end{pmatrix} \tag{2.5}$$

and the angle needs to be $\theta_0 = n\pi$ to satisfy the zero order condition. Being satisfied the former condition, the existence of the continuous limit is guaranteed. We write $\epsilon_m = \epsilon$, $\epsilon_t = \epsilon^\alpha$ and $\epsilon_x = \epsilon^\beta$, to account for the fact that they can tend to zero differently, although the most interesting case belongs to $\alpha = \beta = 1$. Hence, the partial differential equation we are looking for is calculated taking the first order terms when $\epsilon \to 0$, and reads as:

$$\begin{aligned} (\partial_t - \partial_x)\,\psi^{\uparrow} &= i\bar{\theta}\psi^{\downarrow} \\ (\partial_t + \partial_x)\,\psi^{\downarrow} &= i\bar{\theta}\psi^{\uparrow} \end{aligned} \tag{2.6}$$

The former equation can be recast as

$$(i\gamma^\mu\partial_\mu - m)\,\Psi = 0, \tag{2.7}$$

with $\mu = 1,2$ and the matrices gamma $\gamma^0 \equiv \sigma_1$, $\gamma^1 \equiv i\sigma_2$, being σ the Pauli matrices and, as it is mentioned before, $m \equiv -\bar{\theta}$. This equation is the well-known Dirac equation in flat-spacetime, for relativistic masive spin-$\frac{1}{2}$ fermions.

Inhomogeneous DTQWs Let us now consider the case where α, θ, ξ and ζ can be space-time dependent, therefore the evolution reads as:

$$\begin{pmatrix} \psi^{\uparrow}_{j+1,p} \\ \psi^{\downarrow}_{j+1,p} \end{pmatrix} = e^{i\alpha_{j,p}} \begin{pmatrix} e^{i\xi_{j,p}}\cos\theta_{j,p} & e^{i\zeta_{j,p}}\sin\theta_{j,p} \\ -e^{-i\zeta_{j,p}}\sin\theta_{j,p} & e^{-i\xi_{j,p}}\cos\theta_{j,p} \end{pmatrix} \begin{pmatrix} \psi^{\uparrow}_{j,p+1} \\ \psi^{\downarrow}_{j,p-1} \end{pmatrix} \tag{2.8}$$

As we have done before, it is introduced a time step ϵ_t and a space step ϵ_x, which will tend to zero. To study this continuous limit, it is necessary to take into account the space-time dependency of the quantum coin, therefore following the same procedure as in the former section with θ in Eq.(2.4), we split the homogeneous and the in-homogeneous part, for every phase in the coin as:

$$u_i = u_0 + \epsilon_i \bar{u}(t_j, x_p) \tag{2.9}$$

where the use of different $\epsilon_i \in \mathbb{R}$ tending to zero take into account the fact that the angles can tend to zero at a different rate. It is has been very well studied the different choices of these angles to obtain different PDE in the continuous limit. For instance, as a basic example, on can choose the following angles:

$$\begin{aligned} \alpha_{j,p} &= \epsilon_\alpha \bar{\alpha}_{j,p} \\ \xi_{j,p} &= \epsilon_\xi \bar{\xi}_{j,p} \\ \zeta_{j,p} &= \frac{\pi}{2} - \epsilon_\zeta \bar{\xi}_{j,p} \end{aligned} \tag{2.10}$$

where $\epsilon_\alpha = \epsilon_\xi = \epsilon_\zeta = \epsilon$. The reason of this particular choice of the angles will be clearer in the next section when we introduce the discrete gauge transformation in the QW. Therefore, in the limit in which $\epsilon \to 0$, the PDE obtained reads as

$$\left(i\gamma^\mu D_\mu - m\right)\Psi = 0 \tag{2.11}$$

where $D_\mu = \partial_\mu - iA_\mu$ is the usual covariant derivative with the following couplings,

$$\begin{aligned} A_0 &= \bar{\alpha} \\ A_1 &= -\bar{\xi} \end{aligned} \tag{2.12}$$

The above equation is the Dirac equation with the fermion coupled to an electric potential. This result can be extended to higher dimensional DTQW [11, 9] Also DTQW can be used to quantum simulate the action of gravity in relativistic models [47], Sect.(5.5), or the simulation of brane theories which involve an effective mass, which is the motivation of this chapter, Sect.(2.5).

2.3 Localization

Spatial localization of quantum particles in certain regimes has been studied extensively, appearing as a natural phenomenon. In 1958 Anderson studied the absence of diffusion in lattice systems in the case of static disorder [7], i.e the particle wave functionbecomes localized due to impurities in the lattice. Experimental set up of this phenomena has been realized in different scenario such

a semiconductors, [133], phonic lattices [119] or even in Bose-Einstein condensates [94]. On the other hand, it is possible to observe localization in different circumstances, e.g. using external periodic potentials [81, 60] In the context of QWs (discrete and continuous time), Anderson localization and its consequences have been studied theoretically [70, 68, 139] but also have been achieved experimentally by photonics implementation [118, 40]. Also, localization appears due to other causes such a spatial periodic coin [123], via non-linear effects [100], or even via the choice of the coin operator in 2D QWs in square lattices [66] or honeycomb lattices [88].

2.4 Domain wall model

The idea of developing theories with extra dimensions has been considered for many years. The first suggestion of an extra dimension was made by Kaluza and Klein [74] in the attempt of formulating a unified theory of gravitation and electromagnetism, using an extra fifth dimension apart from the usual four of space and time. This extra dimension would be compact and homogeneous, therefore the space-time is essentially four dimensional at distances far from the compactification range, which would be of the order of the Planck scale $l_P \approx 10^{-33}$ cm. Consequently, the energy scale necessary to have direct observation of the indicated extra dimension is the order of $M_P \approx 10^{19}$ GeV, comparing with the actual collision energy at LHC $13 \cdot 10^3$ GeV, it is obvious that probing extra dimensions is hopeless nowadays.

Other theories involving extra dimensions are the so-called "Brane-world" pictures, which assume that matter fields are embedded in a sub-manifold (normally a three-dimensional space) -brane- of a multi-dimensional space. The difference with the Kaluza-Klein scenario is that these extra-dimensions can be large or even infinite. There is a lot of bibliography in this topic [135, 122, 8, 21], where the concept of brane can change depending on the context.

We are inspired in the brane-world model proposed by Rubakov in 1983 [114], in which space-time has an extra dimension $3+1+1$, with low-energy particles confined in the $3D$ ordinary space -brane- via a potential well, which is narrow along the extra spatial direction and flat in the brane. This potential well can be explained as a scalar field in $4+1$ dimensions, as described by the Lagrangian:

$$\mathcal{L} = \frac{1}{2}\partial_A\varphi\partial^A\varphi - \frac{1}{2}m^2\varphi^2 - \frac{1}{4}\lambda\varphi^4, \quad A = 0,1,2,3,4, \tag{2.13}$$

where $g_{AB} = \text{diag}\,(1,-1,-1,-1,-1)$ with coordinates x^A. The classical equation of motion admits a domain wall solution $\varphi^{cl}(x^4)$, which only depends on the

fourth extra-dimension.

$$\varphi^{cl}(x^4) = \frac{m}{\sqrt{\lambda}} \tanh\left(\frac{mx^4}{\sqrt{2}}\right) \tag{2.14}$$

This field provides a narrow potential well narrow in x^4 if m is large. The former model can account to $(3+1)$ dimensional massless fermions if they are coupled to the scalar field φ^{cl},

$$\mathcal{L}_\Psi = i\bar{\Psi}\Gamma^A\partial_A\Psi + h\varphi^{cl}\bar{\Psi}\Psi \tag{2.15}$$

being Ψ is a four component spinor, whereas the γ-matrices are represented by:

$$\Gamma^\mu = \gamma^\mu, \quad \mu = 0, ..., 3, \quad \Gamma^4 = i\gamma^5, \tag{2.16}$$

where γ^μ and γ^5 are the standard Dirac matrices. From Eq.(2.15), we arrive to the corresponding Dirac equation in the presence of the domain wall Eq.(2.14),

$$\Gamma^A\partial_A\Psi + h\varphi^{cl}\Psi = 0 \tag{2.17}$$

which has a solution

$$\Psi^{(0)}(x^0, \vec{x}, x^4) = e^{-h\int_0^{x^4}\varphi^{cl}(x'^4)dx'^4}\psi(x^0, \vec{x}) \tag{2.18}$$

where $\psi(x^0, \vec{x})$ is a left-handed massless $(3+1)$ dimensional spinor, $\gamma^5\psi = \psi$ and $i\gamma^\mu\partial_\mu\psi = 0$. In Sect.(2.5), we will introduce a QW which recovers the former Dirac equation in $(1+1+1)$ space-time in the continuous limit. Because of the confinement, we will be able to localize the walker along one of the axes, which play the role of the extra dimension.

2.5 Publication: "Fermion confinement via quantum walks in $(2+1)$-dimensional and $(3+1)$-dimensional) space-time

In the present paper, we introduce a quantum walk model which simulates a brane model, introduced in Sect.(2.4). We define a 2D and 3D quantum walk, in which the domain wall potential is encoded in an inhomogeneous coin operator. Therefore, as the parameter which controls the particle effective mass increases, the particle probability distribution cannot access to the "extra" dimensions. For instance, in the case of the 2D QW, the probability distribution is confined along a line, whereas in the case of the 3D QW, the probability distribution lives on a surface.

The existence of this localized state can be explained in Sect.(2.6). As our domain wall potential depends on one axis, we have regions with different masses.

Resolving the Dirac equation, we realize that the solution is a bound state living on the interface between these two regions, with different signs of the mass.

The fact that in the previous QW model, Sect.(2.5), the localized probability distribution, in the regime of "low" energy, is an edge state, opens new questions which deserve more study. One possibility to extend this model, is by introducing spatial-dependent noise, to study the effects on the localized state, as it is done in [128]. As it is a bound state what appears on the interface of different masses regions, we expect that the probability distribution could be more robust to a noisy environment, than the case of a standard QW.

Fermion confinement via quantum walks in (2+1)-dimensional and (3+1)-dimensional space-time

I. Márquez-Martín,[1] G. Di Molfetta,[1,2,*] and A. Pérez[1]

[1]*Departamento de Física Teórica and IFIC, Universidad de Valencia-CSIC, Dr. Moliner 50, 46100-Burjassot, Spain*

[2]*Aix-Marseille Université, CNRS, École Centrale de Marseille, CNRS, Laboratoire d'Informatique Fondamentale, Marseille, France*

(Received 3 January 2017; revised manuscript received 9 March 2017; published 10 April 2017)

We analyze the properties of a two- and three-dimensional quantum walk that are inspired by the idea of a brane-world model put forward by Rubakov and Shaposhnikov [Phys. Lett. B **125**, 136 (1983)]. In that model, particles are dynamically confined on the brane due to the interaction with a scalar field. We translated this model into an alternate quantum walk with a coin that depends on the external field, with a dependence which mimics a domain wall solution. As in the original model, fermions (in our case, the walker) become localized in one of the dimensions, not from the action of a random noise on the lattice (as in the case of Anderson localization) but from a regular dependence in space. On the other hand, the resulting quantum walk can move freely along the "ordinary" dimensions.

DOI: 10.1103/PhysRevA.95.042112

I. INTRODUCTION

The quantum walk (QW) is the quantum analog of the classical random walk. As in the case of random walks, QWs can appear either under its discrete-time [1] or continuous-time [2] form. We will concentrate here on discrete-time QWs, first considered by Grössing and Zeilinger [3] in 1988, as simple one-particle quantum cellular automata, and later popularized in the physics community in 1993, by Aharonov [1]. The dynamics of such QWs consists of a quantum particle taking steps on a lattice conditioned on its internal state, typically a (pseudo) spin one-half system. The particle dynamically explores a large Hilbert space associated with the positions of the lattice and thus allows one to simulate a wide range of transport phenomena [4]. With QWs, the transport is driven by an external discrete unitary operation, which sets it apart from other lattice quantum simulation concepts where transport typically rests on tunneling between adjacent sites [5]: all dynamic processes are discrete in space and time. It has been shown that any quantum algorithm can be recast under the form of a QW on a certain graph: QWs can be used for universal quantum computation, this being provable for both the continuous [6] and the discrete version [7]. As models of coherent quantum transport, they are interesting both for fundamental quantum physics and for applications. An important field of applications is quantum algorithmic [8]. QWs were first conceived as a natural tool to explore graphs, for example, for efficient data searching (see, e.g., [9]). They are also useful in condensed matter applications and topological phases [10]. A totally new emergent point of view concerning QWs concerns quantum simulation of gauge fields and high-energy physical laws [11–13]. It is important to note that QWs can be realized experimentally with a wide range of physical objects and setups, for example, as transport of photons in optical networks or optical fibers [14], or atoms in optical lattices [15].

Within the context of diffusion processes in lattices, spatial localization appears as a natural phenomenon. It can result from random noise on the lattice sites, giving rise to Anderson localization [16], but it can also be driven by the action of an external periodic potential (see, e.g., [17–19]). Similarly, one obtains localization for the one-dimensional QW when spatial disorder is included [20–22], via nonlinear effects [23], or using a spatially periodic coin [24]. For higher dimensions, localization may appear, even in the noiseless case, from the choice of the coin operator [25].

In this paper, we propose a different variant of the QW that gives rise to localization, by introducing a site-dependent nonperiodic coin operator. The model is inspired on a brane-world proposal with extra dimensions [26], where particles are confined to live in the ordinary 3+1 dimensions by the action of a potential well created by some additional scalar field. In its simplest form, one accounts for massless fermions which are confined in the brane. This idea can be translated to describe a QW where the potential well manifests as a position-dependent coin operator. Differently to the situations described above, the confining field is not random nor periodic, being instead a monotonous function of the position. As we show, this kind of QW produces a dynamical localization of the QW as in the original model. In fact, it can be shown that, in the continuous space-time limit, one reproduces the dynamics of a massless Dirac fermion. In this way, we establish an interesting parallelism between a high-energy quantum field theory and a QW model that results in localization.

The rest of this paper is organized as follows. In Sec. II we briefly introduce the original brane model [26] that motivated our work. In Sec. III we make use of this model to introduce a QW on two dimensions with a position-dependent coin that simulates the domain wall "scalar field" along the second (or "extra dimension"). We show that this QW in fact results in a confinement of the walker, and that the space-time continuous limit indeed reproduces the dynamics of a Dirac particle coupled to the scalar field. These ideas are generalized to three dimensions in Sec. IV. Finally, Sec. V is devoted to summarizing and discussing our results.

II. DOMAIN WALL MODEL FOR PARTICLE PHYSICS

The possibility of extra dimensions of space was first suggested by Kaluza and Klein [27,28], seeking for a unified

*giuseppe.dimolfetta@lif.univ-mrs.fr

theory of electromagnetic and gravitational fields into a higher-dimensional field, with one of the dimensions compactified. However, experimental data from particle colliders restrict the compactification radius to such small scales that they become virtually impossible to access them experimentally. A way to overcome this difficulty [29] makes use of the ideas put forward by Rubakov and Shaposhnikov [26]. In that paper, the authors propose a brane-world scenario in which space-time has $(3+N+1)$ dimensions, with ordinary (low-energy) particles confined in a potential well which is narrow along N spatial directions and flat along the remaining three directions. The origin of this potential well is suggested to have a dynamical origin. In the simplest case it can be created by an extra scalar field in $4+1$ dimensions, as described by the Lagrangian

$$\mathcal{L} = \tfrac{1}{2}\partial_A\partial^A\varphi - \tfrac{1}{2}m^2\varphi - \tfrac{1}{4}\lambda\varphi^4, \quad A = 0,1,2,3,4, \tag{1}$$

with metrics $g_{AB} = (1,-1,-1,-1,-1)$. The classical equations of motion derived from the above Lagrangian admit a domain wall solution $\varphi(x^4)$ that depends only on the coordinate x^4 along the extra dimension and is given by

$$\varphi(x^4) = \frac{m}{\sqrt{\lambda}}\tanh\left(\frac{mx^4}{\sqrt{2}}\right). \tag{2}$$

This model can account for left-handed massless fermions living in $3+1$ dimensions, if they are coupled to the scalar fields, as in the following Lagrangian:

$$\mathcal{L}_\psi = i\bar{\Psi}\Gamma^A\partial_A\Psi + h\varphi\bar{\Psi}\Psi, \tag{3}$$

where h is the coupling constant, and the $4+1$-dimensional γ matrices are $\Gamma^\mu = \gamma^\mu$, $\mu = 0,\ldots 3$, and $\Gamma^4 = i\gamma^5$, with γ^μ, γ^5 the standard γ matrices. From Eq. (3) the corresponding Dirac equation follows, which reads

$$i\Gamma^A\partial_A\Psi + h\varphi\Psi = 0. \tag{4}$$

As discussed in [26], this equation has a solution that is confined inside the domain wall, while the corresponding particles are left-handed massless fermions in the $3+1$-dimensional world. In the next section, we make use of these ideas to introduce a QW model in $1+1+1$ dimensions that leads to confined fermions in $1+1$.

III. 2D QUANTUM WALKS INSIDE A 1+1 DOMAIN WALL

Consider a QW defined over discrete-time and discrete two-dimensional (2D) space, with axis x, y. The discrete space points are labeled by p and q, respectively, with $p,q \in \mathbb{Z}$, while time steps are labeled by $j \in \mathbb{N}$. This QW is driven by an inhomogeneous coin acting on the 2D Hilbert space $\mathcal{H}_{\text{spin}}$. The evolution equations read

$$\begin{bmatrix}\psi^{\uparrow}_{j+1,p,q}\\ \psi^{\downarrow}_{j+1,p,q}\end{bmatrix} = S_y Q^+(\theta_q) S_x Q^-(\theta_q)\begin{bmatrix}\psi^{\uparrow}_{j,p,q}\\ \psi^{\downarrow}_{j,p,q}\end{bmatrix}, \tag{5}$$

with $Q^\pm(\theta_q)$ defined as

$$Q^\pm(\theta_q) = \begin{pmatrix}\cos\theta^\pm_q & i\sin\theta^\pm_q\\ i\sin\theta^\pm_q & \cos\theta^\pm_q\end{pmatrix}, \tag{6}$$

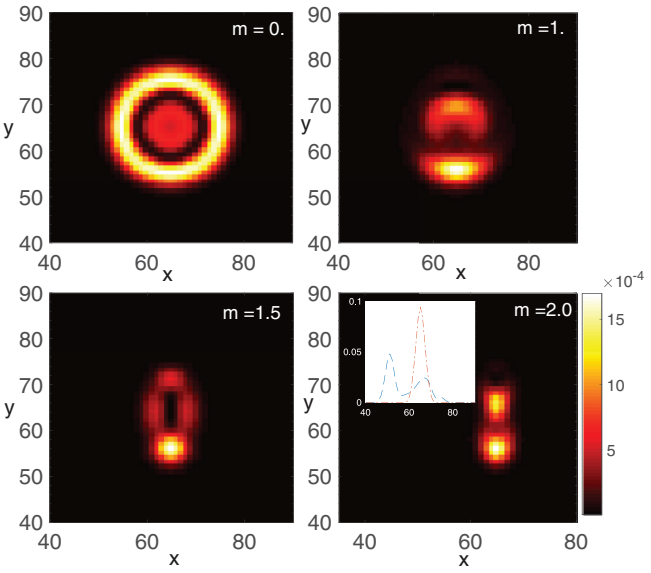

FIG. 1. Probability distribution $||\Psi(t_j,x_p,y_q)||^2$ of the two-dimensional QW for a value $t = 10$ of the time step and different values of m. The rest of the parameters are fixed to $\lambda = 60$, $h = 70$, with the lattice parameter $\epsilon = 0.04$. The inset in the last subfigure also shows the projected density profile along each direction of the lattice (*red dot-dashed line* represents the x direction and *blue dashed line* the y direction). The initial condition is a Gaussian wave packet $\Psi(0,x_p,y_q) = \sqrt{n(x_p,y_q)}\otimes(\frac{1}{\sqrt{2}},\frac{1}{\sqrt{2}})^\top$ centered at the point (64,64), where the Gaussian distribution $n(x_p,y_q)$ has a width $\delta = 0.1$.

where $\theta^\pm_q = \pm\frac{\pi}{4} - \epsilon\bar{\theta}_q$ is the coin angle, which depends only on the coordinate q, and ϵ is a small parameter that allows one to reach the appropriate continuous space-time limit (see discussion below). The operators S^x and S^y are the usual spin-dependent translations along the x direction and the y direction, respectively. They are defined as follows:

$$S^x\Psi_{j,p,q} = (\psi^{\uparrow}_{j,p+1,q}, \psi^{\downarrow}_{j,p-1,q})^\top, \tag{7}$$

and

$$S^y\Psi_{j,p,q} = (\psi^{\uparrow}_{j,p,q+1}, \psi^{\downarrow}_{j,p,q-1})^\top. \tag{8}$$

Equations (5) describe the evolution of a two-level system, e.g., a fermion in two dimensions, and it has been shown that each of them recover, in the continuous limit, the Dirac equation [30], where the parameter θ_q corresponds to a position-dependent potential. Let us now consider $\bar{\theta}_q$ of the form

$$\bar{\theta}_q = h\frac{m}{\sqrt{\lambda}}\tanh\left(\frac{mq}{\sqrt{2}}\right), \tag{9}$$

and notice that it corresponds to a narrow potential in the q direction when m, the "effective mass," is sufficiently large.

Figure 1 shows the evolved probability distribution of this 2D QW, starting from a symmetric Gaussian profile in both directions. As the mass is increased, the probability becomes strongly localized around the y axis, while it evolves as a usual QW on the nonconfining x direction. These features are

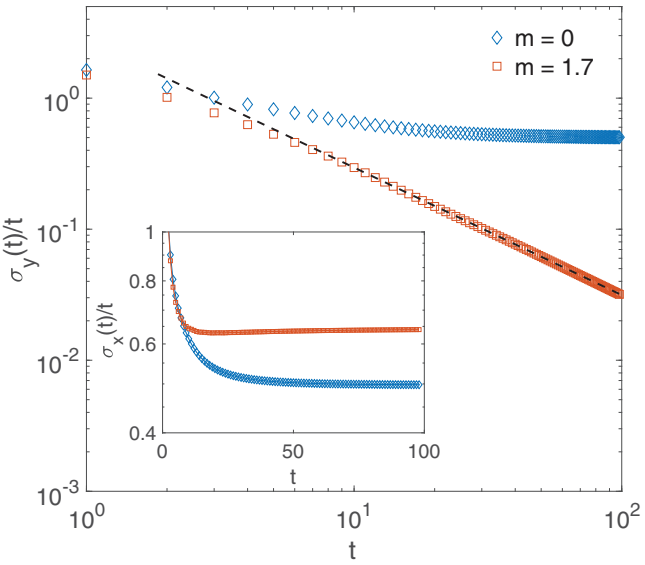

FIG. 2. Time evolution of the standard deviation divided by the time step, i.e., $\sigma_x(t)/t$ (in the inset) and $\sigma_y(t)/t$, calculated independently along the x and y directions, for a localized (red squares) and a free fermion (blue diamonds). The initial condition is a Gaussian wave packet $\Psi(0,x_p,y_q) = \sqrt{n(x_p,y_q)} \otimes (0,1)^\top$ centered around (128,128), and the parameters of the potential are $\lambda = 60$ and $h = 70$, with the lattice parameter $\epsilon = 0.02$.

clearly seen in Fig. 2, where we have represented the standard deviation divided by the time step, i.e., $\sigma_x(t)/t$ and $\sigma_y(t)/t$, calculated independently along the x and y directions. For $m = 0$ (no confinement), both quotients tend to a constant, which corresponds to the normal spreading of a 2D QW in both directions. As m increases, localization acts on the y direction and manifests as an exponential decay of $\sigma_y(t)/t$. On the other hand, the standard deviation corresponding to the x axis behaves as a free-evolving QW, with a spreading velocity that depends on the parameters of the potential well.

As we show below, in the continuous limit Eqs. (5) are in correspondence with Eq. (4), describing the propagation of a massless fermion in a space-time manifold $M^{(1+N,1)}$, the usual Minkowski space with $1+N$ spatial dimensions. When m is nonvanishing, the fermion is confined inside a potential well, which is sufficiently narrow along N directions and flat along the other one (in our case $N = 1$).

Let us introduce new space-time coordinates t_j, x_p, and y_q such that $t_j = j\epsilon$, $x_p = p\epsilon$, and $y_q = q\epsilon$. In the limit when $\varepsilon \longrightarrow 0$, these coordinates become continuous, labeled by t, x, and y, respectively. If we Taylor expand Eqs. (5) around $\epsilon = 0$, we recover the following equation:

$$\partial_t \Psi(t,x,y) = [\sigma_z \partial_x - \sigma_y \partial_y - i\sigma_x \bar{\theta}(y)]\Psi(t,x,y), \qquad (10)$$

which can be recast in covariant form:

$$i\Gamma^A \partial_A \Psi + h\frac{m}{\sqrt{\lambda}} \tanh\left(\frac{my}{\sqrt{2}}\right)\Psi = 0, \qquad (11)$$

where $\Gamma^A = \{\gamma^\mu, \gamma^c\}$, $\mu = 0,1$, and $\gamma^c = i\gamma^5 = i\gamma^0\gamma^1 = -i\sigma_z$. In this equation, $\gamma^0 = -\sigma_x$, $\gamma^1 = -i\sigma_y$. As can be easily seen, Eq. (11) takes the same form as (4) if we make the identification $x^4 \longrightarrow y$ and $\varphi \longrightarrow \frac{m}{\sqrt{\lambda}} \tanh(\frac{my}{\sqrt{2}})$.

IV. 3D QUANTUM WALKS INSIDE A 2+1 DOMAIN WALL

The extension of the previous case to the higher-dimensional case is straightforward. In this section we adopt the same techniques introduced in the last section but we double the spin Hilbert space, in order to recover the standard Dirac equation in 3+1 space-time. Let us recall that in 3+1, γ matrices appearing in Eq. (4) are four dimensional. In the Weyl representation they read

$$\gamma^0 = \begin{pmatrix} 0 & \mathbb{I} \\ \mathbb{I} & 0 \end{pmatrix} \gamma^i = \begin{pmatrix} 0 & \sigma^i \\ -\sigma^i & 0 \end{pmatrix} \gamma^5 = \begin{pmatrix} -\mathbb{I} & 0 \\ 0 & \mathbb{I} \end{pmatrix}. \qquad (12)$$

Now, consider the QW defined over discrete three-dimensional (3D) space, with axes x, y, and z. The discrete space points are labeled by p, q, and r, respectively, with $p,q,r \in \mathbb{Z}$. This QW is driven by an inhomogeneous coin acting on the spinor $(\psi^1_{j,p,q,r}, \psi^2_{j,p,q,r})^\top$, where each $\psi^i_{j,p,q,r}$ belongs to $\mathcal{H}_{\text{spin}}$ for $i = 1,2$.

The evolution equations read

$$\begin{bmatrix} \psi^1_{j+1,p,q,r} \\ \psi^2_{j+1,p,q,r} \end{bmatrix} = \Theta_r \mathcal{S}^z \mathcal{R}_z \mathcal{S}^x \mathcal{R}_x \mathcal{S}^y \mathcal{R}_y \begin{bmatrix} \psi^1_{j+1,p,q,r} \\ \psi^2_{j+1,p,q,r} \end{bmatrix}, \qquad (13)$$

where

$$\Theta_r = \begin{pmatrix} \cos\bar{\theta}_r\epsilon & i\sin\bar{\theta}_r\epsilon \\ i\sin\bar{\theta}_r\epsilon & \cos\bar{\theta}_r\epsilon \end{pmatrix} \otimes \mathbb{I}_2 \qquad (14)$$

and

$$\mathcal{S}^i = \begin{pmatrix} S^i & 0 \\ 0 & S^{i\dagger} \end{pmatrix} \quad \mathcal{R}_i = \begin{pmatrix} R_i & 0 \\ 0 & R_i \end{pmatrix}, \qquad (15)$$

where the operators S^i are the usual spin-dependent translations along each direction of the cubic lattice, and each unitary rotation R_i, for $i = x,y,z$, is an element of U(2).

Notice that Θ_r encodes the coupling between the spinor components, and θ_r is an arbitrary position-dependent function, which can model either the mass term or any other scalar potential. If θ_r identically vanishes, Eq. (13) represents simply a couple of independent split-step QW operators acting on each component of the spinor. In the following, this mass term is defined by Eq. (9) and will model the narrow potential in the r direction, embedding a 3D QW in a 2D space-time lattice.

In order to validate the model, we compute the formal continuous limit of Eq. (13) with the same technique introduced in the previous section. Thus, let us introduce the new spatial coordinate z_r, such that $z_r = r\epsilon$, and again assume that in the limit when $\varepsilon \longrightarrow 0$, this coordinate, together with t_j, x_p, y_q, become continuous, labeled by z and t, x, y, respectively. If we Taylor expand Eqs. (13) around $\epsilon = 0$, the zero order restricts the four-dimensional coins, $\mathcal{R}_i = R_i \otimes \mathbb{I}_2$:

$$\begin{bmatrix} \psi^1 \\ \psi^2 \end{bmatrix} = \mathcal{R}_z \mathcal{R}_x \mathcal{R}_y \begin{bmatrix} \psi^1 \\ \psi^2 \end{bmatrix} + O(\epsilon), \qquad (16)$$

which leads to the condition

$$\mathcal{R}_z \mathcal{R}_x \mathcal{R}_y = \mathbb{I}_4. \qquad (17)$$

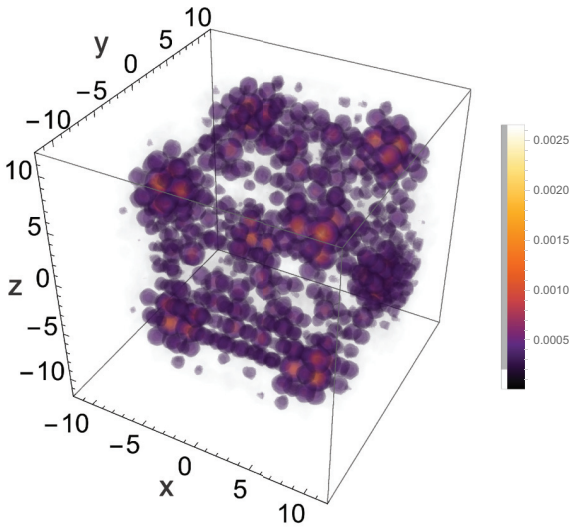

FIG. 3. Density plot in 3D at time $j = 12$ with Gaussian initial wave packet $\Psi(0,x_p,y_q,z_r) = \sqrt{n(x_p,y_q,z_r)} \otimes (1,i,1,i)^\top$ centered around (0,0) and for $m = 0$.

Then the first-order term of the Taylor expansion reads

$$\partial_t \begin{bmatrix} \psi^1 \\ \psi^2 \end{bmatrix} = [B_z\partial_z + B_x\partial_x + B_y\partial_y + iB_0\bar{\theta}(z)] \begin{bmatrix} \psi^1 \\ \psi^2 \end{bmatrix} + O(\epsilon), \tag{18}$$

where

$$\begin{aligned} B_z &= Z\mathcal{R}_z\mathcal{R}_x\mathcal{R}_y \\ B_x &= \mathcal{R}_z Z\mathcal{R}_x\mathcal{R}_y \\ B_y &= \mathcal{R}_z\mathcal{R}_x Z\mathcal{R}_y, \end{aligned} \tag{19}$$

and

$$\begin{aligned} B_0 &= \sigma_x \otimes \mathbb{I}_2 \\ Z &= \mathbb{I}_2 \otimes \sigma_z. \end{aligned} \tag{20}$$

Now, comparing Eq. (18) with Eq. (4), we derive—up to a U(2) rotation—the explicit form of each rotation $\mathcal{R}_i$. In particular, we need to satisfy $\gamma^0\gamma^1 = B_x$, $\gamma^0\gamma^2 = B_y$, and $\gamma^0\gamma^3 = B_z$, which leads to

$$\begin{aligned} R_x &= \frac{1}{\sqrt{2}}\begin{pmatrix} 1 & 1 \\ 1 & -1 \end{pmatrix}, \quad R_z = \frac{1}{\sqrt{2}}\begin{pmatrix} 1 & -i \\ i & -1 \end{pmatrix}, \\ R_y &= R_x R_z. \end{aligned} \tag{21}$$

Thus, numerical simulations of the above QW can model the behavior of a fermion in a 3+1 space-time. In particular, in Fig. 3, the quantum walker spreads on the 3D cubic lattice, starting from a symmetric initial condition, recovering, in the continuous limit, a massless fermion in vacuum ($\bar{\theta} = 0$). In contrast, Fig. 4 shows the evolved probability distribution of this 3D QW when the mass term is different from zero and is position dependent. As in the lower-dimensional case, the probability dynamically localizes on the x-y plane and corresponds to a standard 2D QW, while it possesses a finite size on the z direction, which typically decreases with the lattice parameter ϵ.

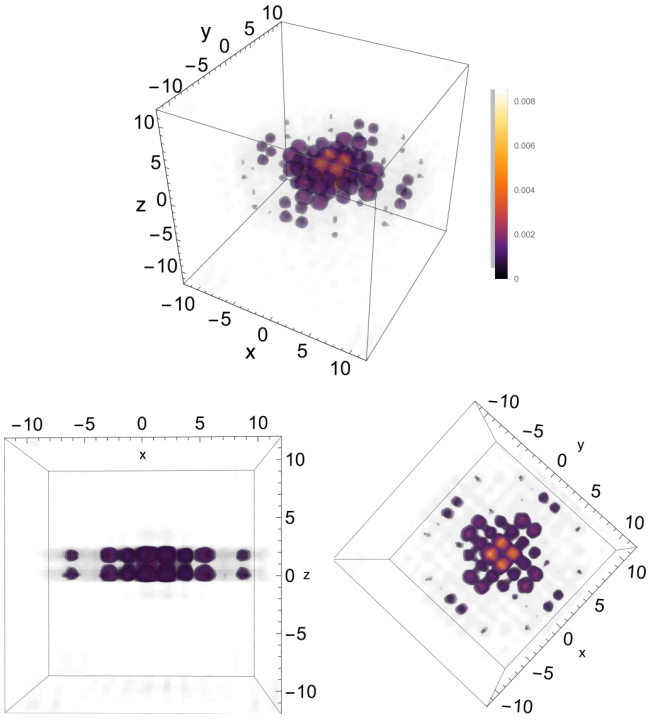

FIG. 4. Density plots in 3D at time $j = 20$ with Gaussian initial wave packet $\Psi(0,x_p,y_q,z_r) = \sqrt{n(x_p,y_q,z_r)} \otimes (0,1,0,1)^\top$ centered around (0,0). The parameters of the potential are $\lambda = 90$, $h = 4$, and $m = 11$. The two subfigures at the bottom display the x-z side view (left) and the x-y side view (right) of the 3D density plot.

V. DISCUSSION

In this paper we have studied the properties of a two- and a three-dimensional QW that are inspired by the idea of a brane-world model put forward by Rubakov and Shaposhnikov [26]. In that model, particles are dynamically confined in the brane due to the interaction with a scalar field. We translated this model into an alternate QW with a coin that depends on the external field, with a dependence which mimics a domain wall solution. As in the original model, fermions (in our case, the walker) become confined in one of the dimensions, while they can move freely on the "ordinary" dimensions. In this way, we can think of the QW as a possibility to simulate brane models of quantum field theories. In the opposite direction of thought, we obtain a QW that shows localization, not from random noise on the lattice or from a periodic coin, as in previous models, but from a coin which changes in space in a regular, nonperiodic manner. In our opinion, this interplay between QWs and high-energy theories can be beneficial for both fields.

ACKNOWLEDGMENTS

This work has been supported by the Spanish Ministerio de Educación e Innovación, MICIN-FEDER Projects No. FPA2014-54459-P and No. SEV-2014-0398, and Generalitat Valenciana Grant No. GVPROMETEOII2014-087.

[1] Y. Aharonov, L. Davidovich, and N. Zagury, Phys. Rev. A **48**, 1687 (1993); K. Rudinger, J. K. Gamble, E. Bach, M. Friesen, R. Joynt *et al.*, J. Comut. Theory. Nanos. **10**(7), 1653 (2013).
[2] E. Farhi and S. Gutmann, Phys. Rev. A **58**, 915 (1998).
[3] G. Grössing and A. Zeilinger, Complex Syst. **2**, 197 (1988).
[4] J. Kempe, Contemp. Phys. **44**, 307 (2003).
[5] I. Bloch, J. Dalibard, and S. Nascimbene, Nat. Phys. **8**, 267 (2012).
[6] A. M. Childs, Phys. Rev. Lett. **102**, 180501 (2009).
[7] N. B. Lovett, S. Cooper, M. Everitt, M. Trevers, and V. Kendon, Phys. Rev. A **81**, 042330 (2010).
[8] A. Ambainis, Int. J. Quantum Inform. **01**, 507 (2003).
[9] F. Magniez, A. Nayak, J. Roland, and M. Santha, SIAM J. Comput. **40**, 142 (2011).
[10] T. Kitagawa, M. A. Broome, A. Fedrizzi, M. S. Rudner, E. Berg, I. Kassal, A. Aspuru-Guzik, E. Demler, and A. G. White, Nat. Commun. **3**, 882 (2012).
[11] P. Arnault, G. Di Molfetta, M. Brachet, and F. Debbasch, Phys. Rev. A **94**, 012335 (2016).
[12] M. Genske, W. Alt, A. Steffen, A. H. Werner, R. F. Werner, D. Meschede, and A. Alberti, Phys. Rev. Lett. **110**, 190601 (2013).
[13] G. D. Molfetta and A. Pérez, New J. Phys. **18**, 103038 (2016).
[14] A. Schreiber, A. Gábris, P. P. Rohde, K. Laiho, M. Štefaňák, V. Potoček, C. Hamilton, I. Jex, and C. Silberhorn, Science **336**, 55 (2012).
[15] R. Côté, A. Russell, E. E. Eyler, and P. L. Gould, New J. Phys. **8**, 156 (2006).
[16] P. W. Anderson, Phys. Rev. **109**, 1492 (1956).
[17] S. Aubry and G. André, Ann. Israel Phys. Soc. **3**, 18 (1980).
[18] D. R. Grempel, S. Fishman, and R. E. Prange, Phys. Rev. Lett. **49**, 833 (1982).
[19] Y. Lahini, R. Pugatch, F. Pozzi, M. Sorel, R. Morandotti, N. Davidson, and Y. Silberberg, Phys. Rev. Lett. **103**, 013901 (2009).
[20] A. Joye and M. Merkli, J. Stat. Phys. **140**, 1025 (2010).
[21] A. Schreiber, K. N. Cassemiro, V. Potoček, A. Gábris, I. Jex, and C. Silberhorn, Phys. Rev. Lett. **106**, 180403 (2011).
[22] A. Crespi, R. Osellame, R. Ramponi, V. Giovannetti, R. Fazio, L. Sansoni, F. De Nicola, F. Sciarrino, and P. Mataloni, Nat. Photonics **7**, 322 (2013).
[23] C. Navarrete-Benlloch, A. Pérez, and E. Roldán, Phys. Rev. A **75**, 062333 (2007).
[24] Y. Shikano and H. Katsura, Phys. Rev. E **82**, 031122 (2010).
[25] N. Inui, Y. Konishi, and N. Konno, Phys. Rev. A **69**, 052323 (2004).
[26] V. Rubakov and M. Shaposhnikov, Phys. Lett. B **125**, 136 (1983).
[27] T. Kaluza, Sitzungsber. Preuss. Akad. Wiss. Berlin (Math. Phys.) **K1**, 966 (1921).
[28] O. Klein, Eur. Phys. J. A **37**, 895 (1926).
[29] N. Arkani-Hamed, S. Dimopoulos, and G. Dvali, Phys. Rev. D **59**, 086004 (1999).
[30] G. Di Molfetta, M. Brachet, and F. Debbasch, Phys. A (Amsterdam, Neth.) **397**, 157 (2014).

2.6 Bound states in the Dirac equation

In the previous article, we observe that, by tuning the coin parameter, it is possible to confine the QW probability distribution along a line, in the case of the 1D QW, or to confine the probability distribution on a surface, in the case of the 2D QW.

We have seen, based on the brane model, that we can couple the Dirac Lagrangian to a scalar field of the form, $\phi^{cl}(x^4) = \frac{m}{\sqrt{\lambda}} \tanh\left(\frac{mx^4}{\sqrt{2}}\right)$, which results on a Dirac equation with a position-dependent (along the extra dimension) effective mass.

The localization along the "extra dimension" can be explained by studying the analytical solution of the Dirac equation, in the case of having a in-homogeneous mass. This localized state is therefore a bound state of the Dirac equation, which lives on interface of two regions with different masses m_1 and m_2. We can consider the 2D Dirac equation, with an in-homogeneous mass $m(y) = m$ for $y > 0$ and $-m$ for $y < 0$. Resolving analytically the equation, two solutions localized along $y = 0$, can be found, given by:

$$\begin{aligned}\psi_1 =& \sqrt{\frac{m}{2}} \begin{pmatrix} i \\ 0 \\ 0 \\ 1 \end{pmatrix} e^{-|m(y)y| + ik_x x} \\ \psi_2 =& \sqrt{\frac{m}{2}} \begin{pmatrix} 0 \\ i \\ 1 \\ 0 \end{pmatrix} e^{-|m(y)y| + ik_x x}\end{aligned} \tag{2.19}$$

with $\hbar = c = 1$. The first solution has a dispersion relation $\omega_1 = k_x$ and the second one $\omega_2 = -k_x$. From these expressions, we observe that the probability amplitude decays exponentially away from the mass interface. These states propagate along the line $y = 0$, but moving in opposite directions. It is also possible to generalize this result to the 3D case, thus observing a bounded surface state. For a further insight in the topic of the Dirac equation and topological states see [120] and the chapter 7 of [19].

3 Gauge invariance in DTQW

Summary

3.1 Gauge invariance in electromagnetism

Since its introduction in the electromagnetic theory, gauge invariance has been a paradigm in physics. It's been introduced at the beginning to help to solve the Maxwell equations, however it plays a more fundamental role in theoretical physics, as it constitutes one of the main properties of successful theories such a the standard model of particle interactions. From the Electromagnetism theory, the electric field $\vec{E}(x,t)$ and magnetic field $\vec{B}(x,t)$ can be written in terms of a scalar potential $\phi(x,t)$ and a vector potential $\vec{A}(x,t)$,

$$\begin{aligned} \vec{E} &= -\nabla\phi - \partial_t \vec{A} \\ \vec{B} &= \nabla \times \vec{A}, \end{aligned} \tag{3.1}$$

where ϕ and $\vec{A}$ are referred to as the gauge fields. The Lagrangian for a charged particle under the effect of an electromagnetic field is given by:

$$\mathcal{L} = \frac{1}{2} m \dot{\vec{x}}^2 + q\dot{\vec{x}} \cdot \vec{A} - q\phi, \tag{3.2}$$

where q refers to the particle charge. Using the classical mechanics theory, from the Lagrangian, it is straightforward to arrive to the equation of motion:

$$\begin{aligned}\partial_{x_i}\mathcal{L} =& -q\partial_{x_i}\phi + q\sum_j \dot{x_j}\partial_{x_i}A_j \\ \partial_{\dot{x}_i}\mathcal{L} =& m\dot{x}_i + qA_i \\ \frac{d}{dt}\partial_{\dot{x}_i}\mathcal{L} =& m\ddot{x}_i + q\partial_t A_i + q\sum \partial_{x_j}A_i\dot{x}_j,\end{aligned} \tag{3.3}$$

where the index i refers to the component of the vector. Therefore, the equations of motion are:

$$m\ddot{x}_i = -q\partial_{x_i}\phi - q\partial_t A_i + q\sum_j \dot{x}_j\left[\partial_{x_i}A_j - \partial_{x_j}A_i\right]. \tag{3.4}$$

Making use of Eq.(3.1), we can recognize the electric and magnetic field. Hence, the equation of motion can be rewritten as:

$$m\ddot{x}_i = q\left(\vec{E} + \dot{\vec{x}}\times\vec{B}\right) \tag{3.5}$$

Gauge transformation The gauge fields are not uniquely defined since they can be transformed by a *gauge transformation*, however yielding to the same electric and magnetic fields.

$$\begin{aligned}\phi &\to \phi - \partial_t\alpha \\ \vec{A} &\to \vec{A} + \vec{\nabla}\alpha\end{aligned} \tag{3.6}$$

for any function $\alpha(x,t)$. In spite of leaving the fields unchanged, the Lagrangian, Eq.(3.2) is not invariant under gauge transformations, but still the equations of motions are invariant. Applying the transformation Eq.(3.6), the Lagrangian transforms as:

$$\mathcal{L}(t) \to \mathcal{L}'(t) = \mathcal{L} + q\frac{d}{dt}\alpha \tag{3.7}$$

Although the Lagrangian is clearly not invariant, the action $\int \mathcal{L}dt$ is gauge invariant (assuming that α vanished as $t \to \pm\infty$). As the equations of motion are given by the principle of least action, which state that the action is stationary under small variations of the dynamical parameters, they are also gauge invariant. Therefore, the existence of gauge transformation implies that systems which differ under the transformation Eq.(3.6), describe the same physical model.

3.1.1 Gauge invariance in quantum mechanics

In the quantum theory we can also apply gauge transformations. In this case we ask the field $\psi(\vec{x},t)$, which is solution of the Schrödinger equation, to be transformed as:

$$\psi(\vec{x},t) \to \psi'(\vec{x},t) = e^{i\alpha}\psi(\vec{x},t) \tag{3.8}$$

where α is the gauge parameter. If α is constant, we are applying a *global gauge transformation*. Thus, substituting $\psi'(\vec{x},t)$ in the Schrödinger equation, we get:

$$i\hbar\partial_t\psi'(\vec{x},t) = -\frac{\hbar^2}{2m}\nabla^2\psi'(\vec{x},t) + U(\vec{x})\psi'(\vec{x},t), \tag{3.9}$$

thus obtaining the same equation, meaning that the Schrödinger equation is invariant under global gauge transformations, and therefore the probability density is also invariant.

If the gauge parameter depends on the space-time coordinates, we call this transformation a *local gauge transformation*:

$$\psi(\vec{x},t) \to \psi'(\vec{x},t) = e^{i\alpha(\vec{x},t)}\psi(\vec{x},t). \tag{3.10}$$

In this case the space and time partial derivatives will act on the gauge parameter. Assuming that $\psi'(\vec{x},t)$ is a solution of the Schrödinger equation, we realize that $\psi(\vec{x},t)$ is not:

$$i\hbar\partial_t\psi(\vec{x},t) = -\frac{\hbar^2}{2m}\left(\nabla + i\nabla\alpha(\vec{x},t)\right)^2\psi(\vec{x},t) + \left(U(\vec{x}) + \hbar\partial_t\alpha(\vec{x},t)\right). \tag{3.11}$$

Therefore, we can conclude that without further modifications, the Schrödinger equation does not preserve local gauge invariance, although the probability density does $|\psi|^2 = |\psi'|^2$. Luckily, the Shrödinger equation is local gauge invariance, by introducing new functions that allow us to cancel out the spoiler terms. Hence, the Schrödinger equation should read as:

$$i\hbar\partial_t\psi(\vec{x},t) = -\frac{\hbar^2}{2m}\left(\nabla + iq\vec{A}(\vec{x},t)\right)^2\psi(\vec{x},t) + \left(U(\vec{x}) + \hbar\phi(\vec{x},t)\right) \tag{3.12}$$

where the new functions are $\vec{A}(\vec{x},t)$ and $\phi(\vec{x},t)$, and q is a constant. In order to preserve gauge invariance, the new functions need to be transformed as:

$$\begin{aligned}\phi(\vec{x},t) &\to \phi(\vec{x},t) - \partial_t\alpha(\vec{x},t)\\ \vec{A}(\vec{x},t) &\to \vec{A} + \frac{1}{q}\nabla\alpha(\vec{x},t)\end{aligned} \tag{3.13}$$

If we compare with the gauge transformation in classical electrodynamics, Eq.(3.6), the functions that we have introduced are completely equivalent to gauge fields,

in this case they play the role of the vector and scalar potential. Therefore, to preserve local gauge transformation, the Schödinger equation demands the presence of electromagnetic fields.

3.1.2 Electromagnetic gauge invariance in relativistic quantum mechanics

We can take a look to the relativistic quantum theory. Let us consider the Lagrangian of a free Dirac field describing a particle of mass m,

$$\mathcal{L} = \bar{\psi}\left(i\gamma^{\mu}\partial_{\mu} - m\right)\psi. \tag{3.14}$$

Again, we can transform the Dirac spinor under a global phase (*global gauge invariance*) that leaves the Lagrangian invariant,

$$\psi \to \psi' = e^{i\alpha}\psi. \tag{3.15}$$

Therefore, the equation of motion is also invariant under this global transformation:

$$\left(i\gamma^{\mu}\partial_{\mu} - m\right)\psi \to \left(i\gamma^{\mu}\partial_{\mu} - m\right)\psi' = \left(i\gamma^{\mu}\partial_{\mu} - m\right)e^{i\alpha}\psi = 0. \tag{3.16}$$

Following the same procedure as in Sect.(3.1.1), the question that arises is what happen if the phase is space-time dependent (*local gauge invariance*) transforming the field as:

$$\psi \to \psi' = e^{i\alpha(x)}\psi. \tag{3.17}$$

In this case, the derivative gives an extra term:

$$\partial_{\mu}\psi \to \partial_{\mu}\psi' = e^{i\alpha(x)}\left(\partial_{\mu}\psi + i\left(\partial_{\mu}\alpha(x)\right)\psi\right), \tag{3.18}$$

and Gauge invariance is spoiled. However, local gauge invariance can be achieved by replacing the derivative by the so-called *covariant derivative*:

$$\partial_{\mu} \to D_{\mu} = \partial_{\mu} + iqA_{\mu}, \tag{3.19}$$

where q is the charge of the particle and A_{μ} is the field, which transforms as:

$$A_{\mu} \to A'_{\mu} = A_{\mu} - \frac{1}{e}\partial_{\mu}\alpha(x). \tag{3.20}$$

Hence, similarly to the Schrödinger equation, in order to achieve local gauge invariance it is necessary to introduce an additional field, which is coupled to the particle. This additional field is the electromagnetic potential A_{μ} in our example.

Fermion current In order to define a conserved current for a particle described by the Dirac equation, we need to define a Lorentz invariant quantity. We define

the adjoint spinor $\bar{\psi} \equiv \psi^\dagger \gamma^0$, where $\psi^\dagger$ is the hermitian conjugate of ψ. The adjoint Dirac equation is written as:

$$i\partial_\mu \bar{\psi}\gamma^\mu + m\bar{\psi} = 0. \tag{3.21}$$

Multiplying the former equation by ψ from the right, gives the continuity equation:

$$\partial_\mu(\bar{\psi}\gamma^\mu\psi) = \partial_\mu j^\mu = 0, \tag{3.22}$$

where j^μ is the four-vector fermion current:

$$j^\mu = (\rho, \vec{j}), \tag{3.23}$$

where ρ is the probability density $\rho = \psi^\dagger\psi$.

Maxwell's equation Making use of the four-vector fermion current, it is possible to write the Maxwell's equations in a Lorentz covariant form:

$$\begin{aligned} \partial^2 A^\mu &= 4\pi j^\mu \\ \partial_\mu A^\mu &= 0 \\ \partial_\mu j^\mu &= 0 \end{aligned} \tag{3.24}$$

where $\partial^2 = \partial_\mu \partial^\mu$.

3.1.3 Discrete local invariance in LGT

Introducing a $U(1)$ gauge invariance in lattice theories is not a trivial problem. In fact, going from the continuum to a lattice formulation is plagued with difficulties and new features [96, 99]. There is not an unique way to define gauge invariance in a lattice model, since different approaches can lead to the same limit in the continuum.

Our proposal to achieve $U(1)$ gauge invariance for the DTQW exhibits close analogies with the method used in lattice quantum field theory [134]. There are some analogies and differences with some recent works, where $U(1)$ gauge invariance is also defined in DTQWs [48, 9].

The method introduced by Wilson [134], to discretize the action on a 4-D hyper-cubic lattice in Euclidean space, breaks translation, rotation and Lorentz symmetry, however it preserves gauge invariance for any lattice spacing. The derivatives are discretized using a symmetric difference:

$$\partial_\mu \psi(x) \to \frac{\psi(n+\mu) - \psi(n-\mu)}{2a}, \tag{3.25}$$

where n is the discrete position and a is the lattice spacing, while μ is the unit

vector along the x direction, Fig.(3.1).

The Dirac action for the electron field transforms as

$$\int d^4x\bar{\psi}(x)\gamma^\mu\nabla_\mu\psi(x) \to \frac{a^3}{2}\sum_n\sum_\mu\left(\bar{\psi}(n)\gamma^\mu\psi(n+\mu) - \bar{\psi}(n+\mu)\gamma^\mu\psi(n)\right). \quad (3.26)$$

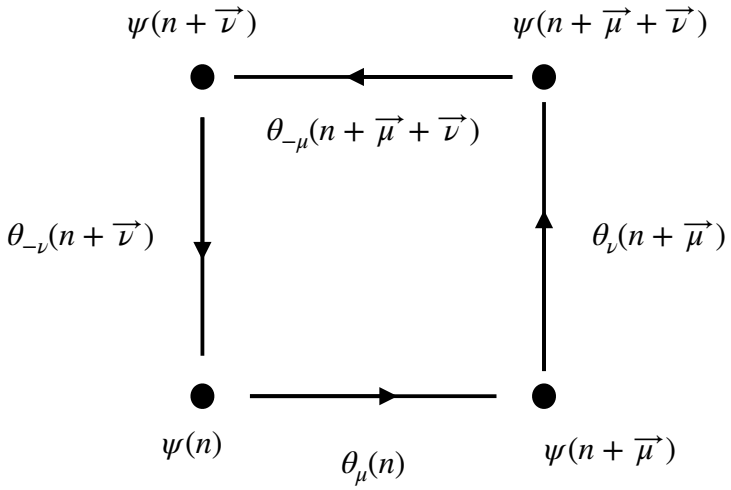

Figure 3.1: A closed path in the basic plaquette. The electron field lives on the sites while the photon field lives on the links. μ is the unit vector in the x direction, whereas ν is the unit vector in the y direction

As this discretization couples the electron field at neighboring sites, the local gauge invariance is broken as the interaction term is discretized,

$$\int d^4x\bar{\psi}(x)\gamma^\mu A_\mu\psi(x) \to a^4\sum_n\sum_\mu\bar{\psi}(n)\gamma^\mu A_\mu(n)\psi(n). \quad (3.27)$$

The solution for preserving gauge invariance consists in replacing the photon field with a periodic angular variable,

$$\theta_\mu(n) = -\theta_{-\mu}(n+\mu), \quad 0 < \theta < 2\pi, \quad (3.28)$$

associating the photon field to the links between neighbors $n \to n+\mu$, Fig.(3.1). Finally local gauge invariance will be preserved, if the electron field and the photon field transform as follows:

$$\psi(n) \to e^{ie\xi(n)}\psi(n) \quad \theta_\mu \to \theta_\mu - e\left(\xi(n+\mu) - \xi(n)\right). \quad (3.29)$$

As mentioned in Sect.(3.2), our additional phases required to preserve gauge

invariance in DTQWs are treated in similar way in terms of discrete derivatives as in Eq.(3.29).

3.2 Publication: "Electromagnetic lattice gauge invariance in two-dimensional discrete-time quantum walks"

In the present paper we discuss the concept of gauge invariance in DTQWs, in one and two dimensions, when there are involved external, synthetic electromagnetic fields. There are some works that discuss this topic already [48, 9]. There are some analogies and differences, however the main contrast is that our discrete derivatives, which intervene in this lattice gauge invariance, treat time and space in the same footing, being very similar to Eq.(3.29). For example, in our 1D DTQWs the gauge fields transform as follows, when we impose a $U(1)$ lattice gauge invariance:

$$(A'_\mu)_{j,p} = (A_\mu)_{j,p} - (d_\mu \xi)_{j,p}, \tag{3.30}$$

being (j, p) the discrete time and position coordinate, for $\mu = 0, 1$, with:

$$\begin{aligned} d_0 &= \frac{1}{\epsilon}\Delta_0\Sigma_1 \\ d_1 &= \frac{1}{\epsilon}\Delta_1\Sigma_0, \end{aligned} \tag{3.31}$$

and the Δ and Σ are defined to act on an arbitrary function $Q_{j,p}$ defined on the lattice as,

$$\begin{aligned} (\Sigma_\mu Q)_{p_\mu} &= Q_{p_\mu+1} + Q_{p_\mu} \\ (\Delta_\mu Q)_{p_\mu} &= Q_{p_\mu+1} - Q_{p_\mu}. \end{aligned} \tag{3.32}$$

Therefore, the discrete derivatives, Eqs.(3.31), treat time and space on the same footing, contrary by to those of [48, 9].

On the other hand, as we mentioned, in standard LGT the gauge fields live on the links, whereas in DTQW the gauge fields live on the sites, as the fermion field does. The fact that our derivatives are a composition of Σ and Δ, underline that it could be appropriate to define the gauge fields and the local phase change on the links rather than on the sites.

We then extend this gauge invariance to two dimensional DTQW following the same procedure, and we also define a continuity equation and conserved current for the 2D QW.

There is a later work [31] which presents a unified framework to understand

$U(1)$ gauge invariance, in discrete-time quantum walks with coin spaces of arbitrary dimensions.

Another related work related which is interesting to mention is [95]. They present a general framework of gauge invariance in 1D DTQW. What it is remarkable is that, apart from studying the electromagnetic gauge invariance in 1D QWs, it is studied the case in which different phases are introduced in both components of the two-dimensional internal space, i.e it considers a local chiral transformation, although it is not mentioned in the paper.

A clear example showing that there is not an unique procedure to arrive to the same continuum limit is presented by [67], where it is introduced a 2D DTQW on a honeycomb and triangular lattice. In this case, three components are necessary to describe the electromagnetic field in the continuum, whereas our phases match exactly with the fields in the continuum theory. This difference indicates that the relation between the connectivity of the lattice and the theory in the continuum deserves a deeper understanding, although some progress has been made [43, 67] and Sect.(4.2).

Electromagnetic lattice gauge invariance in two-dimensional discrete-time quantum walks

Iván Márquez-Martín,[1,2,*] Pablo Arnault,[1,†] Giuseppe Di Molfetta,[1,2,‡] and Armando Pérez[1,§]
[1]*Departamento de Física Teórica and IFIC, Universidad de Valencia and CSIC, Dr. Moliner 50, 46100 Burjassot, Spain*
[2]*Aix-Marseille Univ., Université de Toulon, CNRS, LIS, Marseille, France*

(Received 12 August 2018; published 28 September 2018)

Gauge invariance is one of the more important concepts in physics. We discuss this concept in connection with the unitary evolution of discrete-time quantum walks in one and two spatial dimensions, when they include the interaction with synthetic, external electromagnetic fields. One introduces this interaction as additional phases that play the role of gauge fields. Here, we present a way to incorporate those phases, which differs from previous works. Our proposal allows the discrete derivatives, that appear under a gauge transformation, to treat time and space on the same footing, in a way which is similar to standard lattice gauge theories. By considering two steps of the evolution, we define a density current which is gauge invariant and conserved. In the continuum limit, the dynamics of the particle, under a suitable choice of the parameters, becomes the Dirac equation and the conserved current satisfies the corresponding conservation equation.

DOI: 10.1103/PhysRevA.98.032333

I. INTRODUCTION

Since its introduction in the electromagnetic theory, gauge invariance has been a paradigm in physics, and constitutes one of the main properties of successful theories such as the standard model of particle interactions [1]. On the one side, the gauge principle can be used as a guiding principle to define new theories, where the development of the electroweak interaction theory is just an example. On the other side, the symmetry predicts the existence of a conserved current, which constitutes a powerful tool in the analysis of dynamical phenomena.

In this paper, we discuss the manifestation of U(1) gauge invariance within the context of a discrete-time quantum walk (DTQW) in a two-dimensional (2D) lattice, which could be generalized to 3D lattices. The dynamics of such DTQWs is driven by the action of unitary operators that act both on the spatial and internal degrees of freedom [2]. A particular interest in this gauge-invariant dynamical scheme arises from the possibility of describing with it, artificially, i.e., by engineering an appropriate space-time dependence of the walker's phase, the effect of a magnetic field, or even a combination of electric and magnetic fields, on charged matter. By itself, the magnetic field gives rise to interesting phenomena such as localization or controlled spreading [3] and Landau levels [4]. The magnetic field is also one of the main ingredients of the quantum Hall effect, with associated topological effects [5,6] and edge currents [7]. On the other hand, the combination of both a magnetic and an electric field exhibits richer features, like Bloch oscillations and the $\vec{E} \times \vec{B}$ drift [8]. The observation of these effects with discrete-time schemes as we study here may be available in the future using internal-state-dependent transport of atoms in 2D optical lattices [9–11], or of photons in 3D integrated-photonics circuits [12]. In continuous-time schemes, atoms in optical lattices are also a promising platform [13–16] to observe such effects.

In order to consistently describe these effects with DTQWs, one needs to understand how U(1) gauge invariance can be incorporated within this framework, which differs notably from the electromagnetic theory in the continuum (i.e., in continuous space-time). In fact, this is a general (serious) problem in physics, since going from the continuum to a lattice formulation is plagued with difficulties and new features [17–19]. Moreover, the way of implementing gauge invariance in lattice models is usually not unique, with different approaches leading to the same limit in the continuum. Our proposal to achieve U(1) gauge invariance on the lattice exhibits close analogies both with the method used in quantum field theory [20] and with recent works exhibiting similar but different U(1) lattice gauge invariances, in DTQWs [8,21,22] or in reversible cellular automata [23]. We comment on the similarities and differences with these recent works.

This paper is organized as follows. In Sec. II, we define a family of DTQWs on a line, which satisfy a U(1) gauge invariance on the (1+1)D lattice. The discrete derivatives which intervene in this lattice gauge invariance treat time and space on the same footing, and are very much like those used in standard LGTs, in contrast with those of Refs. [8,22]. This is achieved by applying the gauge-field exponentials either before or after the spatial shift, depending on whether the internal state of the walker is, say, up or down, respectively. We formally compute the continuum limit of these DTQWs, which concides, as desired and as in Refs. [21,22], with the dynamics of a Dirac fermion in (1+1)D space-time, coupled to a U(1), i.e., electro(magnetic) gauge field. In Sec. III, we extend the previous results to 2D walks, constructed by alternating 1D walks in the x and y directions of the spatial lattice. The way we ensure the U(1) lattice gauge invariance

*ivan.marquez@uv.es
†pablo.arnault@ific.uv.es
‡giuseppe.dimolfetta@lis-lab.fr
§armando.perez@uv.es

2469-9926/2018/98(3)/032333(8)

of this 2D scheme is by requiring it *for each one-dimensional substep*, in contrast with the gauge invariance of Ref. [8]. This ensures that time and space are still treated on the same footing at the level of the discrete derivatives, up to the fact that there are now, in 2D, two discrete derivatives in time, one for the even discrete-time coordinates, corresponding to the motion in the, say, x direction and another one for the odd ones, corresponding to the motion in the y direction. In Sec. IV, finally, we derive analytically a lattice continuity equation, stating the conservation of a certain current on the lattice which is computed exactly. We comment on the differences between this continuity equation and that of Ref. [8].

II. NEW U(1) LATTICE GAUGE INVARIANCE FOR THE DTQW ON THE LINE

A. Defining the 1D walk

The state $|\psi_j\rangle$ of the walker at some arbitrary discrete time $j \in \mathbb{N}$ belongs to a Hilbert space $\mathcal{H} = \mathcal{H}_{\text{coin}} \otimes \mathcal{H}_{\text{position}}$. The Hilbert space $\mathcal{H}_{\text{position}}$ describes the external, spatial degree of freedom of the walker and is spanned by the basis states $\{|x = p\epsilon\rangle\}_{p\in\mathbb{Z}}$, where ϵ is the lattice spacing. The two-dimensional Hilbert space $\mathcal{H}_{\text{coin}} = \text{span}\{|R\rangle, |L\rangle\}$ describes the internal, so-called coin degree of freedom of the walker, where "R" and "L" stand for "right" and "left." The projection of the walker's state on the position state $|x = p\epsilon\rangle$ at time j is $\psi_{j,p} \equiv \langle x = p\epsilon|\psi_j\rangle$. We identify $|R\rangle = (1, 0)^\top$ and $|L\rangle = (0, 1)^\top$, where $\top$ denotes matrix transposition. The dynamics of the DTQW is defined by its one-time-step evolution operator U_j, which is unitary and may depend on j,

$$|\psi_{j+1}\rangle = U_{j+1}\,|\psi_j\rangle\,. \tag{1}$$

As usual for DTQWs, the dynamics alternates between (i) rotations, C, of the coin degree of freedom and (ii) spatial coin-state-dependent shifts, S:

$$U = SC, \tag{2}$$

where, to lighten notations, the multiplication of C by the identity tensor factor of the position Hilbert space has been, and will be, in similar cases, omitted. We choose, for the coin rotation, the following one:

$$C(\theta) = e^{i\sigma^1\frac{\theta}{2}} = \begin{bmatrix} \cos\frac{\theta}{2} & i\,\sin\frac{\theta}{2} \\ i\,\sin\frac{\theta}{2} & \cos\frac{\theta}{2} \end{bmatrix}, \tag{3}$$

where σ^n is the nth Pauli matrix and θ is some angle, constant in time and uniform in position.

Now, one of the distinctive features of the present work is the way we gauge our walk. In Refs. [8,21,22], gauging the walk amounts to gauging the standard coin-state-dependent shift, $S_{\text{free}} = e^{-i\sigma^3\mathcal{K}}$, where $\mathcal{K}$ is the quasimomentum operator, as $S_{\text{free}} \to e^{i\alpha_j} S_{\text{free}}\, e^{-i\sigma^3\xi_j}$, where $\alpha_{j,p}$ and $\xi_{j,p}$ are lattice counterparts of the temporal and spatial components of an electric potential of the continuum, (A^0, A^1), with which they coincide in the continuum limit of the DTQW. We have used the notation $\varphi_j : p \mapsto \varphi_{j,p}$ for diagonal operators in the position basis, such as α_j and ξ_j. In the present work, we gauge the shift as follows: the relative order in which the shift and the gauge-field exponentials are applied depend on the coin state, that is,

$$S(\alpha_j, \xi_j) = \begin{bmatrix} e^{-i\mathcal{K}}e^{i(\xi_j-\alpha_j)} & 0 \\ 0 & e^{-i(\xi_j+\alpha_j)}e^{i\mathcal{K}} \end{bmatrix} \tag{4a}$$

$$= T\,e^{i(\beta_-)_j}\Lambda_R + e^{-i(\beta_+)_j}T^\dagger\Lambda_L, \tag{4b}$$

where $\dagger$ denotes Hermitian conjugation. We have introduced the following objects: (i) the translation operator by one lattice site to the right,

$$T = e^{-i\mathcal{K}}, \tag{5}$$

(ii) the two projectors associated to the coin space,

$$\Lambda_s = |s\rangle\langle s|\,, \quad s = R, L, \tag{6}$$

and (iii) the difference and sum of ξ and α,

$$\beta_- = \xi - \alpha, \tag{7a}$$

$$\beta_+ = \xi + \alpha. \tag{7b}$$

The nongauged coin-state-dependent shift is of course $S_{\text{free}} = S(0, 0)$. We have chosen the superscripts R and L for, respectively, the upper and lower components of the wave function, because S_{free} shifts the upper one to the right and the lower one to the left. To make notations clear, we introduce an auxiliary notation $\tilde{U}$ for the evolution operator, such that

$$U_j \equiv \tilde{U}(\alpha_j, \xi_j, \theta) \tag{8a}$$

$$\equiv S(\alpha_j, \xi_j)C(\theta). \tag{8b}$$

B. Continuum limit of the 1D walk

A first fact to mention is that this way of gauging the walk does not change the continuum limit $\epsilon \to 0$ obtained in Refs. [8,21,22]. Indeed, the fact that $e^{i\mathcal{K}}$ and $e^{if(\mathcal{P})}$, where $\mathcal{P}$ is the position operator and f an arbitrary function, do not commute, does make an important difference between the gauge procedure of the present work and that of Refs. [8,21,22] at the level of the DTQW, i.e., for a finite space-time-lattice spacing. However, this becomes irrelevant in the continuum limit, since the latter is obtained by Taylor expanding all exponentials in their argument, and keeping only the first-order terms: in other words, at first order in their arguments, the exponentials always commute.

Let us now recall this continuum limit $\epsilon \to 0$. Assume that, for a given quantity Q defined on the space-time lattice, $Q_{j,p}$ coincides with the value $Q(t = j\epsilon, x = p\epsilon)$ of some continuous function Q of t and x. First, rotate the coin state by a small amount at each time step, that is, set

$$\theta = -2\epsilon_m m, \tag{9}$$

with ϵ_m going to zero with ϵ, which is the necessary condition for the continuum limit to exist; now, when going to the continuum, we will actually choose $\epsilon_m = \epsilon$ and the parameter m will be identified as the mass of the walker. Second, consider small gauge fields, that is, set

$$\alpha_{j,p} = \epsilon_A q A^0_{j,p}, \tag{10a}$$

$$\xi_{j,p} = \epsilon_A q A^1_{j,p}, \tag{10b}$$

with ϵ_A going to zero with ϵ, which is also a necessary condition for the continuum limit to exist; again, when going to the continuum, we will actually choose $\epsilon_A = \epsilon$ and the parameter q will be identified as the electromagnetic charge of the walker. Assuming now that all Q's are twice differentiable in both t and x, and Taylor expanding the dynamics of the walker, Eq. (1), at first order in ϵ, delivers (i) zeroth-order terms that, by construction of our walk, cancel each other, which is a necessary condition for the continuum limit to exist, and (ii) first-order terms, which deliver a Hamiltonian equation that can be identified as the Dirac equation in (1+1)D space-time, with a coupling to a U(1) (and thus Abelian) gauge field. This equation reads, in manifestly covariant form,

$$\left(i\gamma^{\mu}_{1\mathrm{D}} D_{\mu} - m\right)\psi = 0, \tag{11}$$

with $\mu = 0, 1$, the covariant derivative $D_{\mu} = \partial_{\mu} + iqA_{\mu}$, where

$$A_0 = A^0, \quad A_1 = -A^1, \tag{12}$$

are the covariant components of the electric potential, and with the following gamma matrices:

$$\gamma^0_{1\mathrm{D}} = \sigma^1, \quad \gamma^1_{1\mathrm{D}} = -i\sigma^2. \tag{13}$$

As announced, we obtain, in the limit of small coin-rotation angles and small phases, the same continuum limit as if we had used the gauge procedure of Refs. [8,21,22].

C. New U(1) lattice gauge invariance

Our DTQW, Eq. (1), exhibits a remarkable U(1) lattice gauge invariance: it is invariant under local phase shifts of the form $\psi_{j,p} \to \psi'_{j,p} = e^{iq\chi_{j,p}}\psi_{j,p}$, where $\chi_{j,p}$ is an arbitrary space- and time-dependent quantity, provided the gauge fields become

$$(A'_{\mu})_{j,p} = (A_{\mu})_{j,p} - (d_{\mu}\chi)_{j,p}, \tag{14}$$

for $\mu = 0, 1$, with

$$d_0 = \frac{1}{\epsilon_A}\Delta_0\Sigma_1, \tag{15a}$$

$$d_1 = \frac{1}{\epsilon_A}\Delta_1\Sigma_0, \tag{15b}$$

where the Σ's and Δ's act on sequences $Q_{j,p}$ of time and space as

$$(\Sigma_{\mu}Q)_{p_{\mu}} = Q_{p_{\mu}+1} + Q_{p_{\mu}}, \tag{16a}$$

$$(\Delta_{\mu}Q)_{p_{\mu}} = Q_{p_{\mu}+1} - Q_{p_{\mu}}, \tag{16b}$$

having introduced $p_0 \equiv j$ and $p_1 \equiv p$ for a more compact notation. The discrete derivatives, Eqs. (15), treat time and space on the same footing, on the contrary to those of Refs. [8,22]. Morever, the Σ's and Δ's defined here are sums and differences over one lattice spacing, or link between two sites, while in Refs. [8,22] they were over two links. Notice that the Δ's are nothing but standard finite differences over one link. The fact that, here, one has to apply the Σ's in addition to the Δ's underlines that it may be appropriate that the gauge variables, that is, both the gauge fields and the local phase change, be defined on the links rather than on the sites, as in standard LGTs. We leave this matter to future work. Up to these extra Σ's, the discrete derivatives involved in Eqs. (15) are the same as those used in standard LGTs, that is, standard finite differences.

As done in Ref. [22] for the 1D case, Ref. [8] for the 2D case, and Ref. [24] for the non-Abelian 1D case, one can define a lattice counterpart to the electromagnetic tensor in the continuum,

$$(F_{\mu\nu})_{j,p} = (d_{\mu}A_{\nu})_{j,p} - (d_{\nu}A_{\mu})_{j,p}, \tag{17}$$

which is antisymmetric by construction. Since we are in 1D space, the only nonvanishing components are $(F_{01})_{j,p} = -(F_{10})_{j,p}$, which encode a lattice counterpart to the electric field, and there is no magnetic field. This quantity, $(F_{\mu\nu})_{j,p}$, is, as in the continuum, gauge invariant by construction (on the space-time lattice, obviously), since the d_{μ}'s commute with each other.

In the continuum limit, d_{μ} tends towards the partial derivative ∂_{μ}, the gauge transformation of Eq. (15) becomes the standard one of the continuum, and the lattice counterpart to the electro(magnetic) tensor, Eq. (17), becomes that electro(magnetic) tensor.

III. 2D GENERALIZATION BY ALTERNATING 1D WALKS ALONG THE *x* AND y DIRECTIONS

A. Defining the 2D walk

The walker can now move on a 2D lattice, and has spatial coordinates $x = p\epsilon$ and $y = q\epsilon$, where $p, q \in \mathbb{Z}$. We will also use the notation $p = p_1$ and $q = p_2$. Now, the 1D walk defined in the previous section admits a 2D generalization via a walk which alternates 1D walks in the x and y directions of the 2D lattice. This generalization reads

$$|\psi_{2l}\rangle = U^{(1)}_{2l}\,|\psi_{2l-1}\rangle\,, \tag{18a}$$

$$|\psi_{2l+1}\rangle = U^{(2)}_{2l+1}\,|\psi_{2l}\rangle\,, \tag{18b}$$

with $l \in \mathbb{N}$ and where, for $i = 1, 2$,

$$U^{(i)}_j \equiv \tilde{U}^{(i)}\left(\tfrac{1}{2}\alpha_j, \xi^i_j, \theta^i\right) \tag{19a}$$

$$\equiv S^{(i)}\left(\tfrac{1}{2}\alpha_j, \xi^i_j\right)C(\theta^i) \tag{19b}$$

and

$$S^{(i)}\left(\tfrac{1}{2}\alpha_j, \xi^i_j\right) = T_i e^{i(\beta^{(i)}_-)_j}\Lambda_R + e^{-i(\beta^{(i)}_+)_j}T_i^{\dagger}\Lambda_L, \tag{20}$$

where

$$T_i = e^{-i\mathcal{K}_i}, \tag{21}$$

$\mathcal{K}_i$ being the quasimomentum operator along direction i, and

$$(\beta^{(i)}_-)_{j,p,q} = \xi^i_{j,p,q} - \tfrac{1}{2}\alpha_{j,p,q}, \tag{22a}$$

$$(\beta^{(i)}_+)_{j,p,q} = \xi^i_{j,p,q} + \tfrac{1}{2}\alpha_{j,p,q}. \tag{22b}$$

When the gauge fields, α_j, ξ^1_j, and ξ^2_j, vanish, the alternate walk is translationally invariant in both time and space every two time steps. We will thus sometimes use the wording "substep" for the time evolutions $2l-1 \to 2l$ and $2l \to 2l+1$, and the wording "step" for $2l-1 \to 2l+1$. We also

introduce the two-substep walk,

$$|\psi_{2l+1}\rangle = U^{2D}_{2l+1}\,|\psi_{2l-1}\rangle\,, \tag{23}$$

where

$$U^{2D}_{2l+1} = U^{(2)}_{2l+1}U^{(1)}_{2l}. \tag{24}$$

B. Continuum limit for the 2D walk

We perform the continuum limit of the two-substep walk. Adapting the 1D-case procedure, we write

$$\alpha_{j,p,q} = \epsilon_A q A^0_{j,p,q}, \tag{25a}$$

$$\xi^i_{j,p,q} = \epsilon_A q A^i_{j,p,q}, \tag{25b}$$

for $i = 1, 2$. Moreover, we choose

$$\theta^1 = \frac{\pi}{2} - \epsilon_m m, \tag{26a}$$

$$\theta^2 = -\frac{\pi}{2} - \epsilon_m m. \tag{26b}$$

Assume now that, for a quantity defined on the space-time lattice, $Q_{j,p,q}$ coincides with the value $Q(t = j\epsilon/2, x = p\epsilon, y = q\epsilon)$ of some continuous function $Q(t, x, y)$. The factor $1/2$ in the time variable is necessary to make the continuum limit of this two-substep DTQW match with the standard form of the Dirac equation. Taking the continuum limit, $\epsilon \to 0$, of Eq. (18), with $\epsilon_A = \epsilon_m = \epsilon$, we obtain

$$(i\gamma^\mu D_\mu - m)\psi = 0\,, \tag{27}$$

with

$$\gamma^0 = \sigma^1, \quad \gamma^1 = -i\sigma^3, \quad \gamma^2 = -i\sigma^2. \tag{28}$$

C. Two-substep U(1) lattice gauge invariance

By construction from 1D gauge-invariant walks, the 2D walk we have introduced, Eq. (18), is invariant under the local phase shift $\psi_{j,p,q} \to \psi'_{j,p,q} = e^{iq\chi_{j,p,q}}\psi_{j,p,q}$, provided the gauge fields become

$$(A'_0)_{j,p,q} = \begin{cases} (A_0)_{j,p,q} - \left(d^1_0\chi\right)_{j,p,q} & \text{for } j \text{ even}, \\ (A_0)_{j,p,q} - \left(d^2_0\chi\right)_{j,p,q} & \text{for } j \text{ odd}, \end{cases} \tag{29a}$$

$$(A'_i)_{j,p,q} = (A_i)_{j,p,q} - (d_i\chi)_{j,p,q}, \tag{29b}$$

for $i = 1, 2$, with

$$d^k_0 = \frac{1}{\epsilon_A}\Delta_0\Sigma_k, \tag{30a}$$

$$d_i = \frac{1}{\epsilon_A}\Delta_i\Sigma_0. \tag{30b}$$

A first comment to make is that this 2D U(1) lattice gauge invariance differs from that of Ref. [8] in the following: we have required, here, the gauge invariance *for each one-dimensional substep*; we thus call this 2D U(1) lattice gauge invariance a two-substep gauge invariance. In such a two-substep gauge invariance, A_0 transforms, by construction, differently at even and odd times: indeed, we have two different difference operators in time, d^1_0 for even times, and d^2_0 for odd times, which manifests the alternate construction of the walk.

Apart from this, the difference operators of Eq. (30) are a straightforward generalization of those used above in the 1D case, Eq. (15). As in the 1D case, the difference operators of Eq. (30) treat space and time on the same footing (up to the two discrete derivatives in time), in constrast with Ref. [8]. Additionally, in the present 2D case, these difference operators also treat the two directions of the lattice on the same footing, which is also in contrast with Ref. [8].

Finally, one can define a lattice counterpart to the electromagnetic tensor, by generalizing the 1D lattice tensor, Eq. (17), to the present 2D setting. Notice that one has to use the discrete temporal derivative d^i_0 in the definition of F_{0i}, so that F_{01} and F_{02} involve *different* discrete temporal derivatives. This 2D lattice tensor has by construction the same properties of antisymmetry and of U(1) lattice gauge invariance as in the 1D case, and contains, additionally, a "lattice magnetic field" orthogonal to the 2D plane, namely, $(F_{12})_{j,p,q}$, for which there is no room in the 1D case.

In Ref. [25], a three-substep U(1) lattice gauge invariance is suggested for a 2D DTQW on an equilateral triangular lattice, which is likely to be generalizable to the other DTQWs presented in this reference (isosceles triangular and honeycomb lattices). There are two main differences between this work and the present one. First, the correspondence between the spatial components of the lattice gauge field and those of the continuum is, in Ref. [25], not one to one: three such components are needed on the lattice—one for each substep—while, the scheme being in 2D space, only two such components are needed in the continuum, which can be expressed as linear combinations of the three former ones; see Eqs. (18) of that reference. In the present work, in contrast, the spatial components of the lattice gauge field match exactly those of the continuum. This difference between Ref. [25] and the present work reflects the connectivity of the lattice, and calls for an understanding, in *arbitrary* nD lattices, $n \in \mathbb{N}$, of the coupling of DTQWs to lattice counterparts of the electric and magnetic fields of the nD continuum. Reference [26] opens the way to such an understanding.

The second main difference between Ref. [25] and the present work is that, in the former, the relative order in which one applies the gauge field and the shift is not coin-state dependent, in contrast with ours. As a consequence, the difference operators appearing in Ref. [25] do not treat time and space on the same footing as we do. More precisely, the temporal difference operator of Ref. [25], see, e.g., the first equation of Eqs. (17) of that reference, is the same as that of the earlier work already mentioned previously, namely, Ref. [8] (see Ref. [27]), and we already mentioned above that, in that earlier work, time and space are not treated on the same footing at the level of the difference operators, in contrast with the present work.

Eventually, notice the two following facts. If one tries to impose to the 2D walk of Ref. [8] a U(1) lattice gauge invariance for each one-dimensional substep, one needs at least to choose, for the corresponding gauge fields, linear combinations of those introduced in that reference—for the no-substep gauge invariance—but at *different* space-time-lattice sites. The same thing happens when trying to impose, conversely, a no-substep U(1) lattice gauge invariance to the present 2D walk.

IV. CONTINUITY EQUATION AND CONSERVED CURRENT FOR THE 2D WALK

In this section, we derive a lattice continuity equation from the dynamics of the DTQW, allowing us to introduce a current density which is both conserved and gauge invariant. In the whole section, we work on the space-time lattice, and use the notations $t = j\epsilon$, $x = p\epsilon$, and $y = q\epsilon$, already introduced previously. By construction, the probability density at time t and point (x, y) is

$$J^0(t, x, y) = \langle\psi_t|\,\Lambda_{x,y}\,|\psi_t\rangle\,, \tag{31}$$

where $\Lambda_{x,y} = |x, y\rangle\langle x, y|$ is the projector on state $|x, y\rangle$.

Now, another distinctive feature of the present work with respect to Ref. [8], apart from the way we gauge our walk, discussed in the previous sections, is that we are going to derive our continuity equation and define the current density over *two* time steps, i.e., 2ϵ, of evolution (23), i.e., four integers steps in the discrete-time variable j, since $t = j\epsilon/2$, while Ref. [8] considers a single time step of this evolution to define the current density. As the reader shall see, this—i.e., considering two time steps to derive the continuity equation, instead of a single one—will lead to the appearance of the standard (symmetric) finite difference as discrete derivatives, both in time and space, while the discrete derivatives of Ref. [8] are more complicated, in particular the temporal one.

So, from this evolution over two time steps, one can easily derive a formula for the difference $J^0(t+\epsilon, x, y) - J^0(t-\epsilon, x, y)$, which can be written as

$$\begin{aligned}&\left[\Delta_0^{\text{sym}} J^0\right](t, x, y)\\ &\quad= \tfrac{1}{2}\langle\psi_t|\left(U^{2\text{D}\,\dagger}_{t+\epsilon}\Lambda_{x,y}U^{2\text{D}}_{t+\epsilon} - U^{2\text{D}}_{t-\epsilon}\Lambda_{x,y}U^{2\text{D}\,\dagger}_{t-\epsilon}\right)|\psi_t\rangle,\end{aligned} \tag{32}$$

where note that we have used the following notation of the Hermitian conjugate for the backwards evolution: $U^{2\text{D}\dagger}_{t-\epsilon} \equiv U^{(1)\dagger}_{t-\epsilon/2}\,U^{(2)\dagger}_{t}$, and where $[\Delta_0^{\text{sym}} f](t, x, y) \equiv \frac{1}{2}[f(t+\epsilon, x, y) - f(t-\epsilon, x, y)]$, which defines a symmetric finite difference in time. We compute this quantity in Appendix A, and the result is given by Eq. (A6). We can then recast Eq. (A6), i.e., Eq. (32), as

$$\Delta_\mu^{\text{sym}} J^\mu = 0, \tag{33}$$

with implicit sum over $\mu = 0, 1, 2$, and where we have introduced the symmetric finite differences in the x and y directions, $[\Delta_1^{\text{sym}} f](t, x, y) \equiv \frac{1}{2}[f(t, x+\epsilon, y) - f(t, x-\epsilon, y)]$ and $[\Delta_2^{\text{sym}} f](t, x, y) \equiv \frac{1}{2}[f(t, x, y+\epsilon) - f(t, x, y-\epsilon)]$. Equation (33) has the form of a continuity equation on the lattice. $J^1 = J^x$ and $J^2 = J^y$, appearing naturally as the current densities along the x and y directions, respectively, are defined by

$$\begin{aligned}J^x(t, x, y) = \langle\psi_t|\,\Lambda_x\big[&e^{i\beta^y_-(t,x,y)}e^{i\beta^y_+(t,x,y-\epsilon)}D_2M_x^{(1)}\\ &+ e^{-i\beta^y_+(t,x,y-\epsilon)}e^{-i\beta^y_-(t,x,y)}D_2^\dagger M_x^{(2)}\\ &+ \Lambda_{y-\epsilon}M_x^{(3)} + \Lambda_{y+\epsilon}M_x^{(4)}\big]\,|\psi_t\rangle\end{aligned} \tag{34}$$

and

$$\begin{aligned}J^y(t, x, y) = \langle\psi_t|\,\Lambda_y\big[&e^{i\beta^x_+(t+\frac{\epsilon}{2},x,y)}e^{i\beta^x_-(t+\frac{\epsilon}{2},x-\epsilon,y)}D_1M_y^{(1)}\\ &+ e^{-i\beta^x_-(t+\frac{\epsilon}{2},x-\epsilon,y)}e^{-i\beta^x_+(t+\frac{\epsilon}{2},x,y)}D_1^\dagger M_y^{(2)}\\ &+ \Lambda_{x+\epsilon}M_y^{(3)} + \Lambda_{x-\epsilon}M_y^{(4)}\big]\,|\psi_t\rangle\,,\end{aligned} \tag{35}$$

where we have used the following notations:

$$\beta^x_\pm = \beta^{(1)}_\pm, \quad \beta^y_\pm = \beta^{(2)}_\pm, \tag{36a}$$

$$S_x = S^{(1)}, \quad S_y = S^{(2)}, \tag{36b}$$

$$C_x = C(\theta^1), \quad C_y = C(\theta^2). \tag{36c}$$

The rest of the notations we have introduced are defined in Appendix A.

Both the time and space differences are symmetric, which implies that they can be used to approximate true derivatives with a truncation error $O(\epsilon^3)$, in contrast with the difference schemes over one time step, as that in Ref. [8], where the error is $O(\epsilon^2)$. There is a price to pay for this at the level of the discrete-space-time scheme: the current is only defined at times t which are even multiples of the time step Δt, while the walk is defined at all times—less importantly, one needs in practice, in order to compute the current dynamics over a given area on a finite-size 2D lattice, more sites on the edges of that area with a two-step current than with a single-step one.

In terms of formal simplicity and connection to standard lattice gauge theories, notable advantages of the present continuity equation, Eq. (33), with respect to that of Ref. [8], is that the difference operators involved in it, i.e., the Δ^{sym}'s, not only (i) treat all three space-time coordinates on the same footing (while *all* three are treated differently in Ref. [8]), but (ii) correspond, in addition, to standard symmetric finite differences, while more complicated operators are used in Ref. [8]. As in Ref. [8], however, the present difference operators intervening in the continuity equation are still different from those intervening in the gauge invariance.

It is easy to check (i) that the current densities defined above are gauge invariant under the transformations of Eq. (29), and (ii) that Eq. (33) ensures the conservation of the total probability, i.e., $\sum_{x,y} J^0(t, x, y)$ does not change with time.

Eventually, we notice the following. On the one hand, one can check that the present 2D DTQW, defined by Eqs. (18), satisfies, in addition to the present two-step lattice continuity equation, a single-step one—obtained by comparing the probability densities between two consecutive instants—which has the same structure as that of Ref. [8], and involves, in particular, the same discrete derivatives—the corresponding current is gauge invariant under the gauge transformations defined in the present work. On the other hand, one can also check that the 2D DTQW defined in Ref. [8] satisfies, in addition to the single-step lattice continuity equation presented in that reference, a two-step one, which has the same structure as that of the present work, and involves, in particular, *also symmetric finite differences as discrete derivatives*—the corresponding current is gauge invariant under the gauge invariance of Ref. [8], which, we recall, is different from the present one. These two combined results indicate that the "symmetrization" of the discrete derivatives when going from single-step to two-step continuity equations is independent from the way one gauges the walk and is solely due to the alternate construction of the 2D walk.

V. CONCLUSION

In this paper we have discussed some of the subtleties related to gauge invariance on discrete-time quantum walks that include the interaction with external, synthetic electromagnetic fields, appearing as additional phases related to those fields. As in standard lattice gauge theories, the way to introduce such interactions is not unique and can lead to interesting new features. We introduce these additional phases in a way that differs from previous works in the literature. We have first described how this definition works for one-dimensional discrete-time quantum walks. This procedure has the advantage that the discrete derivatives which intervene in this lattice gauge invariance treat time and space on the same footing, and are very much like those used in standard LGTs, in contrast with those of Refs. [8,22].

We extended the above dynamics to 2D lattices, by alternating 1D walks in the x and y directions of the spatial lattice, where we ensure the U(1) lattice gauge invariance of this 2D scheme by requiring it *for each one-dimensional substep*, in contrast with the gauge invariance of Ref. [8]. Also, here, time and space are treated on the same footing at the level of the discrete derivatives—up to the fact that there are now, in 2D space, two discrete derivatives in time, one for the even discrete-time coordinates, corresponding to the motion in the, say, x direction, and another one for the odd ones, corresponding to the motion in the y direction.

By taking two time steps of the alternate walk, we introduced a density current which is both conserved and gauge invariant. Both in the 1D and in the 2D cases, we have computed the continuum limit of these DTQWs. They coincide, as desired and as in Refs. [21,22] and [8,22], respectively, with the dynamics of a Dirac fermion in (1+1)D and (1+2)D space-time, respectively, coupled to a U(1), i.e., electromagnetic gauge field. We also showed that, in two dimensions, the current conservation reproduces, in the continuum, that corresponding to the Dirac field. The procedure discussed here could be easily extended to the case of 3D lattices.

In our opinion, this work represents a sensible step on the way to quantum simulating the dynamics of a Dirac particle coupled to an external electromagnetic field. In addition to this, the quantum walk, as a dynamical process taking place on a lattice, introduces by itself interesting phenomena, which are still to be fully explored even in the case of two-dimensional lattices, which is the minimum dimensionality allowing for the description of both an electric and a magnetic field.

Let us finally mention that a recent work [28] presents a unified framework to understand U(1) gauge invariance in discrete-time quantum walks on lattices and with coin spaces of arbitrary dimensions. This work should at the very least enlighten this field.

ACKNOWLEDGMENTS

P.A. acknowledges inspiring discussions with Christopher Cedzich, Terry Farrelly, and Reinhard F. Werner, and is grateful for their one-week hosting in the Quantum Information Group, Institut für Theoretische Physik, Leibniz Universität Hannover, Germany. This work has been funded by No. ANR-12-BS02-007-01 TARMAC grant, the STICAmSud Project No. 16STIC05 FoQCoSS, CSIC No. PIC2017FR6, and the Spanish Ministerio de Economía, Industria y Competitividad, MINECO-FEDER Projects No. FPA2017-84543-P, No. SEV-2014-0398, and Generalitat Valenciana Grant No. GVPROMETEOII2014-087.

APPENDIX A: DERIVATION OF THE CONTINUITY EQUATION

We start from Eq. (32), with the purpose of obtaining the continuity equation, Eq. (33). First, we work out the term

$$\begin{aligned} &U^{2\mathrm{D}}_{t-\epsilon}\Lambda_{x,y}U^{2\mathrm{D}\,\dagger}_{t-\epsilon} \\ &\quad\equiv \left(T_y e^{i\beta^y_-(t,x,y)}M_{R_y}+e^{-i\beta^y_+(t,x,y)}T_y^\dagger M_{L_y}\right) \\ &\qquad\times\left(T_x e^{i\beta^x_-(t-\frac{\epsilon}{2},x,y)}M_{R_x}+e^{-i\beta^x_+(t-\frac{\epsilon}{2},x,y)}T_x^\dagger M_{L_x}\right)\Lambda_{x,y} \\ &\qquad\times\left(e^{-i\beta^x_-(t-\frac{\epsilon}{2},x,y)}T_x^\dagger M^\dagger_{R_x}+T_x e^{i\beta^x_+(t-\frac{\epsilon}{2},x,y)}M^\dagger_{L_x}\right) \\ &\qquad\times\left(e^{-i\beta^y_-(t,x,y)}T_y^\dagger M^\dagger_{R_y}+T_y e^{i\beta^y_+(t,x,y)}M^\dagger_{L_y}\right), \end{aligned} \tag{A1}$$

having used the notations

$$T_x = T_1, \quad T_y = T_2, \tag{A2a}$$

$$M_{s_i} = \Lambda_s C_i, \quad s = R, L, \quad i = x, y. \tag{A2b}$$

After some tedious algebra, we arrive at

$$\begin{aligned} &U^{2\mathrm{D}}_{t-\epsilon}\Lambda_{x,y}U^{2\mathrm{D}\,\dagger}_{t-\epsilon} \\ &\quad= \Lambda_{x+\epsilon,y+\epsilon}M_{R_y}M_{R_x}M^\dagger_{R_x}M^\dagger_{R_y} \\ &\qquad+e^{i\beta^y_-(t,x+\epsilon,y)}e^{i\beta^y_+(t,x+\epsilon,y-\epsilon)}\Lambda_{x+\epsilon}D_2M_x^{(1)} \\ &\qquad+\Lambda_{x-\epsilon,y+\epsilon}M_{R_y}M_{L_x}M^\dagger_{L_x}M^\dagger_{R_y} \\ &\qquad-e^{i\beta^y_-(t,x-\epsilon,y)}e^{i\beta^y_+(t,x-\epsilon,y-\epsilon)}\Lambda_{x-\epsilon}D_2M_x^{(1)} \\ &\qquad+e^{-i\beta^y_+(t,x+\epsilon,y-\epsilon)}e^{-i\beta^y_-(t,x+\epsilon,y)}\Lambda_{x+\epsilon}D_2^\dagger M_x^{(2)} \\ &\qquad+\Lambda_{x+\epsilon,y-\epsilon}M_{L_y}M_{R_x}M^\dagger_{R_x}M^\dagger_{L_y} \\ &\qquad-e^{-i\beta^y_+(t,x-\epsilon,y-\epsilon)}e^{-i\beta^y_-(t,x-\epsilon,y)}\Lambda_{x-\epsilon}D_2^\dagger M_x^{(2)} \\ &\qquad+\Lambda_{x-\epsilon,y-\epsilon}M_{L_y}M_{L_x}M^\dagger_{L_x}M^\dagger_{L_y}. \end{aligned} \tag{A3}$$

Similarly, the Hermitian conjugate is given by

$$\begin{aligned} &U^{2\mathrm{D}\,\dagger}_{t+\epsilon}\Lambda_{x,y}U^{2\mathrm{D}}_{t+\epsilon} \\ &\quad= \Lambda_{x-\epsilon,y-\epsilon}M^\dagger_{R_x}M^\dagger_{R_y}M_{R_y}M_{R_x} \\ &\qquad+e^{-i\beta^x_-(t+\frac{\epsilon}{2},x-\epsilon,y-\epsilon)}e^{-i\beta^x_+(t+\frac{\epsilon}{2},x,y-\epsilon)}D_1^\dagger\Lambda_{y-\epsilon}M_y^{(2)} \\ &\qquad+\Lambda_{x-\epsilon,y+\epsilon}M^\dagger_{R_x}M^\dagger_{L_y}M_{L_y}M_{R_x} \\ &\qquad-e^{-i\beta^x_-(t+\frac{\epsilon}{2},x-\epsilon,y+\epsilon)}e^{-i\beta^x_+(t+\frac{\epsilon}{2},x,y+\epsilon)}D_1^\dagger\Lambda_{y+\epsilon}M_y^{(2)} \\ &\qquad+e^{i\beta^x_+(t+\frac{\epsilon}{2},x,y-\epsilon)}e^{i\beta^x_-(t+\frac{\epsilon}{2},x-\epsilon,y-\epsilon)}D_1\Lambda_{y-\epsilon}M_y^{(1)} \\ &\qquad+\Lambda_{x+\epsilon,y-\epsilon}M^\dagger_{L_x}M^\dagger_{R_y}M_{R_y}M_{L_x} \\ &\qquad-e^{i\beta^x_-(t+\frac{\epsilon}{2},x-\epsilon,y+\epsilon)}e^{i\beta^x_+(t+\frac{\epsilon}{2},x,y+\epsilon)}D_1\Lambda_{y+\epsilon}M_y^{(1)} \\ &\qquad+\Lambda_{x+\epsilon,y+\epsilon}M^\dagger_{L_x}M^\dagger_{L_y}M_{L_y}M_{L_x}. \end{aligned} \tag{A4}$$

In the above equations, we have introduced the projectors $\Lambda_x = |x\rangle\langle x|$, $\Lambda_y = |y\rangle\langle y|$, the operators $D_1 = |x+\epsilon\rangle\langle x-\epsilon|$, $D_2 = |y+\epsilon\rangle\langle y-\epsilon|$, and

$$M_x^{(1)} = M_{R_y} M_{R_x} M_{R_x}^\dagger M_{L_y}^\dagger, \tag{A5a}$$

$$M_x^{(2)} = M_{L_y} M_{R_x} M_{R_x}^\dagger M_{R_y}^\dagger, \tag{A5b}$$

$$M_y^{(1)} = M_{Lx}^\dagger M_{R_y}^\dagger M_{R_y} M_{Rx}, \tag{A5c}$$

$$M_y^{(2)} = M_{R_x}^\dagger M_{R_y}^\dagger M_{R_y} M_{L_x}. \tag{A5d}$$

Performing in Eq. (32) the substraction $U_{t+\epsilon}^{2\mathrm{D}\,\dagger} \Lambda_{x,y} U_{t+\epsilon}^{2\mathrm{D}} - U_{t-\epsilon}^{2\mathrm{D}} \Lambda_{x,y} U_{t-\epsilon}^{2\mathrm{D}\,\dagger}$ with the expressions obtained just above yields

$$\begin{aligned}
2\big[\Delta_0^{\mathrm{sym}} J^0\big](t,x,y) = {} & \Lambda_{x+\epsilon,y+\epsilon} M_\Lambda^{(2)} + \Lambda_{x-\epsilon,y+\epsilon} M_\Lambda^{(4)} + \Lambda_{x+\epsilon,y-\epsilon} M_\Lambda^{(1)} + \Lambda_{x-\epsilon,y-\epsilon} M_\Lambda^{(3)} \\
& + \big(e^{i\beta_+^x(t+\frac{\epsilon}{2},x,y-\epsilon)} e^{i\beta_-^x(t+\frac{\epsilon}{2},x-\epsilon,y-\epsilon)} \Lambda_{y-\epsilon} - e^{i\beta_+^x(t+\frac{\epsilon}{2},x,y+\epsilon)} e^{i\beta_-^x(t+\frac{\epsilon}{2},x-\epsilon,y+\epsilon)} \Lambda_{y+\epsilon}\big) D_1 M_y^{(1)} \\
& + \big(e^{-i\beta_-^x(t+\frac{\epsilon}{2},x-\epsilon,y-\epsilon)} e^{-i\beta_+^x(t+\frac{\epsilon}{2},x,y-\epsilon)} \Lambda_{y-\epsilon} - e^{-i\beta_-^x(t+\frac{\epsilon}{2},x-\epsilon,y+\epsilon)} e^{-i\beta_+^x(t+\frac{\epsilon}{2},x,y+\epsilon)} \Lambda_{y+\epsilon}\big) D_1^\dagger M_y^{(2)} \\
& + \big(e^{i\beta_-^y(t,x-\epsilon,y)} e^{i\beta_+^y(t,x-\epsilon,y-\epsilon)} \Lambda_{x-\epsilon} - e^{i\beta_-^y(t,x+\epsilon,y)} e^{i\beta_+^y(t,x+\epsilon,y-\epsilon)} \Lambda_{x+\epsilon}\big) D_2 M_x^{(1)} \\
& + \big(e^{-i\beta_+^y(t,x-\epsilon,y-\epsilon)} e^{-i\beta_-^y(t,x-\epsilon,y)} \Lambda_{x-\epsilon} - e^{-i\beta_+^y(t,x+\epsilon,y-\epsilon)} e^{-i\beta_-^y(t,x+\epsilon,y)} \Lambda_{x+\epsilon}\big) D_2^\dagger M_x^{(2)},
\end{aligned} \tag{A6}$$

having introduced

$$M_\Lambda^{(1)} = M_{L_x}^\dagger M_{R_y}^\dagger M_{R_y} M_{L_x} - M_{L_y} M_{R_x} M_{R_x}^\dagger M_{L_y}^\dagger, \tag{A7a}$$

$$M_\Lambda^{(2)} = M_{L_x}^\dagger M_{L_y}^\dagger M_{L_y} M_{L_x} - M_{R_y} M_{R_x} M_{R_x}^\dagger M_{R_y}^\dagger, \tag{A7b}$$

$$M_\Lambda^{(3)} = M_{R_x}^\dagger M_{R_y}^\dagger M_{R_y} M_{R_x} - M_{L_y} M_{L_x} M_{L_x}^\dagger M_{L_y}^\dagger, \tag{A7c}$$

$$M_\Lambda^{(4)} = M_{R_x}^\dagger M_{L_y}^\dagger M_{L_y} M_{R_x} - M_{R_y} M_{L_x} M_{L_x}^\dagger M_{R_y}^\dagger. \tag{A7d}$$

Now, one can check that the following relations hold:

$$M_\Lambda^{(1)} = M_y^{(3)} - M_x^{(3)}, \tag{A8a}$$

$$M_\Lambda^{(2)} = -M_y^{(3)} - M_x^{(4)}, \tag{A8b}$$

$$M_\Lambda^{(3)} = M_y^{(4)} + M_x^{(3)}, \tag{A8c}$$

$$M_\Lambda^{(4)} = -M_y^{(4)} + M_x^{(4)}, \tag{A8d}$$

having introduced

$$M_x^{(3)} = \Lambda_L C_y \Lambda_R C_y^\dagger \Lambda_L, \tag{A9a}$$

$$M_x^{(4)} = \Lambda_R C_y \Lambda_R C_y^\dagger \Lambda_R - C_x^\dagger \Lambda_L C_x, \tag{A9b}$$

$$M_y^{(3)} = C_x^\dagger \Lambda_L C_y^\dagger \Lambda_R C_y \Lambda_L C_x, \tag{A9c}$$

$$M_y^{(4)} = C_x^\dagger \Lambda_R C_y^\dagger \Lambda_R C_y \Lambda_R C_x - \Lambda_L, \tag{A9d}$$

so that the above continuity equation, Eq. (A6), can be recast as Eq. (33).

APPENDIX B: CONTINUUM LIMIT OF THE CURRENT

Let us check that the lattice continuity (or current-conservation) equation, Eq. (A6), tends, in the continuum limit, towards the standard continuity equation involving the Dirac current $j^\mu = \bar\psi \gamma^\mu \psi$. Taylor expanding the following quantities at first order in ϵ yields

$$J_0(t+\epsilon,x,y) - J_0(t-\epsilon,x,y) = 2\epsilon \partial_t J_0(t,x,y), \tag{B1a}$$

$$(\Lambda_{x-\epsilon} - \Lambda_{x+\epsilon}) = -2\epsilon \partial_x \Lambda_x, \tag{B1b}$$

$$(\Lambda_{y-\epsilon} - \Lambda_{y+\epsilon}) = -2\epsilon \partial_y \Lambda_y. \tag{B1c}$$

Making use of Eqs. (34) and (35), one arrives at

$$\begin{aligned}
\partial_t J_0(t,x,y) = {} & -\partial_x \langle\psi_t|\Lambda_{xy}\big(M_x^{(1)} + M_x^{(2)} + M_x^{(3)} + M_x^{(4)}\big)|\psi_t\rangle \\
& - \partial_y \langle\psi_t|\Lambda_{xy}\big(M_y^{(1)} + M_y^{(2)} + M_y^{(3)} + M_y^{(4)}\big)|\psi_t\rangle.
\end{aligned} \tag{B2}$$

In our particular case, the coin matrices are, at zeroth order in ϵ, $C_x = \frac{1}{\sqrt{2}}\begin{bmatrix} 1 & i \\ i & 1 \end{bmatrix}$ and $C_y = \frac{1}{\sqrt{2}}\begin{bmatrix} 1 & -i \\ -i & 1 \end{bmatrix}$, so that

$$M_x^{(1)} + M_x^{(2)} + M_x^{(3)} + M_x^{(4)} = \begin{bmatrix} 0 & i \\ -i & 0 \end{bmatrix} = \gamma^0\gamma^1, \tag{B3a}$$

$$M_y^{(1)} + M_y^{(2)} + M_y^{(3)} + M_y^{(4)} = \begin{bmatrix} 1 & 0 \\ 0 & -1 \end{bmatrix} = \gamma^0\gamma^2. \tag{B3b}$$

Finally, the continuum limit of our continuity equation reads

$$\begin{aligned}
\partial_t J_0(t,x,y) = {} & -\partial_x \langle\psi_t|\Lambda_{xy}\gamma^0\gamma^1|\psi_t\rangle \\
& - \partial_y \langle\psi_t|\Lambda_{xy}\gamma^0\gamma^2|\psi_t\rangle.
\end{aligned} \tag{B4}$$

This equation can be recast as $\partial_\mu(\bar\psi\gamma^\mu\psi) = 0$, the expected current-conservation equation.

[1] C. Quigg, *Gauge Theories of the Strong, Weak, and Electromagnetic Interactions*, 2nd ed. (Princeton University Press, Princeton, NJ, 2013).

[2] D. A. Meyer, From quantum cellular automata to quantum lattice gases, J. Stat. Phys. **85**, 551 (1996).

[3] İ. Yalçınkaya and Z. Gedik, Two-dimensional quantum walk under artificial magnetic field, Phys. Rev. A **92**, 042324 (2015).

[4] P. Arnault and F. Debbasch, Landau levels for discrete-time quantum walks in artificial magnetic fields, Physica A **443**, 179 (2016).

[5] T. Kitagawa, Topological phenomena in quantum walks: elementary introduction to the physics of topological phases, Quantum Inf. Process. **11**, 1107 (2012).

[6] T. Kitagawa, M. A. Broome, A. Fedrizzi, M. S. Rudner, E. Berg, I. Kassal, A. Aspuru-Guzik, E. Demler, and A. G. White, Observation of topologically protected bound states in photonic quantum walks, Nat. Commun. **3**, 882 (2012).

[7] A. D. Verga, Edge states in a two-dimensional quantum walk with disorder, Eur. Phys. J. B **90**, 41 (2017).

[8] P. Arnault and F. Debbasch, Quantum walks and discrete gauge theories, Phys. Rev. A **93**, 052301 (2016).

[9] T. Groh, S. Brakhane, W. Alt, D. Meschede, J. K. Asbóth, and A. Alberti, Robustness of topologically protected edge states in quantum walk experiments with neutral atoms, Phys. Rev. A **94**, 013620 (2016).

[10] S. Brakhane, The quantum walk microscope, Ph.D. thesis, Universität Bonn, 2016.

[11] M. Sajid, J. K. Asbóth, D. Meschede, R. F. Werner, and A. Alberti, Creating Floquet Chern insulators with magnetic quantum walks, arXiv:1808.08923.

[12] O. Boada, L. Novo, F. Sciarrino, and Y. Omar, Quantum walks in synthetic gauge fields with three-dimensional integrated photonics, Phys. Rev. A **95**, 013830 (2017).

[13] D. Jaksch and P. Zoller, The cold atom Hubbard toolbox, Ann. Phys. (NY) **315**, 52 (2005).

[14] J. Dalibard, F. Gerbier, G. Juzeliūnas, and P. Öhberg, Artificial gauge potential for neutral atoms, Rev. Mod. Phys. **83**, 1523 (2011).

[15] I. Bloch, J. Dalibard, and S. Nascimbène, Quantum simulations with ultracold quantum gases, Nat. Phys. **8**, 267 (2012).

[16] J. Dalibard, Introduction to the physics of artificial gauge fields, arXiv:1504.05520.

[17] I. Montvay and G. Münster, *Quantum Fields on a Lattice*, Cambridge Monographs on Mathematical Physics (Cambridge University Press, Cambridge, UK, 1994).

[18] G. Münster and M. Walzl, Lattice gauge theory - a short primer, arXiv:hep-lat/0012005.

[19] J. Smit, *Introduction to Quantum Fields on a Lattice*, Cambridge Lecture Notes in Physics (Cambridge University Press, Cambridge, UK, 2002).

[20] K. G. Wilson, Confinement of quarks, Phys. Rev. D **10**, 2445 (1974).

[21] G. Di Molfetta, F. Debbasch, and M. Brachet, Quantum walks in artificial electric and gravitational fields, Physica A **397**, 157 (2014).

[22] P. Arnault, Discrete-time quantum walk and gauge theories, Ph.D. thesis, Université Pierre et Marie Curie, 2017.

[23] P. Arrighi, G. D. Molfetta, and N. Eon, A gauge-invariant reversible cellular automaton, in *Cellular Automata and Discrete Complex Systems* (Springer International Publishing, Cham, 2018), pp. 1–12.

[24] P. Arnault, G. Di Molfetta, M. Brachet, and F. Debbasch, Quantum walks and non-Abelian discrete gauge theory, Phys. Rev. A **94**, 012335 (2016).

[25] G. Jay, J. B. Wang, and F. Debbasch, Dirac quantum walks on triangular and honeycomb lattices, arXiv:1803.01304.

[26] F. Debbasch, Action principles for quantum automata and Lorentz invariance of discrete time quantum walks, arXiv:1806.02313.

[27] This is of course true up to the fact that only one "spatial symmetrization" σ_i, i labeling the direction taken by the walker at each sub time step, appears in Ref. [25], instead of the double one, $\Sigma_2\Sigma_1$, of the earlier reference [8]; see the first equation of Eqs. (9) in that reference. This difference is simply due to the fact that, in the earlier reference, the lattice gauge invariance is not multisubstep.

[28] C. Cedzich, T. Geib, A. H. Werner, and R. F. Werner, Quantum walks in external gauge fields, arXiv:1808.10850.

4 Quantum walks over the honeycomb and triangular lattice

Summary

4.1 Motivation

In the present chapter we present QW-based schemes which do not rely on the regular grid, indeed the QW models that we will describe are defined on the honeycomb and triangular lattices.

There are already DTQWs studies on these type of lattices such a the implementation of the Grover quantum search on the honeycomb lattice [2] and the triangular lattice [1]. As the graphene has a hexagonal structure, QWs-based scheme on the honeycomb can be used to study the possibility of using graphene armchair and zigzag nanoribbons [1] to implement quantum gates [69] and QWs also can be used to explore transport properties in these graphene structures [28]. On the other hand, QWs have been defined over triangular lattices to study topological phases due to their non-trivial topology [73]; however no actual continuum limit is studied in these works, what it will be introduced in Sect.(4.2).

Our motivation is proving that quantum simulation schemes do not depend on the type of lattice, therefore being possible to simulate physical theories in the continuum limit, in our case the Dirac equation, on honeycomb and triangular lattices, Sect.(4.2). Apart from the mathematical interest itself, there are other motivations for this departure from the rectangular lattice to the honeycomb and triangular lattices. As it is mentioned in Sect.(2.1), quantum simulation of

[1] The carrier velocity is determined by the shape of the nanoribbon border.

condensed-matter system dynamics is a hot topic nowadays, e.g. systems driven by the Dirac-like Hamiltonian in the honeycomb graphene [104, 115],

Other important topic is related to topological phases. QWs on triangular and hexagonal lattices would help to study the transport properties of systems which converges to the Dirac equation in the continuum, in lattices with non-trivial topological phases [73].

Before introducing our model, we would like to give an introduction on quantum walks in triangular and honeycomb lattices by reviewing other previous model and their motivations.

4.1.1 Spatial search on hexagonal and triangular lattices

This section is based on the works by G. Abal *et al* [2, 1] in which QWs models are defined on the honeycomb and triangular lattices for the purpose of building quantum algorithms in QW-based schemes, in particular for doing *spatial search*. Spatial search is defined as *the problem of finding a marked location in a rigid structure using local operators*. The most efficient QW-based spatial search algorithm in two-dimensional square lattice has a time complexity of $\mathcal{O}(\sqrt{N \log N})$, proposed by Tulsi [127], which algorithm is based on the work of Ambainis, Kempe and Rivosh (AKR) [6]. The aim of these QWs-based spatial search on different type of lattices is to study whether the time complexity of the search algorithm depends on the number of connection of each node. In both articles they prove that the time complexity remains equal as in the case of the rectangular grid $\mathcal{O}(\sqrt{N \log N})$.

We are not going to enter in the details of the search algorithm because what we would like to do is introducing their DTQWs definitions, in both kind of lattices, in order to compare with our QW proposals.

Quantum walk on the honeycomb lattice Since the hexagonal lattice is not a Bravais lattice, the connection number per node is $d = 3$, and can be divided into two sub-lattices with $N/2$ vertices each, Fig.(4.1). Therefore the vectors a_1 and a_2 connects neighbors of the same sub-lattice whereas the unit vector b moves from one sub-lattice to the other, from the white to the black or vice versa. Hence any arbitrary point can be addressed as $r = n_1 a_1 + n_2 a_2$, taking into account that each point has a reciprocal in the other sub-lattice $r + b$. Thus, we can express a state in the position subspace as $|s, n_1, n_2\rangle$, where $s = 0, 1$ indicates in which sub-lattice the state is.

On the other hand, at every site the walker has three possible direction of motion, for this reason it is encoded in a three dimensional coin space, referred with the index $j = 0, 1, 2$ for each direction.

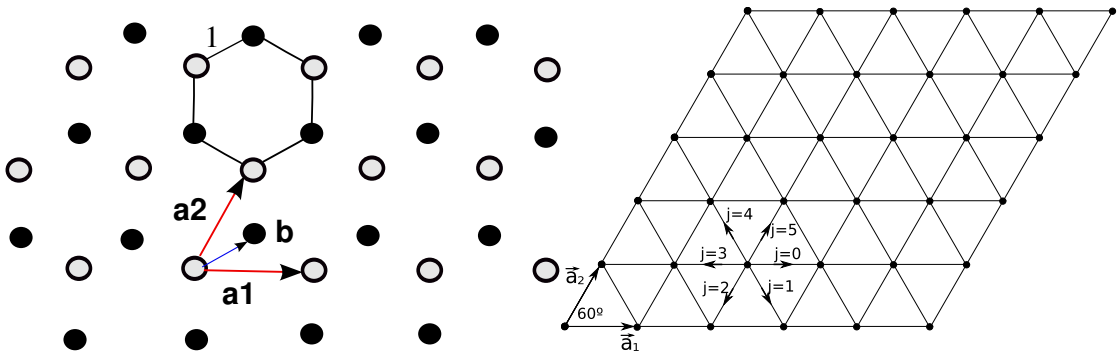

(a) Honeycomb lattice (b) Triangular lattice

Figure 4.1: (a) On the honeycomb lattice there are two sub-sublattices, the white and black sites. a_1 and a_2 are the vectors which connect to the sites living in the same sublattice whereas b is the moves from the white to the black sub-lattice. (b) On the triangular lattice, the walker has six direction of motion which are labeled by j. Images taken from [2, 1]

The entire Hilbert space $\mathcal{H} = \mathcal{H}_C \otimes \mathcal{H}_P$ is spanned by $|j, s; \vec{n}\rangle$ where $\vec{n}$ refers (n_1, n_2). In this basis, the walker $\psi \in \mathcal{H}$ can be written as:

$$\psi = \sum_{j;n_1,n_2} a_{j;n_1,n_2} |j; 0, \vec{n}\rangle + b_{j;n_1,n_2} |j; 1, \vec{n}\rangle . \tag{4.1}$$

Then, the conditional shift operator is defined as:

$$S = \sum_{j,s,\vec{n}} |j, s \oplus 1, \vec{n} - (-1)^s v_j\rangle \langle j, s, \vec{n}| , \tag{4.2}$$

where $\oplus$ refers to the binary sum and $\vec{v}_j$ are the directional vectors:

$$v_0 = (0, 0) \quad v_1 = (1, 0) \quad v_2 = (0, 1). \tag{4.3}$$

According to the propagation rule, the walker change the sub-lattice at every step. The evolution operator reads as:

$$U = S(G_3 \otimes \mathcal{I}_P), \tag{4.4}$$

where $\mathcal{I}_P$ is the identity in $\mathcal{H}_P$ and G_3 is the 3-dimensional standard Grover matrix:

$$G_3 = \frac{1}{3} \begin{pmatrix} -1 & 2 & 2 \\ 2 & -1 & 2 \\ 2 & 2 & -1 \end{pmatrix}, \tag{4.5}$$

coin proposed by [97], which is given for any dimension as $G^d_{ij} = \frac{2}{d} - \delta_{ij}$. The Grover coin is symmetric, treating all d directions equally, and also it is the per-

mutation invariant operator farthest away from the identity operator.

Quantum walk on the triangular lattice G.Abal et al [1] propose another QW-based scheme for doing spatial search, however the use a triangular network, with connection number per node $d = 6$. Since it is obtained the same time complexity scaling of the previous models in different type of lattices, $\mathcal{O}(\sqrt{N \log N})$, they suggest that the time complexity does not depend on the degree of the lattice.

Considering N sites arranged in a triangular network paving a 2D region, an arbitrary point is identified as $r = n_1 a_1 + n_2 a_2$, where a_1 and a_2 are showed in Fig.(4.1). As there are not two kind of sub-lattices this time, it is not necessary to include an extra label s. Therefore, the entire position Hilbert space is spanned by $|n_1, n_2\rangle$. As it is indicated before the connectivity of the lattice is $d = 6$, hence the walker has six possible directions to hop, labeled by $j \in [0, 5]$. These six possible directions are encoded in the coin space $\mathcal{H}_C$.

Then, the entire Hilbert space $\mathcal{H} = \mathcal{H}_C \otimes \mathcal{H}_P$ is 6N- dimensional, a state $|\psi\rangle$ being written as:

$$|\psi\rangle = \sum_{j,\vec{n}} a_{j,\vec{n}} \, |j, \vec{n}\rangle \, , \tag{4.6}$$

where $a_{j,\vec{n}}$ are the complex amplitudes and we define again $\vec{n} = (n_1, n_2)$.

The shift operator acting on the states $|j, \vec{n}\rangle$ is defined as:

$$\begin{aligned}
S\,|0, \vec{n}\rangle &= |3, \vec{n} + (1, 0)\rangle \\
S\,|1, \vec{n}\rangle &= |4, \vec{n} + (1, -1)\rangle \\
S\,|2, \vec{n}\rangle &= |5, \vec{n} + (0, -1)\rangle \\
S\,|3, \vec{n}\rangle &= |0, \vec{n} + (-1, 0)\rangle \\
S\,|4, \vec{n}\rangle &= |1, \vec{n} + (-1, 1)\rangle \\
S\,|5, \vec{n}\rangle &= |2, \vec{n} + (0, 1)\rangle \, ,
\end{aligned} \tag{4.7}$$

whereas the coin operator is the usual Grover coin, which elements are given by $G^d_{ij} = \frac{2}{d} - \delta_{ij}$, for $d = 6$.

4.1.2 Localization on the honeycomb and triangular lattices

We introduce in Sect.(4.1.1) a QW-based scheme over the honeycomb lattice. QWs over honeycomb lattices present some interesting features, such as localization phenomena [88, 89, 65, 88] (see Sect.(2.3)). In contrast, it seems that this phenomenon is not usual in the triangular lattice [78].

In particular, Changyuan Lyu *et al* [88], study in great detail the localization effect on a QW over the honeycomb network, focusing on the Grover walk. They derive analytically the long time limit of the walker's state, depending on the

initial condition. They also introduce other coin operators, and study the sufficient conditions for localization. Based on the average probabilities of finding the particle at the starting position, they conclude that the trapping effect of a honeycomb network is relatively strong. In addition there are previous works that analyzed the localization in quantum walks on hexagonal lattices [89, 65] which are in concordance with the results exhibited in [88].

On the other hand, Kollár *et al* in [78] studied a QW model in the triangular network [2]. They found that, despite of using a Grover's operator, the walker has a rapidly decaying probability to be localized at the origin. Instead of getting localization of the walker around the starting point, they find a subclass of coin operators that transform the quantum walk on the 2D plane to a quantum walk confined along a quasi one-dimensional line.

4.1.3 Topological phases in the triangular lattice

Motivated by a variety of exotic phenomena, from the quantum Hall effect to a new class of materials known as topological insulators, the study of nontrivial topological phases has been increased considerably in the recent years in quantum walks-based schemes [32, 18, 23, 136, 17, 105].

Kitagawa et al [73] introduce the study of topological phases very nicely, classifying the different kind of nontrivial topologies in 1D and 2D QWs, depending on the type of symmetry the system has. To analyze the two-dimensional case, they define a quantum walk on the triangular lattice. Apart from the interest itself in studying topological phases, what it is also noticeable is that the model is quite similar to our honeycomb [3] quantum walk.

In contrast to the previous models , the Hilbert space of the coin $\mathcal{H}_C$ is two dimensional. In our case, the one step operator is defined as:

$$U_{2D}(\theta_1, \theta_2) = T_3 R(\theta_1) T_2 R(\theta_2) T_1 R(\theta_1), \tag{4.8}$$

where $R(\theta)$ is given by:

$$R(\theta) = \begin{pmatrix} \cos(\frac{\theta}{2}) & -\sin(\frac{\theta}{2}) \\ \sin(\frac{\theta}{2}) & \cos(\frac{\theta}{2}) \end{pmatrix} \tag{4.9}$$

and T_i, $i = 1, 2, 3$, are the usual translation operators which shift the spin up (down) in the +(-)v_i direction, Fig.(4.2). The evolution in one time step is equivalent to that generated by an effective Hamiltonian $H(\theta_1, \theta_2)$ over the time step

[2] They define the QW over the triangular network using a three dimensional coin, whereas the QW we have introduced in the previous section (4.1.1), has a six dimensional coin. It could be interesting studying the connection between both models

[3] We define the honeycomb and triangular lattice contrary to the standard definitions in literature. What we call 'honeycomb' lattice is equivalent to a triangular lattice, and our 'triangular' lattice is equivalent to the honeycomb lattice (see explanation in Sect.(4.2))

δt:

$$U(\theta_1, \theta_2) = e^{-iH(\theta_1,\theta_2)t}. \tag{4.10}$$

Since the DTQW is translationally invariant, it is possible to diagonalize the evolution operator $U(\theta_1, \theta_2)$ and the effective Hamiltonian $H(\theta_1, \theta_2)$ in the Fourier basis. Thus the effective Hamiltonian can be written as:

$$H(\theta_1, \theta_2) = \int_{BZ} d^2\mathbf{k} \left(E(\mathbf{k})\vec{n} \cdot \vec{\sigma}\right), \tag{4.11}$$

where $\vec{\sigma} = (\sigma_1, \sigma_2, \sigma_3)$ is the vector of Pauli matrices, BZ refers to the first Brillouin zone for $\tilde{\mathbf{k}} = (k_1, k_2)$, and $E(\vec{k})$ represents by the eigenvalues of $H(\theta_1, \theta_2)$. The unit vector $\vec{n} = (n_x, n_y, n_z)$ defines the quantization axis for the spinor eigenstates at each momentum $\vec{k}$, i.e. the eigenstates of $H(\theta_1, \theta_2)$ are the superposition of spin up and spin down states, hence they can be represented as a point on the Bloch sphere. The vector $\vec{n}$ determines the direction of this point.

The topological phases can be characterized by an integer-valued topological invariant called the Chern number, determined by:

$$C = \frac{1}{4\pi} \int_{BZ} d^2\mathbf{k} \left[\vec{n} \cdot \left(\partial_{k_x}\vec{n} \times \partial_{k_y}\vec{n}\right)\right]. \tag{4.12}$$

The Chern number can be calculated numerically for the full range of angle parameters (θ_1, θ_2), Fig.(4.2). The nontrivial topology of the model can be manifested in the interface between two regions with topologically distinct phases. Introducing an initial condition in this interface, the presence of protected midgap modes is manifested. This gapless modes are bound to the interface, and they are robust against perturbations. Following the example of Kitagawa *et al*, we define two regions in the 2D QW by taking the spin-rotation angles to be site independent. Hence there are two regions with different Chern number, $C = -1$ for $25 \leq y < 75$, and $C = 0$ for the rest, Fig.(4.2). To confirm these edge modes they calculate the quasienergies numerically, Fig.(4.2). Two counter-propagating chiral edge modes appears in the interface between the two regions with different topological phases.

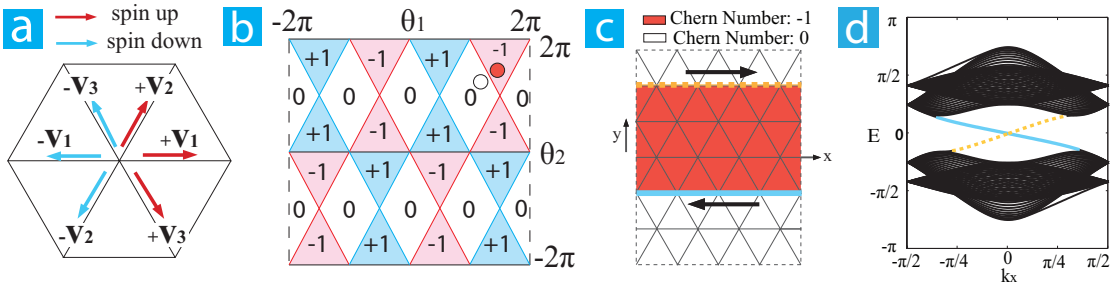

Figure 4.2: (a) Possible directions that the walker can take on the triangular lattice. (b) Chern number for different values of the coin angles θ_1 and θ_2. (c) Two different regions in the 2D QW with different Chern number. In the red region the Chern number is equal to -1 with $\theta_1 = \theta_2 = \frac{3\pi}{2}$, whereas in the white region the Chern number is 0 with $\theta_1 = \theta_2 = \frac{7\pi}{6}$. The arrows refer to the propagation of the edge modes at the boundaries. (d) Quasi-energy spectrum of the 2D QW with the two different regions. Two edge state appears with energies connecting the upper and lower branches. Image taken from [73]

It would be interesting, using our QW proposal over the honeycomb and triangular lattice, Sect.(4.2), to study nontrivial topological systems, e.g. the model proposed by Haldane [63], which is a 2D model on a honeycomb lattice exhibiting the quantum Hall effect without an external magnetic field.

4.1.4 Quantum walks over graphene structures

Graphene has been a focus of interest during the last decades due to its remarkable electronic properties [115, 131, 104, 103, 30, 108]. Since this material has a considerable number of interesting properties, it has been proposed as a physical platform for quantum information processing [53]. Since graphene is arranged on a honeycomb lattice, it is possible to use quantum walks on the hexagonal lattice to study the transport properties of this material [28] or even as a material for implementing experimentally quantum walks [69].

In [69] it is investigated different graphene nanostructures, such a nanoflakes and nanoribbons, to implement universal discrete time quantum walks. They define the quantum walk over a two-dimensional hexagonal lattice, which is quite similar to the case studied in Sect.(4.1.1). However, the main difference between both models is that, in this QW, the coin space is four-dimensional, thus the extra amplitude defined remains stuck on the same site after one time step. Instead of using a specific coin operator, they implement universal quantum gates as coins to drive the quantum walk. These coins can represent a physical action such an external field or a laser pulse on the graphene nanostructure.

On the other hand, in [28] it is defined a QW over the honeycomb lattice, however this work is focused on the transport properties of different graphene struc-

tures. By means of numerical simulations, they demonstrate that the transport for discrete-time quantum walks on graphs corresponding to a different classes of graphene nanostructures is significantly faster than transport on simple graphs like cycles or lines.

Since the behavior on these graphene materials can be related to the massless behavior of electrons at the Dirac points, we believe that our QW scheme over the triangular lattice, Sect.(4.2), can help to understand in a deeper way the transport properties over graphene nanostructures, since our model has the advantage of obtaining the exact Dirac equation in the continuous limit.

4.2 Publication: "Dirac equation as a quantum walk over the honeycomb and triangular lattices"

In this section we introduce a discrete-time quantum walk over the honeycomb and triangular lattices, which admits as the continuum limit the Dirac equation. The aim is showing that these simulations results can be achieved in lattices which are not the rectangular one. This result opens the door for a generalization of the Dirac equation to arbitrary discrete surfaces.

On the other hand, we have seen in the previous sections that these quantum walks models on nonrectangular lattices, such a the honeycomb and the triangular, are subject of interest in different topics. We are going to summarize our quantum walk proposals to easily compare with the previous models.

The first difference is that we call *honeycomb lattice* what the rest of the authors call *triangular lattice*, and the same occurs with the equivalence between our *triangular lattice* and the *honeycomb lattice* of the other previous models. The reason of discrepancy is the site definition of the walker in the lattice. In the honeycomb lattice, our waker is defined on the center of the hexagons, whereas in our triangular QW the amplitudes are defined on the edges of the triangles. This means that our honeycomb QW has a connectivity of degree six, while our triangular QW has a degree three. This is only a difference in the notation with respect to the previous works, however it is important to specify this divergence in naming notation to do not confuse the reader.

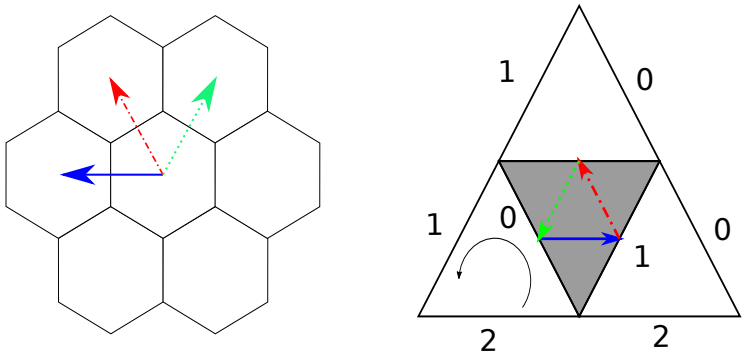

(a) Honeycomb QW (b) Triangular QW

Figure 4.3: (a) The walker moves at every step in one of the three u_i direction. First it moves along u_0 (blue solid line), then u_1 (red dot-dashed) and finally u_2 (green dot line). (b) The walker lives on the shared edge between triangles. The dynamics, after three steps, is similar to the honeycomb QW.

Honeycomb QW We introduce a QW over the honeycomb lattice, Fig.(4.3), defining the walker in the center of every hexagon, as we pointed out before. In contrast with the QW on the triangular lattice defined in Sect.(4.1.1), our coin Hilbert space $\mathcal{H}_C$ is defined to be two dimensional since we require to recover two-dimensional spinors in the continuum limit. Thus our honeycomb QW is given by:

$$|\psi(t+\epsilon)\rangle = (WT_{2,\epsilon}WT_{1,\epsilon}WT_{0,\epsilon})\,|\psi(t)\rangle \tag{4.13}$$

where T_i shifts the $\pm$ components along $\pm u_i$, which are written as:

$$u_i = \cos\left(i\frac{2\pi}{3}\right)u_x + \sin\left(i\frac{2\pi}{3}\right)u_y, \tag{4.14}$$

where u_x and u_y are the unit vectors along the x and y directions. W is the coin operator required to recover the Dirac equation in the limit $\epsilon \to 0$, which details are explained in the following article.

As compared to previous QW models, our definition Eq.(4.13) is quite similar to Eq.(4.8), in which they study the topological properties of the quantum walk in a two dimensional lattice, whereas the coin space changes with respect to [1].

Triangular QW In this case we define the quantum walk over a equilateral triangular lattice, Fig.(4.3). Our two-dimensional spinors lie on the edges shared by two neighboring triangles. We denote them by $\psi(t,v,k) = \begin{pmatrix}\psi^{\uparrow}(t,v,k)\\ \psi^{\downarrow}(t,v,k)\end{pmatrix}$, with v a triangle and k a side. We take the convention that the upper (lower) compo-

nent of the spinor lies on the white (gray) triangle's side.

The dynamics of the triangular QW is the composition of two operators. The first operator is a anticlockwise rotation R at every triangle. For instance, the amplitude components at side k hops to side $(k+1 \bmod 3)$. The second operator is the 2×2 matrix W defined in the honeycomb lattice. This operator acts on the spinor $\psi(t, v, k)$ of every edge shared by two neighboring triangles.

This elegant way to define the quantum walk over the triangular lattice has the advantage of not taking care of two sub-lattices, making the evolution more simple than in previous models.

On the one hand, since we recover the transport of free electrons in the continuous limit, our QW model could add more insight in the study of graphene structures.

On the other hand, a question that arises is whether this QW can be used as a Grover search algorithm. Recently, in [62], it is studied that QW models which recover the Dirac equation in the continuum can behave like a Grover search when there are defects in the lattice. They use the square and the triangular lattice. In the case of using the triangular QW, the contribution of behaving like a Grover walk can be enhanced due to the non-trivial topology of the system, which produces the appearance of an edge state around the defect.

Apart from our discrete-time Dirac quantum walk, another group tackled the same problem [67]. On the one side, our QW is more elegant and simpler to implement than their model, as we only use one coin every step, whereas they use three different coins. On the other side, their work goes further in terms of applications since it includes gauge fields, gauge invariance and numerical simulations.

Dirac equation as a quantum walk over the honeycomb and triangular lattices

Pablo Arrighi[*]
Aix-Marseille Univ, Université de Toulon, CNRS, LIS, Marseille, France and IXXI, Lyon, France

Giuseppe Di Molfetta[†] and Iván Márquez-Martín[‡]
Aix-Marseille Univ, Université de Toulon, CNRS, LIS, Marseille, France
and Departamento de Física Teórica and IFIC, Universidad de Valencia-CSIC, Dr. Moliner 50, 46100-Burjassot, Spain

Armando Pérez[§]
Departamento de Física Teórica and IFIC, Universidad de Valencia-CSIC, Dr. Moliner 50, 46100-Burjassot, Spain

(Received 3 March 2018; published 13 June 2018)

A discrete-time quantum walk (QW) is essentially an operator driving the evolution of a single particle on the lattice, through local unitaries. Some QWs admit a continuum limit, leading to well-known physics partial differential equations, such as the Dirac equation. We show that these simulation results need not rely on the grid: the Dirac equation in $(2+1)$ dimensions can also be simulated, through local unitaries, on the honeycomb or the triangular lattice, both of interest in the study of quantum propagation on the nonrectangular grids, as in graphene-like materials. The latter, in particular, we argue, opens the door for a generalization of the Dirac equation to arbitrary discrete surfaces.

DOI: 10.1103/PhysRevA.97.062111

I. INTRODUCTION

We will describe two discrete-time quantum walks (QWs), one the honeycomb lattice, and the other the triangular lattice, whose continuum limit is the Dirac equation in $(2+1)$ dimensions. Let us put this result in context.

Quantum walks. QWs are dynamics having the following characteristics: (i) the state space is restricted to the one particle sector (also called one "walker"); (ii) space-time is discrete; (iii) the evolution is unitary; (iv) the evolution is homogeneous, that is, translation invariant and time independent; and (v) causal (or "nonsignaling"), meaning that information propagates at a strictly bounded speed. Their study is blossoming, for two parallel reasons.

One reason is that a whole series of novel quantum computing algorithms, for the future quantum computers, have been discovered via QWs, e.g., [1,2], and are better expressed using QWs. The Grover search has also been reformulated in this manner. In these QW-based algorithms, the walker usually explores a graph, which is encoding the instance of the problem. No continuum limit is taken.

The other reason is that a whole series of novel quantum simulation schemes, for the near-future quantum simulation devices, have been discovered via QWs, and are better expressed as QWs [3,4]. Recall that quantum simulation is what motivated Feynman to introduce the concept of quantum computing in the first place [5]. While a universal quantum computer remains out of reach experimentally, more special-purpose quantum simulation devices are seeing the light, whose architecture in fact often resembles that of a QW [6,7]. In these QW-based schemes, the walker propagates on the regular lattice, and a continuum limit is taken to show that this converges toward some well-known physics equation that one wishes to simulate. As an added bonus, QW-based schemes provide: (1) stable numerical schemes, even for classical computers, thereby guaranteeing convergence as soon as they are consistent [8]; and (2) simple discrete toy models of the physical phenomena, which conserve most symmetries (unitarity, homogeneity, causality, sometimes even Lorentz-covariance [9,10], perhaps even general covariance [11,12]), thereby providing playgrounds to discuss foundational questions in physics [13]. It seems that QWs are becoming a new language to express quantum physical phenomena.

While the present work is clearly within the latter trend, technically it borrows from the former. Indeed, the QW-based schemes that we will describe depart from the regular lattice, to go to the honeycomb and triangular grid—which opens the way for QW-based simulation schemes on trivalent graphs.

Motivations. That quantum simulation schemes need not rely on the regular lattice grid is mathematically interesting—but there are numerous other motivations for this departure from the rectangular grid. One is the hot topic of simulating or modeling many quantum condensed-matter system dynamics, driven by the usual high-binding Hamiltonian or by the Dirac-like Hamiltonian, for example, in graphene, and within crystals in general [14]. This work would establish a connection between such physical phenomena and QWs. Another hot topic is related to topological phases. QWs on triangulations should allow us to model all sorts of topologies as simplicial complexes, and hopefully help predict their transport properties

[*]pablo.arrighi@univ-amu.fr
[†]giuseppe.dimolfetta@lis-lab.fr
[‡]ivan.marquez@uv.es
[§]armando.perez@uv.es

2469-9926/2018/97(6)/062111(5)

[15]. The fact that our triangular QW converges to the Dirac equation shows that we have the right prediction at least in the flat case.

Yet another motivation for exploring nonflat geometries is general relativity. In fact, two of the authors have already developed QW models of the curved space-time Dirac equation [11,12,16]. These were on the regular lattice, using a nonhomogeneous coin to code for the space-time-dependent metric. We wonder whether a QW on triangulations can also model the curved space-time Dirac equation, using a homogeneous coin but a space-time-dependent triangulation. This problem is reminiscent of the question of matter propagation in triangulated space-time, as arising, e.g., in loop quantum gravity [17]. Here again, the fact that our triangular QW converges toward the Dirac equation demonstrates that we have the right prediction at least in the triangulation-of-flat-space case. Finally, let us mention the work of two of the authors which models the massive Dirac equation as a Dirac QW on a cylinder [18]. QWs on triangulations should allow us to vary the geometry of this cylinder, so as to model richer fields with just the massless Dirac QW.

Related works. The Grover quantum search algorithm has been expressed as a QW on the honeycomb lattice in [19] (and also in [20] with continuous time). It has also been expressed as a QW on the triangular lattice [21,22]. Again for quantum algorithmic purposes, Ref. [23] studies the possibility to use graphene nanoribbons to implement quantum gates. From the quantum simulation perspective, QWs on triangular lattices have been used to explore transport in graphene structures [24,25], and they have also been used to explore topological phases [15]; but no actual continuum limit is taken in these works. A work that does take a continuum limit of a discrete-time QW while departing from the regular lattice is [26], where a Dirac-like Hamiltonian is recovered. What we show is that the exact Dirac Hamiltonian can be recovered, both in the honeycomb and the triangular lattices. That this can be done is somewhat surprising. Indeed, in [27], the authors conducted a thorough investigation of isotropic QWs of coin dimension 2 over arbitrary Caley graphs Abelian groups, from which it follows that only the square lattice supports the Dirac equation. Our results circumvent this no-go theorem, while keeping things simple, by making use of two-dimensional spinors that lie on the edges shared by adjacent triangles, instead of lying on the triangles themselves. Thus means that, per triangle, there are three thus including an additional degree of freedom associated with these edges.

Plan. To start gently, Sec. II, explains how the Dirac equation in $(2+1)$ dimensions can be simulated by a QW on the regular lattice. In Sec. III, we express the $(2+1)$-dimensional Dirac Hamiltonian in terms of derivatives along arbitrary three $2\pi/3$–rotated axes u_i. We use this expression to simulate the Dirac equation with a QW on the honeycomb lattice. In Sec. IV, we introduce a QW on the triangular lattice, which will turn out to be equivalent to that on the honeycomb lattice. In V we provide a summary and some perspectives.

II. REGULAR LATTICE

In this section, we recall a well-known QW on the regular lattice with axis x, y and spacing ε, which has the Dirac equation in the continuum limit. It arises by operator-splitting [28] the original, one-dimensional Dirac QW [3,4,29].

A possible representation of this equation is (in units such as $\hbar = c = 1$)

$$i\,\partial_t|\psi\rangle = H_D|\psi\rangle, \quad \text{with} \quad H_D = p_x\sigma_x + p_y\sigma_y + m\sigma_z \qquad (1)$$

the Dirac Hamiltonian, σ_i $(i = 1,2,3)$ the Pauli matrices, p_i the momentum operator components, and m the particle mass.

To simulate the above dynamics on the lattice, we define a Hilbert space $\mathcal{H} = \mathcal{H}_l \otimes \mathcal{H}_s$, where $\mathcal{H}_l$ represents the space degrees of freedom and is spanned by the basis states $|x = \varepsilon l_1, y = \varepsilon l_2\rangle$ with $l_1, l_2 \in \mathbb{Z}$, whereas $\mathcal{H}_s = \text{Span}\{|s\rangle / s \in \{-1,1\}\}$ describes the internal (spin) configuration. When acting on $\mathcal{H}_l$, the p_i are called quasimomentum operators (since they no longer satisfy the canonical commutation rules with the position operators). Still, the translation operators are given by $\mathbf{T}(j,\varepsilon) = \exp(-i\varepsilon p_j)$ and verify that

$$\mathbf{T}(1,\varepsilon)|x,y\rangle = |x+\varepsilon, y\rangle, \quad \mathbf{T}(2,\varepsilon)|x,y\rangle = |x, y+\varepsilon\rangle.$$

By analogy with these notations, we introduce the time evolution operator as $\mathbf{T}(0,\varepsilon) = \exp(-i\varepsilon H_D)$. In this way, the time evolution of a state $|\psi(t)\rangle$ is given by

$$|\psi(t+\varepsilon)\rangle = \mathbf{T}(0,\varepsilon)|\psi(t)\rangle = \exp(-i\varepsilon H_D)|\psi(t)\rangle. \qquad (2)$$

After substitution of Eq. (1) into this definition, and making use of the Lie-Trotter product formula (assuming that ε is small) we arrive at

$$\begin{aligned}\mathbf{T}(0,\varepsilon) &\simeq e^{-i\varepsilon m\sigma_z} e^{-i\varepsilon p_x\sigma_x} e^{-i\varepsilon p_y\sigma_y} \\ &= e^{-i\varepsilon m\sigma_z} H e^{-i\varepsilon p_x\sigma_z} H H_1 e^{-i\varepsilon p_y\sigma_z} H_1^\dagger,\end{aligned}$$

since $\sigma_x = H\sigma_z H$ with H the Hadamard gate, and $\sigma_y = H_1\sigma_z H_1^\dagger$ with $H_1 = \frac{1}{\sqrt{2}}\begin{pmatrix} i & 1 \\ -i & 1 \end{pmatrix}$. Using the definition of σ_z, we get

$$\begin{aligned}&\mathbf{T}(0,\varepsilon) \simeq C_\varepsilon H T_{1,\varepsilon} H H_1 T_{2,\varepsilon} H_1^\dagger, \qquad (3)\\ &\text{with} \quad C_\varepsilon = \exp(-i\varepsilon m\sigma_z) \\ &\text{and} \quad T_{j,\varepsilon} = \sum_{s\in\{-1,1\}} |s\rangle\langle s|\mathbf{T}(j,s\varepsilon),\end{aligned}$$

where the $T_{j,\varepsilon}$ matrices are partial shifts. This defines the Dirac QW, which is known to converge toward the Dirac equation in $(2+1)$ dimensions [8].

III. HONEYCOMB LATTICE

We now introduce a QW over the honeycomb lattice (Fig. 1) which we show has the Dirac equation as its continuum limit. The results of this section will also help us in the next section, when we introduce a QW over the triangular lattice. Our starting point is Eq. (2), with H_D as defined in Eq. (1). The basic idea is to rewrite this Hamiltonian using partial derivatives (which will then turn into translations) along the three (u_i) vectors that characterize nearest neighbors in the hexagonal lattice, instead of the u_x and u_y vectors that do so in the regular lattice. The vectors u_i, $i = 0,1,2$ are given by

$$u_i = \cos\left(i\frac{2\pi}{3}\right)u_x + \sin\left(i\frac{2\pi}{3}\right)u_y, \qquad (4)$$

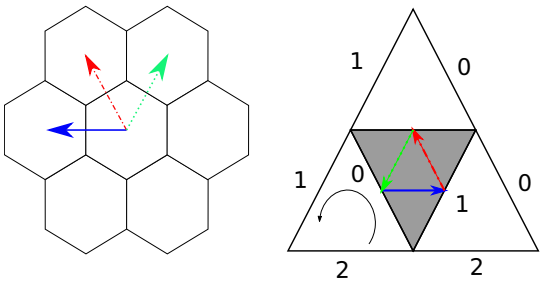

FIG. 1. Left: Honeycomb QW. The particle moves first along the u_0 direction (blue solid line), then u_1 (red dot-dashed line) and finally u_2 (green dot line). Right: Triangular QW. Starting at the edge $k = 0$, the dynamics is equivalent to the honeycomb QW, in three time steps. The circle line represents the counterclockwise rotation operator.

with u_x and u_y the unit vectors along the x and y directions. In terms of momentum operators,

$$\pi_i = \cos\left(i\frac{2\pi}{3}\right)p_x + \sin\left(i\frac{2\pi}{3}\right)p_y.$$

We then look for three 2×2 matrices τ_i satisfying the following conditions:

(C1) Each of them has $\{-1,1\}$ as eigenvalues, i.e., there exists a unitary U_i such that

$$\tau_i = U_i^\dagger \sigma_z U_i.$$

(C2) We impose that $\sum_{i=0}^{2}\tau_i\pi_i = p_x\sigma_x + p_y\sigma_y$, i.e., the Dirac Hamiltonian adopts the form

$$H_D = \sum_{i=0}^{2}\tau_i\pi_i + m\sigma_z.$$

It was surprising to us that these conditions lead to unique (τ_i) matrices, up to a sign:

$$\tau_0 = \frac{2}{3}\sigma_x + \xi\sigma_z,$$
$$\tau_1 = -\frac{1}{3}\sigma_x + \frac{\sqrt{3}}{3}\sigma_y + \xi\sigma_z,$$
$$\tau_2 = -\frac{1}{3}\sigma_x - \frac{\sqrt{3}}{3}\sigma_y + \xi\sigma_z,$$

with $\xi = \pm\frac{\sqrt{5}}{3}$. Let us choose $\xi = \frac{\sqrt{5}}{3}$, and notice that

$$\sum_i \tau_i = \frac{\sqrt{5}}{3}\sigma_z. \tag{5}$$

Thus

$$e^{-i\varepsilon H_D} = e^{-i\varepsilon(\sum_i \tau_i\pi_i + \frac{3}{\sqrt{5}}m\sum_i \tau_i)}.$$

As before, we use the Lie-Trotter product formula and obtain

$$e^{-i\varepsilon(\sum_i \frac{3}{\sqrt{5}}m\tau_i + \tau_i\pi_i)} \simeq \prod_{i=0}^{2} e^{-i\varepsilon\frac{3}{\sqrt{5}}m\tau_i}e^{-i\varepsilon\tau_i\pi_i}. \tag{6}$$

We now make use of condition (C1) to rewrite, for each i,

$$e^{-i\varepsilon\tau_i\pi_i} = e^{-i\varepsilon U_i^\dagger\sigma_z U_i\pi_i} = U_i^\dagger e^{-i\varepsilon\sigma_z\pi_i}U_i = U_i^\dagger T_{i,\varepsilon}U_i,$$

where now the partial shifts $T_{i,\varepsilon}$ are defined through the π_i operators, instead of p_x and p_y. Similarly, for all i,

$$e^{-i\varepsilon\frac{3}{\sqrt{5}}m\tau_i} = U_i^\dagger e^{-i\varepsilon\frac{3}{\sqrt{5}}m\sigma_z}U_i.$$

Let $M = e^{-i\varepsilon\frac{3}{\sqrt{5}}m\sigma_z}$. Wrapping it up, we have obtained a QW over the honeycomb lattice:

$$|\psi(t+\varepsilon)\rangle = \left(\prod_{i=0}^{2} U_i^\dagger M T_{i,\varepsilon}U_i\right)|\psi(t)\rangle, \tag{7}$$

which, by construction, has the Dirac equation (1) as its continuum limit as $\varepsilon\to 0$. By mere associativity the QW rewrites as

$$U_0|\psi(t+\varepsilon)\rangle = \left(\prod_{i=0}^{2} U_{i+1}U_i^\dagger M T_{i,\varepsilon}\right)U_0|\psi(t)\rangle.$$

Thus, if the matrix products $U_{i+1}U_i^\dagger$ could be made independent of i (with $i+1$ understood modulo 3), the QW could be reformulated to have a constant coin operator. Surprisingly, this can be done thanks to a natural choice of the U_i matrices, expressed in terms of well-chosen rotations in the Bloch sphere, understood as the set of possible spin operators. The natural choice for U_0 is $\mathcal{R}_{\sigma_y}(\alpha) = e^{-i\alpha\sigma_y/2}$, the rotation of angle $\alpha = \arccos\frac{\sqrt{5}}{3}$ around σ_y. Indeed $\mathcal{R}_{\sigma_y}(\alpha)$ maps the Bloch vector of τ_0 into the Bloch vector of σ_z:

$$\sigma_z = \mathcal{R}_{\sigma_y}(\alpha)\tau_0\mathcal{R}_{\sigma_y}^\dagger(\alpha). \tag{8}$$

Next, we observe that the Bloch vectors τ_i are related by a rotation of angle $2\pi/3$ around σ_z. For reasons that will become apparent, it matters to us that the cube of this rotation is the identity, which is obviously not the case for $\mathcal{R}_{\sigma_z}(\frac{2\pi}{3}) = e^{-i\pi/3\sigma_z}$, since it represents a spin-1/2 rotation and will acquire a minus sign when applied three times. Hence we take $\mathcal{S} = e^{i\frac{\pi}{3}}\mathcal{R}_{\sigma_z}(\frac{2\pi}{3})$ instead. Then, the natural choices for the matrices U_1 and U_2 are

$$U_1 = U_0\mathcal{S}, \quad U_2 = U_1\mathcal{S}.$$

Indeed, these again fulfill (C1): first the $\mathcal{S}$ unitary brings τ_i to τ_0, and then the U_0 rotation brings τ_0 to σ_z. Now, the fact that the U_i matrices are related by a unitary which cubes to the identity entails that the products $U_{i+1}U_i^\dagger = U_0\mathcal{S}U_0^\dagger$ are independent of i. We introduce

$$W = U_0\mathcal{S}U_0^\dagger M. \tag{9}$$

Then, if we redefine the field up to an encoding, via

$$|\widetilde{\psi}(t)\rangle \equiv U_0|\psi(t)\rangle,$$

Then the honeycomb QW rewrites as just

$$|\widetilde{\psi}(t+\varepsilon)\rangle = (WT_{2,\varepsilon}WT_{1,\varepsilon}WT_{0,\varepsilon})|\widetilde{\psi}(t)\rangle. \tag{10}$$

In other words, the honeycomb QW just shifts the $\pm$ components along $\pm u_0$, applies the fixed $U(2)$ matrix W at each lattice point, shifts the $\pm$ components along $\pm u_1$, applies W again, etc. For certain architectures it could well be that the time homogeneity of the coins makes the scheme easier to

implement experimentally, compared to earlier alternate QWs on the regular lattice [8].

IV. TRIANGULAR LATTICE

Having understood how to obtain the Dirac equation over the honeycomb lattice will make it much easier to tackle the triangular or related lattice such as the kagome lattice [30]. Let us first describe the lattice and its state space. Our triangles are equilateral with sides $k = 0,1,2$, see Fig. 1. Albeit the drawing shows white and gray triangles, these differ only by the way in which they were laid—they have the same orientation, for instance. Our two-dimensional spinors lie on the edges shared by neighboring triangles. We label them $\psi(t,v,k) = \left(\begin{smallmatrix}\psi^{\uparrow}(t,v,k)\\ \psi^{\downarrow}(t,v,k)\end{smallmatrix}\right)$, with v a triangle and k a side. But, since each spinor lies on an edge, we can get to it from two triangles. For instance, if triangle v_0 (white) and v_1 (grey) are glued along their $k = 1$ side, then $\psi(t,v_0,1) = \psi(t,v_1,1)$. In fact let us take the convention that the upper (lower) component of the spinor, namely $\psi^{\uparrow}$ ($\psi^{\downarrow}$), lies on the white (gray) triangle's side. From this perspective each triangle hosts a $\mathbb{C}^3$ vector, e.g., $\psi(t,v_0) = [\psi^{\uparrow}(t,v_0,k)]^T_{k=0\ldots2}$ and $\psi(t,v_1) = [\psi^{\downarrow}(t,v_1,k)]^T_{k=0\ldots2}$.

The dynamics of the triangular QW is the composition of two operators. The first operator, R, simply rotates every triangle anticlockwise. Phrased in terms of the hosted $\mathbb{C}^3$ vectors, the component at side k hops to side $(k+1 \mod 3)$. For instance $R\psi(t,v_0) = [\psi^{\uparrow}(t,v_0,k-1)]_{k=2,0,1}$. The second operator is just the application of the 2×2 unitary matrix W given in Eq. (9), to every two-dimensional spinor of every edge shared by two neighboring triangles. Again we work on pre-encoded spinors

$$\widetilde{\psi}(t,v,k) = U_k\psi(t,v,k), \tag{11}$$

where the U_k are those of Sec. III, but this time the chosen encoding depends on side k. Altogether, the triangular QW dynamics is given by

$$\begin{pmatrix}\widetilde{\psi}^{\uparrow}(t+\varepsilon,v,k)\\ \widetilde{\psi}^{\downarrow}(t+\varepsilon,v,k)\end{pmatrix} = W\begin{pmatrix}\widetilde{\psi}^{\uparrow}(t,v,k-1)\\ \widetilde{\psi}^{\downarrow}(t,e(v,k),k-1)\end{pmatrix}, \tag{12}$$

where $e(v,k)$ is the neighbor of triangle v alongside k.

This triangular QW is actually implementing the honeycomb QW in a covert way. Indeed, whereas the honeycomb QW propagates the walker along the three directions successively, the triangular QW propagates the walker along the three translation simultaneously—depending on the edge at which it currently lies. Thus the walker will start moving along one of the three directions depending on its starting point, then another, etc. For instance, focusing on what happens to spinors on edges $k = 0$, we readily get

$$\begin{pmatrix}\widetilde{\psi}^{\uparrow}(\varepsilon,v,1)\\ \widetilde{\psi}^{\downarrow}(\varepsilon,v,1)\end{pmatrix} = VM\begin{pmatrix}\widetilde{\psi}^{\uparrow}(0,v,0)\\ \widetilde{\psi}^{\downarrow}(0,e(v,2),0)\end{pmatrix},$$

which is equivalent to a translation along u_0 (as is clear from Fig. 1), followed by the action of W. But the result now lies on edges $k = 1$, and will undergo a translation along u_1 followed by the action of W, etc.

As a sanity check we computed the continuum limit obtained by letting $\varepsilon \to 0$ after three iterations of Eq. (12). The 0th order is trivial. The 1st is what defines the dynamics. Let us align the middle of side 1 of triangle v with the origin of the Euclidean space, so that $\psi(0,v,1) = \psi(0,0,0)$ in Cartesian coordinates. Expand the initial condition $\psi(0,x,y)$ as

$$\psi(0,x,y) = \psi(0,0,0) + \varepsilon x\partial_x\psi(0,0,0) + \varepsilon y\partial_y\psi(0,0,0),$$

where x and y are the coordinates in the lattice. As usual we also expand the M inside the W as $\mathbb{I} - 3i\varepsilon m\sigma_z/\sqrt{5}$. After three steps of the triangular QW we obtain (with the help of a computer algebra system)

$$\begin{aligned}\mathbf{T}(0,3\varepsilon)\psi = \psi(0,0) - \frac{\sqrt{3}}{2}\varepsilon(\sigma_x\partial_x + \sigma_y\partial_y)\psi(0,0)\\ - 3i\varepsilon m\sigma_z\psi(0,0) + O(\varepsilon^2).\end{aligned}$$

Using that $\mathbf{T}(0,3\varepsilon) = \psi(0,0) + 3\varepsilon\partial_t\psi(0,0) + O(\varepsilon^2)$, and taking the limit $\varepsilon \to 0$, we arrive at the Dirac equation under the following form:

$$i\partial_t\psi(0,0) = \frac{\sqrt{3}}{6}(p_x\sigma_x + \sigma_y p_y)\psi(0,0) + m\sigma_z\psi(0,0).$$

The factor $\frac{\sqrt{3}}{6}$ comes from two sources: the fact that a continuous limit results from three time steps and the fact that the distance between the middles of the sides of a triangle is $\frac{\sqrt{3}}{2}$. To get rid of this factor, it suffices to rescale the length of the spatial coordinates of the triangles by the same factor, or conversely to rescale time as $t' = \frac{6}{\sqrt{3}}t$.

V. SUMMARY AND PERSPECTIVES

Summary. We constructed a 2×2 unitary W, defined in Eq. (9), which serves as the "coin" for both the honeycomb QW and the triangular QW. On the honeycomb lattice, each hexagon carries a $\mathbb{C}^2$ spin. The honeycomb QW, defined in Eq. (10), simply alternates a partial shift along the u_i direction of Eq. (4), followed by a W on each hexagon, for $i = 0,1,2$. On the triangular lattice, each side of each triangle carries a $\mathbb{C}$, so that each edge shared by two neighboring triangles carries a $\mathbb{C}^2$ spin. The triangular QW, defined in Eq. (12), simply alternates a rotation of each triangle, and the application of W at each edge. The simplicity of these QW-based schemes, compared to those of the regular lattice [Eq. (3)], makes them not only elegant, but also easy to implement. Our main result states that up to a simple, local unitary encoding given by Eq. (11), both the honeycomb QW and the triangular QW admit, as their continuum limit, the Dirac equation in $(2+1)$ dimensions.

Perspectives. Thus we have shown that such quantum simulation results need not rely on the grid. We believe that this constitutes an important step toward modeling propagation in crystalline materials, identifying substrates for QW implementations, studying topological phases, understanding propagation in discretized curved space-time, and coding fields in closed dimensions. In the near future, we wish to run numerical simulations, and to understand what happens when deforming the triangles, and whether similar results can be achieved in $(3+1)$ dimensions.

Note added. We recently became aware that a French-Australian team is tackling the same problem. We agreed to swap papers so that the two works would be independent and yet cite each other. Manuscript [31] is indeed very recommendable, as it goes further in terms of applications: electromagnetic field, gauge invariance, and numerical simulations. Their triangular walk is, however, an alternation of three different steps that use different coins—whereas the present paper just iterates the very same step. This is both mathematically more elegant, and easier to implement. Thus the two works have turned out to be nicely complementary.

ACKNOWLEDGMENTS

We acknowledge an interesting discussion with M. C. Bañuls. This work has been funded by the ANR-12-BS02-007-01 TARMAC grant, the STICAmSud project 16STIC05 FoQCoSS and the Spanish Ministerio de Economía, Industria y Competitividad, MINECO-FEDER Projects No. FPA2017-84543-P and No. SEV-2014-0398 and Generalitat Valenciana Grant No. GVPROMETEOII2014-087, Défi InFinitTI 2018 - Project: Lattice Quantum Simulation Theory (LaQuST) CNRS.

[1] A. Ambainis, A. M. Childs, Ben W. Reichardt, R. Špalek, and S. Zhang, Any and-or formula of size n can be evaluated in time $n^{1/2+o(1)}$ on a quantum computer, SIAM J. Comput. **39**, 2513 (2010).

[2] G. Wang, Efficient quantum algorithms for analyzing large sparse electrical networks, Quantum Inf. Comput. **17**, 987 (2017).

[3] I. Bialynicki-Birula, Weyl, Dirac, and Maxwell equations on a lattice as unitary cellular automata, Phys. Rev. D **49**, 6920 (1994).

[4] D. A. Meyer, From quantum cellular automata to quantum lattice gases, J. Stat. Phys. **85**, 551 (1996).

[5] R. P. Feynman, Simulating physics with computers, Int. J. Theor. Phys. **21**, 467 (1982).

[6] M. Genske, W. Alt, A. Steffen, A. H. Werner, R. F. Werner, D. Meschede, and A. Alberti, Electric Quantum Walks with Individual Atoms, Phys. Rev. Lett. **110**, 190601 (2013).

[7] L. Sansoni, F. Sciarrino, G. Vallone, P. Mataloni, A. Crespi, R. Ramponi, and R. Osellame, Two-Particle Bosonic-Fermionic Quantum Walk Via Integrated Photonics, Phys. Rev. Lett. **108**, 010502 (2012).

[8] P. Arrighi, V. Nesme, and M. Forets, The Dirac equation as a quantum walk: Higher-dimensions, observational convergence, J. Phys. A: Math. Theor. **47** 465302 (2014).

[9] P. Arrighi, S. Facchini, and M. Forets, Discrete Lorentz covariance for quantum walks and quantum cellular automata, New J. Phys. **16**, 093007 (2014).

[10] A. Bisio, G. M. D. Ariano, and P. Perinotti, Quantum walks, Weyl equation and the Lorentz group, Found. Phys. **47**, 1065 (2017).

[11] P. Arrighi, S. Facchini, and M. Forets, Quantum walking in curved spacetime, Quantum Inf. Process. **15**, 3467 (2016).

[12] G. Di Molfetta, M. Brachet, and F. Debbasch, Quantum walks in artificial electric and gravitational fields, Phys. Stat. Mech. Appl. **397**, 157 (2014).

[13] S. Lloyd, A theory of quantum gravity based on quantum computation, arXiv:quant-ph/0501135.

[14] A. H. C. Neto, F. Guinea, N. M. R. Peres, K. S. Novoselov, and A. K. Geim, The electronic properties of graphene, Rev. Mod. Phys. **81**, 109 (2009).

[15] T. Kitagawa, M. S. Rudner, E. Berg, and E. Demler, Exploring topological phases with quantum walks, Phys. Rev. A **82**, 033429 (2010).

[16] P. Arnault and F. Debbasch, Quantum walks and gravitational waves, Ann. Phys. (NY) **383**, 645 (2017).

[17] E. Bianchi, M. Han, C. Rovelli, W. Wieland, E. Magliaro, and C. Perini, Spinfoam fermions, Classical Quant. Grav. **30**, 235023 (2013).

[18] L. A. Bru, G. J. De Valcarcel, G. Di Molfetta, A. Pérez, E. Roldán, and F. Silva, Quantum walk on a cylinder, Phys. Rev. A **94**, 032328 (2016).

[19] G. Abal, R. Donangelo, F. L. Marquezino, and R. Portugal, Spatial search on a honeycomb network, Math. Struct. Comput. Sci. **20**, 999 (2010).

[20] I. Foulger, S. Gnutzmann, and G. Tanner, Quantum walks and quantum search on graphene lattices, Phys. Rev. A **91**, 062323 (2015).

[21] G. Abal, R. Donangelo, M. Forets, and R. Portugal, Spatial quantum search in a triangular network, Math. Struct. Comput. Sci. **22**, 521 (2012).

[22] K. Matsue, O. Ogurisu, and E. Segawa, Quantum walks on simplicial complexes, Quantum Inf. Process. **15**, 1865 (2016).

[23] I. G. Karafyllidis, Quantum walks on graphene nanoribbons using quantum gates as coins, J. Comput. Sci. **11**, 326 (2015).

[24] H. Bougroura, H. Aissaoui, N. Chancellor, and V. Kendon, Quantum-walk transport properties on graphene structures, Phys. Rev. A **94**, 062331 (2016).

[25] C. M. Chandrashekar, Two-component Dirac-like Hamiltonian for generating quantum walk on one-, two-, and three-dimensional lattices, Sci. Rep. **3**, 2829 (2013).

[26] D. Sarkar, N. Paul, K. Bhattacharya, and T. K. Ghosh, An effective Hamiltonian approach to quantum random walk, Pramana **88**, 45 (2017).

[27] G. M. D'Ariano, M. Erba, and P. Perinotti, Isotropic quantum walks on lattices and the Weyl equation, Phys. Rev. A **96**, 062101 (2017).

[28] F. Fillion-Gourdeau, E. Lorin, and A. D. Bandrauk, Numerical solution of the time-dependent Dirac equation in coordinate space without fermion-doubling, Comput. Phys. Commun. **183**, 1403 (2012).

[29] S. Succi and R. Benzi, Lattice boltzmann equation for quantum mechanics, Phys. Nonlinear Phenom. **69**, 327 (1993).

[30] L. Ye, M. Kang, J. Liu, F. von Cube, C. R. Wicker, T. Suzuki, C. Jozwiak, A. Bostwick, E. Rotenberg, D. C. Bell *et al.*, Massive Dirac fermions in a ferromagnetic kagome metal, Nature **555**, 638 (2018).

[31] G. Jay, F. Debbasch, and J. B. Wang, Dirac quantum walks on triangular and honeycomb lattices, arXiv:1803.01304 (2018).

5 Curved space-time Dirac equation in the honeycomb and triangular lattice

Summary

5.1 Motivation

In the previous chapter, we introduced a QW-based model over the honeycomb and triangular lattices. We have proved that it is possible to reproduce the dynamics of the Dirac equation, in the continuous limit, even in the case of a QW defined over a non-rectangular lattice.

On the other hand, we have remarked the possible interest of using honeycomb lattices. For example, graphene materials, which have honeycomb nanostructures,are potential candidates to implement quantum walks, Sect.(4.1.4). In recent years, the interest of simulating the Dirac equation under gauge fields have been increased, including the Dirac equation under gravitational fields. In the field of QW-based models, there are several proposals to study the dynamics of fermions under the effects of a gravitational field [15, 14, 13, 10, 47].

Furthemore, there are also proposals to study the properties of Dirac-like Hamiltonians, under curved spaces (such a the energy spectrum, dynamics, conductivity, etc), using graphene deformed sheets, e.g. graphene in a cylindrical structure [58, 44, 106, 56]. This opens the question to whether the QW model defined over the honeycomb and triangular lattices in Sect.(4.2), could be useful for simulating fermions under gravitational fields.

This chapter is organized as follows: first, we make an introduction to the Dirac equation in a curved space-time. Then, we introduce techniques to introduce a spatial deformation, which can be used to introduce effective metric or curvature in certain systems. Finally, in Sect.(5.5), we introduce an extension of our previous model, Sect.(4.2), which recovers the behavior of fermions under a curved spacetime, in the continuum.

As it will be explained, what it is remarkable in the model introduced in Sect.(5.5), is that we are able to simulate curvature without deforming the lattice. By a concept that we call *duality*, we absorb the possible lattice deformation in a set of space-time dependent unitaries. This could open the possibility of using standard, undeformed, graphene to simulate the dynamics of fermions under gravitational fields, by applying local unitaries.

5.2 The Dirac equation in a curved space time

5.2.1 General covariance

> *Mathematics was not sufficiently refined in 1917 to cleave apart the demands for "no prior geometry" and for a geometric, coordinate-independent formulation of physics. Einstein described both demands by a single phrase, "general covariance." The "no prior geometry" demand actually fathered general relativity, but by doing so anonymously, disguised as "general covariance", it also fathered half a century of confusion*
>
> Gravitation
> John Weeler

The two guiding principles in general relativity are the *principle of equivalence* and the *principle of general covariance*. In the case of the Minkowski spacetime, the equations of motion need to be covariant under Poincaré transformations, however in curved space time, it is not possible to leave the metric unchanged by a general coordinate transformation.

On the other hand, any coordinate systems is only an artifice in theoretical physics that enables us to describe points of spacetime, however they do not play any fundamental role in nature. As there cannot be any preference for a coordinate system, the equations of motion need to be generally covariant, if they are to be derived from an action that remains unchanged under any kind of transformation. This is what we call *general covariancie*.

5.2.2 Affine connection

The equations of motion are expressed entirely in terms of tensors. It is known that the derivatives of a scalar field $\partial_\mu f$ are the component of a one-form field.

However, the derivatives of the components of a vector field $\partial_\mu V^\nu$ are not component of a tensor field. As an example, let us transform the derivative into a new coordinate system, by the transformation $x^{\mu'} = \Lambda^{\mu'}_{\mu} x^\mu$.

Hence:

$$\partial_{\mu'} V^{\mu'} = \Lambda^{\mu}_{\mu'} \partial_\mu \left(\Lambda^{\nu'}_{\nu} V^\nu \right) = \Lambda^{\mu}_{\mu'} \Lambda^{\nu'}_{\nu} \partial_\mu V^\nu + \Lambda^{\mu}_{\mu'} \left(\partial_\mu \Lambda^{\nu'}_{\nu} \right) V^\nu \tag{5.1}$$

The last term spoils the transformation law for a second-rank tensor.

Due to the fact that the partial derivative $\partial\mu$ depends on the coordinate system, it becomes necessary to define a *covariant derivative*, which plays the role of the partial derivative, but being independent of coordinates.

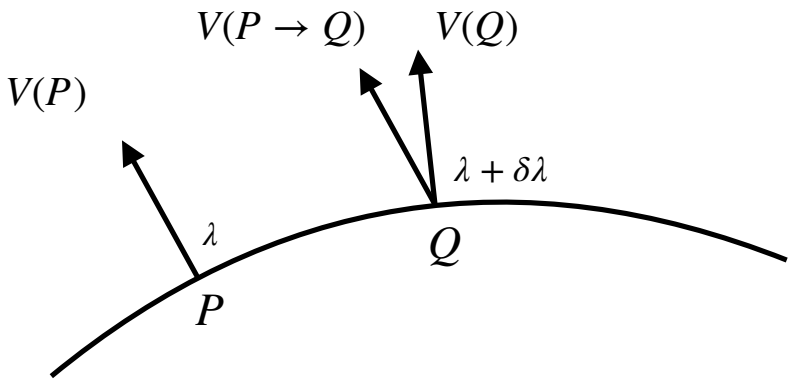

Figure 5.1: $V(Q)$ and $V(O)$ are the vectors at P and Q of the vector field V, on the curve described by the parameter λ. $V(P \to Q)$ is the result of parallel transport of $V(P)$ along the curve.

Let us consider the mathematical definition of the derivative of a vector field component along a curve, Fig.(5.1):

$$\frac{dV^\mu}{d\lambda} = \frac{dx^\mu}{d\lambda} \frac{\partial V^\mu}{\partial x^\mu} = \lim_{\delta\lambda \to 0} \frac{V^\mu(Q) - V^\mu(P)}{\delta\lambda} \tag{5.2}$$

where P and Q are points on the spacetime curve at λ and $\lambda + \delta\lambda$ respectively. In the case of a scalar field, which has unique values at P and Q, the former definition makes sense, however in the case of a vector field, the comparison between $V(Q)$ and $V(P)$ is not, in general, the tangent vector to a curve at a specific point.

In order to define a correct derivative for a vector field, it is necessary to compare two vectors at the same point, for example Q, Fig.(5.1). To do it, we

need the concept of *parallel transport*, which moves the vector $V(P)$ to Q keeping it parallel to the original vector at the spacetime point P. The key ingredient to parallel transport a vector is the so called *affine connection*, Γ:

$$V^\mu(P \to Q) = V^\mu - \delta\lambda \Gamma^\mu_{\nu\sigma}(P) V^\nu(P) \frac{dx^\sigma}{d\lambda} \tag{5.3}$$

where $\Gamma^\mu_{\nu\sigma}$ are the affine connection coefficients. Then, the covariant derivative is defined as:

$$\nabla_\sigma V^\mu = \frac{V^\mu(Q) - V^\mu(P \to Q)}{\delta x^\sigma} = \partial_\sigma V^\mu + \Gamma^\mu_{\nu\sigma} V^\nu, \tag{5.4}$$

Demanding that $\nabla_\sigma V^\mu$ transforms as a tensor, we can deduce the transformation law for the connection coefficients,

$$\nabla_{\sigma'} V^{\mu'} = \Lambda^\sigma_{\sigma'} \Lambda^{\mu'}_\mu \nabla_\sigma V^\mu, \tag{5.5}$$

yielding:

$$\Gamma^{\mu'}_{\nu'\sigma'} = \left(\Lambda^{\mu'}_\mu \Lambda^\nu_{\nu'} \Lambda^\sigma_{\sigma'}\right) \Gamma^\nu_{\nu\sigma} + \Lambda^{\nu'}_\nu \left(\partial_{\sigma'} \Lambda^\nu_{\nu'}\right). \tag{5.6}$$

In spite of Γ being not a tensor, the covariant derivative, acting on any tensor, produces another tensor of one higher covariant rank.

The metric connection If two vectors are parallel transported along a curve, the angle between them should remain constant. This requisite allows us to derive a relation between the metric and the affine connection. Demanding that the angle remains constant is equivalent to say that the scalar product of two arbitrary parallel-transported vectors is constant, and this condition is expressed as:

$$\frac{dx^\sigma}{d\lambda} \nabla_\sigma \left(g_{\mu\nu} U^\mu V^\nu\right) = 0 \tag{5.7}$$

Using the Leibniz rule, as in the case of an ordinary derivative, we arrive to:

$$\nabla_\sigma \left(g_{\mu\nu} U^\mu V^\nu\right) = \left(\nabla_\sigma g_{\mu\nu}\right) U^\mu V^\nu + g_{\mu\nu} \left(\nabla_\sigma U^\mu\right) V^\nu + g_{\mu\nu} U^\mu \left(\nabla_\sigma V^\nu\right). \tag{5.8}$$

Applying $\frac{dx^\sigma}{d\lambda}$ as in Eq.(5.7), the last two terms are zero due to the parallel transport condition, $\frac{dx^\sigma}{d\lambda} \nabla_\sigma U^\mu = 0$. Then we get,

$$\frac{dx^\sigma}{d\lambda} \left(\nabla_\sigma g_{\mu\nu}\right) U^\mu V^\nu = 0, \tag{5.9}$$

hence the covariant derivative of $g_{\mu\nu}$ must be zero:

$$\nabla_\sigma g_{\mu\nu} = g_{\mu\nu,\sigma} - \Gamma^\tau_{\mu\sigma} g_{\tau\nu} - \Gamma^\tau_{\nu\sigma} g_{\mu\tau} = 0. \tag{5.10}$$

Combining the last equation with two additional ones, which are obtained by renaming the indices, the following relation is achieved:

$$g_{\sigma\mu,\nu} + g_{\sigma\nu,\mu} - g_{\mu\nu,\sigma} = \left(\Gamma^{\tau}_{\sigma\nu} - \Gamma^{\tau}_{\nu\sigma}\right) g_{\tau\mu} + \left(\Gamma^{\tau}_{\sigma\mu} - \Gamma^{\tau}_{\mu\sigma}\right) g_{\tau\nu} + \left(\Gamma^{\tau}_{\mu\nu} + \Gamma^{\tau}_{\nu\mu}\right) g_{\tau\sigma}. \quad (5.11)$$

Assuming that the connection is torsion free, then it is symmetric in its lower indices. Finally, multiplying by $g^{\lambda\sigma}$, the connection is determined by the metric tensor as:

$$\Gamma^{\lambda}_{\mu\nu} = \frac{1}{2} g^{\lambda\sigma} \left(g_{\sigma\mu,\nu} + g_{\sigma\nu,\mu} - g_{\mu\nu,\sigma}\right). \quad (5.12)$$

Therefore the former expression connects the affine connection with the metric coefficients. This metric connection is called *Christoffel symbols*.

5.2.3 Spin connection

In order to introduce the covariant derivative for spinor wavefunctions, we start with a system of local inertial Cartesian coordinates. Let us refer to these local coordinates by y^a, using Latin indices to label the local inertial coordinates, where greek indices are used to label the general coordinates.

Therefore, at each point x it is possible to define a collection of four vectors $\{e^a_\mu(x)/a, \mu = 0, ...4\}$, named as the tetrad or *vierbein*, that locally diagonalizes the metric tensor:

$$g_{\mu\nu}(x) = e_\mu{}^a(x) e_\nu{}^b(x) \eta_{ab}, \quad (5.13)$$

where $\eta_{ab} = \text{Diag}(1, -1, -1, -1)$. The tetrad transform as $4-$vectors under Lorentz transformations, therefore there is not only a unique tetrad field that satisfies Eq.(5.13).

The inverse of the vierbein is denoted $e^\mu{}_a$ (interchanged indices), satisfying:

$$e^\mu{}_a(x) e_\nu{}^a = \delta^\mu_\nu \qquad e_\mu{}^a(x) e^\mu{}_b = \delta^a_b \quad (5.14)$$

Making use of Eq.(5.13) and Eq.(5.14), one gets:

$$g_{\mu\nu}(x) e^\mu{}_a(x) e^\nu{}_b(x) = \eta_{ab} \quad (5.15)$$

Hence, the vierbein relates the original coordinates to a local inertial frame. In the local inertial frame, the γ-matrices are referred as $\{\gamma^a, \gamma^b\} = 2\eta_{ab}$. Now, it is possible to define any vector $V^\mu(x)$, in terms of the local coordinate directions as:

$$V^\mu(x) = e^\mu_a(x) V^a(x) \quad \text{and} \quad V^a(x) = e^a_\mu(x) V^\mu(x). \quad (5.16)$$

We can translate Eq.(5.3) in terms of these local inertial directions,

$$V^a(x \to x + dx) = V^a(x) - \omega^a_{b\mu} V^b(x) dx^\nu, \quad (5.17)$$

where $\omega^a_{b\nu}(x)$ are the components of the *spin connection*, which can be written in terms of the affine connections as:

$$\omega^a_{b\nu} = e^a_\mu \partial_\mu (e^\mu_b) + e^a_\mu e^\sigma_b \Gamma^\mu_{\sigma\nu} \tag{5.18}$$

The spin connection allows us to derive the covariant derivative for spinors, which satisfy the parallel transport of the form:

$$\psi(x \to x + dx) = \psi(x) - \Omega_\nu \psi(x) dx^\nu \tag{5.19}$$

where $\Omega_\nu(x)$ is a connection coefficient, described by an $n \times n$ matrix for each ν. For a 4-dimensional spacetime $n = 4$.

In order to determine the coefficients Ω_ν, we demand that the scalar quantity $S(x) = \bar{\psi}(x)\psi(x)$ should be invariant under parallel transport, whereas the vector $V^a(x) = \bar{\psi}(x)\gamma^a\psi(x)$ should be transported according to Eq.(5.17).

Using Eq.(5.19), $S(x)$ transforms as:

$$S(x \to x + dx) = S(x) - \bar{\Psi}(x) \left[\gamma^0 \Omega^\dagger_\nu(x) \gamma^0 + \Omega_\nu(x)\right] \psi(x) dx^\nu, \tag{5.20}$$

in order to be invariant, we find the following relation:

$$\gamma^0 \Omega^\dagger_\nu(x) \gamma^0 = -\Omega_\nu(x) \tag{5.21}$$

On the other hand, $V^a(x)$ transforms as:

$$\begin{aligned} V^a(x \to x + dx) - V^a(x) &= -\bar{\psi}(x) \left[\gamma^a \Omega_\nu + \gamma^0 \Omega^\dagger_\mu \gamma^0 \gamma^a\right] \psi(x) dx^\nu, \\ &= -\bar{\psi}(x) \left[\gamma^a \Omega_\nu - \Omega_\nu \gamma^a\right] \psi(x) dx^\nu, \\ &= -\omega^a_{b\nu} \gamma^b dx^\nu, \end{aligned} \tag{5.22}$$

where we defined the spin connection as:

$$[\gamma^a, \Omega_\nu] = \omega^a_{b\nu} \gamma^b. \tag{5.23}$$

Taking into account that the spin connection is also antisymmetric, $\omega_{ab\nu}(x) = -\omega_{ba\nu}$, one can arrive to:

$$\Omega_\nu(x) = \frac{1}{8} \omega_{ab\nu} \left[\gamma^a, \gamma^b\right] = -\frac{i}{4} \left(e^a_\mu \partial_\mu (e^\mu_b) + e^a_\mu e^\sigma_b \Gamma^\mu_{\sigma\nu}\right) \sigma^{ab} \tag{5.24}$$

where $\sigma^{bc} = \frac{i}{2}\left[\gamma^b, \gamma^c\right]$.

Finally, the covariant version the Dirac equation is written as:

$$\left[i e^\mu_a(x) \gamma^a \nabla_\mu - m\right] \psi(x) = 0, \tag{5.25}$$

where $\nabla_\mu = \partial_\mu + \Omega_\nu(x)$. We can write this equation in a simpler form by defining

$\gamma^\mu = e^\mu_a(x)\gamma^a$. These covariant γ matrices satisfy $\{\gamma^\mu, \gamma^\nu\} = 2g^{\mu\nu}(x)$.

$(2+1)$- dimensions We are interested in the $(2+1)$-dimensional case, since we are working on a 2D lattice. As the space dimension is lower than 3, the γ-matrices become 2×2. Eq.(5.25) can then be significantly simplified . We will include some steps to arrive to the final equation in $(2+1)$, for further details we refer to [107]. Let us consider the following relation:

$$\gamma_a \sigma_{bc} = \frac{1}{2} 2i \left(\eta_{ab}\gamma_c - \eta_{ac}\gamma_b \gamma\right) + \frac{1}{2}(-2i)\epsilon_{abcd}\gamma^d \gamma_5, \tag{5.26}$$

where $\gamma_5 = \gamma_0\gamma_1\gamma_2\gamma_3$ and ϵ_{abcd} is the antisymmetric unit tensor. In this case a, b , c, $d \in \{0, 1, 2\}$, therefore $\epsilon_{abcd} = 0$, leaving the former relation in the form:

$$\gamma^a \sigma_{bc} = \frac{1}{2} 2i \left(\eta^{ab}\gamma^c - \eta^{ac}\gamma^b \gamma\right). \tag{5.27}$$

On the other hand, using the previous relation, we can rewrite $\gamma^a e^\mu{}_a \Omega_\mu$, as:

$$\begin{aligned}\gamma^a e^\mu{}_a \Omega_\mu &= \gamma^a e^\mu{}_a (-\frac{i}{4}\omega_{bc\nu}\sigma^{bc}) = -\frac{i}{4} e^\mu{}_a \omega_{bc\nu}\gamma^a \sigma^{bc} = \frac{i}{4} e^\mu{}_a \omega_{bc\nu}\left(\eta^{ab}\gamma^c - \eta^{ac}\gamma^b\right) \\ &= \frac{1}{4} 2 e^\mu{}_a \omega_{bc\nu}\eta^{ab}\gamma^c = \frac{1}{2} e^\mu{}_a \omega^a_{c\nu}\gamma^c \end{aligned} \tag{5.28}$$

Moreover,

$$e^\mu{}_a \omega^a_{c\mu} = e^\mu{}_a \left(e_\nu{}^a \partial_\mu e^\nu{}_c + e_\nu{}^a e^\sigma{}_c \Gamma^\nu_{\sigma\mu}\right), \tag{5.29}$$

where $e^\mu{}_a e_\nu{}^a = \delta^\mu_\nu$, and we arrive to:

$$\gamma^a e^\mu{}_a \Omega_\mu = \partial_\mu e^\mu{}_c + e^\sigma{}_c \Gamma^\mu_{\sigma\mu}, \tag{5.30}$$

where

$$\Gamma^\mu_{\sigma\mu} = \frac{1}{\sqrt{-g}} \partial_\sigma \sqrt{-g}, \tag{5.31}$$

with g the absolute value of the determinant of the metric.

Finally, making use of the previous relations and some intermediate steps, we arrive to a simplified version of the Dirac equation in $(2+1)$ space-time:

$$i\gamma^a \left[e^\mu_a \partial_\mu + \frac{1}{2\sqrt{g}} \partial_\mu (e^\mu_a \sqrt{g}) - m\right] \psi = 0 \tag{5.32}$$

where, $\mu = t, x, y$ and $a = 0, 1, 2$.

We can express Eq.(5.32) in Hamiltonian form. First, we introduce a local Lorentz transformation in order to arrive to a form of the tetrad such that $e^t_a = 0$ for $a = 1, 2$. Then, we need to introduce the change of wavefunction [107],

given by:

$$\chi = g^{1/4}(e_0^t)^{1/2}\psi, \tag{5.33}$$

After multiplying Eq.(5.32) by $\beta \equiv \gamma^0$, one arrives to:

$$i\partial_t\chi + \frac{i}{2}\{B^s, \partial_s\}\chi - \frac{m}{e_0^t}\beta\chi = 0 \tag{5.34}$$

where $s = 1, 2$ and $B^s = \alpha^a \frac{e_a^s}{e_0^t}$, with the Dirac α-matrices $\alpha^a \equiv \beta\gamma^a$. In this particular example, one can make the choice $\gamma^0 = \sigma_z$, $\gamma^1 = i\sigma_y$ and $\gamma^2 = -i\sigma_x$.

5.3 Continuum Deformation Mechanics

In Sect.(5.5) we introduce the concept of *duality* in a QW, a distortion of the metric via a coordinate transformation on the lattice, that can be transfered into a encoding local unitarities. The local coordinate transformation is motivated by two reasons: i) *The equivalence principle* states that one can introduce a local transformation of coordinates at a given point, which allows to recover the flat spacetime locally at that point. ii) From the theory of finite strain theory in continuous media, it is possible to study some deformed systems that exhibits a modification of the metric tensor. For further study, we recommend Chapter 8 of [87].

Let us consider a local deformation in a material. A point without deformation are denoted by $\vec{X}$, whereas a point in the displaced configuration is labeled as $\vec{x}$. The motion of the body is described by the relation:

$$\vec{x} = \chi(\vec{X}, t). \tag{5.35}$$

Then, we define the *deformation gradient* at $\vec{X}$ as:

$$F_{iI} = \frac{\partial\chi_i}{\partial X_I}, \tag{5.36}$$

where i and I go from 1 to 3. Consider two neighboring points $\vec{X}$ and $\vec{X}' = \vec{X} + \vec{u}$, where $\vec{u}$ is a "small" vector. The displaced positions of $\vec{X}$ and $\vec{X}'$ are given by $\vec{x}$ and $\vec{x}'$, and they can be expressed as:

$$\vec{x}' = \vec{x} + F(\vec{X}, t)\vec{u} + \mathcal{O}(|u|) \quad as \quad |u| \to 0. \tag{5.37}$$

We can compare the distance between $\vec{x}$ and $\vec{x}'$ with respect to the distance

between the rigid points $\vec{X}$ and $\vec{X}'$:

$$|\vec{x}' - \vec{x}| = \sqrt{(\vec{x}' - \vec{x})^T (\vec{x}' - \vec{x})} = \sqrt{\vec{u}^T F^T(\vec{X}, t) F(\vec{X}, t)\vec{u} + \mathcal{O}(|\vec{u}|^2)}$$
$$= \sqrt{\vec{u}^T C(\vec{X}, t)\vec{u}} + \mathcal{O}(|\vec{u}|) \tag{5.38}$$

where the *Cauchy-Green tensor* is defined as $C = F^T(\vec{X}, t)F(\vec{X}, t)$.

This Cauchy-Green tensor C is also known as the *metric tensor*. If the coordinates x_i describe points in the displaced body, they are not necessary Euclidean coordinates. The square of an infinitesimal vector $d\vec{x}$ in the altered body is given by:

$$|d\vec{x}|^2 = C_{IJ} dx_I dx_J \tag{5.39}$$

Hence, C is the metric tensor in the modified body.

However, the *compatibility condition*, i.e. the condition under which a displacement field can be guaranteed, for the Cauchy-Green tensor, states that the *Riemann-Christoffel tensor* or the *curvature tensor* vanishes.

5.4 Crystallographic defects

Defects in crystalline structures have a profound impact on the macroscopic properties of materials. We can distinguish to different types of defects: translational defects, called *dislocations*, and rotation-type or *disclinations*.

In *dislocations* processes a single-atom is removed from the crystal, Fig.(5.2). In *disclinations*, an entire wegde from the crystal is removed, and then the rest of the surface is re-glued, which means that rotational symmetry is violated, Fig.(5.2).

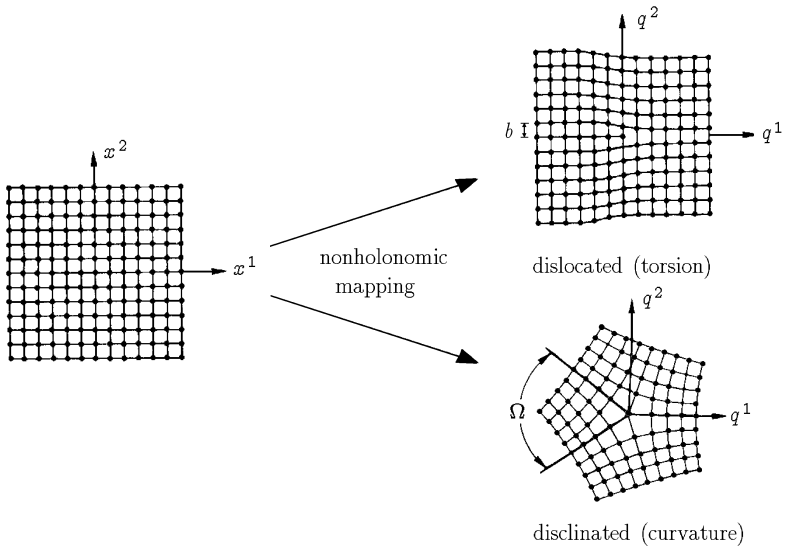

Figure 5.2: Both types of defects on crystals, dislocations and disclinations. The first introduces torsion and the latter introduces curvature. Image taken from [75]

What it is interesting to us is that studying these defects using the affine differential geometry, we can relate the dislocation with the *torsion tensor* of the Riemann-Cartan geometry, whereas the disclinations play the role of the Einstein tensor associated with the *curvature tensor*. For further study, we recommend [80, 75].

Therefore, we believe that it is possible to include these types of defects on DTQWs to study the effects of disclinations and dislocations on the QW dynamics.

On the other hand, studying the impacts of defects in non-rectangular lattices has the advange of having a non-trivial topology, which makes the system itself more interesting to study. A recent work, already mentioned, is [62] in which they include defects on square and triangular DTQWs, in order to perform a Grover walk. In the case of the triangular lattice, the topology of the network can help to find the defect faster, as an edge state is produced around it.

5.5 Publication: "From curved spacetime to spacetime-dependent local unitaries over the honeycomb and triangular Quantum Walks"

In the present article, we make an extension of the DTQW model introduced in Sect.(4.2), in which we proved that the Dirac equation can be obtained in

the continuous spacetime limit, using a non-rectangular lattice. Then, what we introduce is a set of local spacetime dependent unitaries, which allow the DTQW to recover the behavior of electrons under a curved spacetime, in the continuous limit. Based on the *equivalence principle* and the *finite strain theory*, we introduce a local deformation on the lattice that later is encoded into local unitaries. We refer to this equivalence between distorting the lattice and changing the unitaries as *duality*.

We have introduced two methods to distort the lattice, by continuum deformation or introducing defects, it is not clear how to use this transformations, in order to obtain a given metric in the QW dynamics, since analytical calculations are quite difficult

Fortunately, the concept of duality is quite helpful in this situation. What we can do is *imposing* a theoretical deformation in the Dirac equation, in order to have a certain space-time described by the metric tensor $g_{\mu\nu}$. Then, we can transfer the information of this distortion into the local unitaries, that rule the dynamics of the quantum walk. In that manner, we are not changing at all the lattice, whereas the coins will be space-dependent, and they will act on the particle as behaving under a particular given metric $g_{\mu\nu}$.

SCIENTIFIC REPORTS
nature research

OPEN

From curved spacetime to spacetime-dependent local unitaries over the honeycomb and triangular Quantum Walks

Received: 7 February 2019
Accepted: 15 July 2019
Published online: 29 July 2019

Pablo Arrighi[1], Giuseppe Di Molfetta[2], Ivan Marquez-Martin[2] & Armando Perez[3]

A discrete-time Quantum Walk (QW) is an operator driving the evolution of a single particle on the lattice, through local unitaries. In a previous paper, we showed that QWs over the honeycomb and triangular lattices can be used to simulate the Dirac equation. We apply a spacetime coordinate transformation upon the lattice of this QW, and show that it is equivalent to introducing spacetime-dependent local unitaries —whilst keeping the lattice fixed. By exploiting this duality between changes in geometry, and changes in local unitaries, we show that the spacetime-dependent QW simulates the Dirac equation in (2 + 1)–dimensional curved spacetime. Interestingly, the duality crucially relies on the non linear-independence of the three preferred directions of the honeycomb and triangular lattices: The same construction would fail for the square lattice. At the practical level, this result opens the possibility to simulate field theories on curved manifolds, via the quantum walk on different kinds of lattices.

Quantum walks. QWs are quantum dynamical systems characterized by: *(i)* a state space which is restricted to the one-particle sector (i.e. to a single 'walker'); *(ii)* a discrete spacetime; *(iii)* the unitarity of its evolution; *(iv)* the homogeneity of its evolution, meaning its translation-invariance and time-independence, and *(v)* its causality (i.e. it is 'non-signalling'), meaning that information has a bounded speed of propagation. QWs are blossoming, for two good reasons.

The first is that a number of novel Quantum Computation algorithms, to be run on Quantum Computers, were discovered via QWs[1,2], or were elegantly expressed using QWs (the Grover search for instance). Typically in these quantum algorithms, the QW explores a graph, whose shape encodes the instance of the problem. No continuous spacetime limit is taken in these works.

The second is that a number of novel Quantum Simulation schemes, to be run on quantum simulation devices, were first expressed as QWs[3,4], which seems to be the natural language for doing so. Quantum simulation was Feynman's initial motivation to invent Quantum Computing[5]. Whilst full-blown Quantum Computers remain out-of-reach at the experimental level, a number of special-purpose Quantum Simulation devices are appearing, whose architecture is often directly inspired by QWs[6,7]. In QW-based quantum simulation schemes, the quantum walker propagates on a grid, and a spacetime continuum limit towards some well-known target physics equation is taken. These schemes provide: a/ numerical schemes that are stable even for classical computers— from which one can derive convergence[8]; b/simple toy models of the target physical phenomena, with most symmetries conserved (homogeneity, causality, unitarity… sometimes even Lorentz-covariance[9,10].

The present work falls within the second class. However it borrows from the first. Indeed, we describe depart from the square lattice, to go to the honeycomb and triangular lattice— which can be seen as trivalent graphs.

Rationale. A motivation for this work is the possibility to describe and implement the quantum simulation of certain physical systems, without the need to rely on the square lattice architecture. Rather, one would like to phrase a quantum simulation scheme in terms of naturally occurring lattices in well-controlled substrates.

[1]Aix-Marseille Univ, Université de Toulon, CNRS, LIS, Marseille, France and IXXI, Lyon, France. [2]Aix-Marseille Univ, Université de Toulon, CNRS, LIS, Marseille, France and Departamento de Física Teórica and IFIC, Universidad de Valencia-CSIC, Dr. Moliner 50, 46100, Burjassot, Spain. [3]Departamento de Física Teórica and IFIC, Universidad de Valencia-CSIC, Dr. Moliner 50, 46100, Burjassot, Spain. Correspondence and requests for materials should be addressed to P.A. (email: pablo.arrighi@univ-amu.fr) or G.D.M. (email: giuseppe.dimolfetta@lis-lab.fr) or I.M.-M. (email: ivan.marquez@uv.es) or A.P. (email: armando.perez@uv.es)

Examples of this class are the simulation of condensed matter systems modeled by a tight-binding Hamiltonian, such as graphene[11] or the Kagome lattices[12]— where the dynamics of electrons can be effectively recast as a Dirac-like equation. In fact the QW introduced in this paper may be useful as a simple point of departure to predict electronic transport properties in the graphene like-materials[13] and exploring how varying their geometry may influence the dispersion relations, and lead to topological phases[14], with interesting consequences on the conducting properties.

Another motivation for this work is to understand how fermions would propagate if spacetime were a triangulated manifold, at the fundamental level. Indeed, triangulated manifolds are being used to describe curved spacetime since[15]– when Regge introduced his simplicial, discrete formulation of General Relativity. This discrete formulation then motivated a number of quantum gravity theories, such as Loop Quantum Gravity[16] and Causal Dynamical Triangulation[17]— which seek to recover Regge calculus in the classical limit. Most often quantum gravity research focuses on the core issue of the quantum dynamics of discrete spacetime itself— overlooking the question of how matter would propagate within the discrete spacetime structure it prescribes. The present ideas may help address the question.

Duality. In a previous work, we showed how a QW can be defined on the honeycomb and the triangular lattice[18] (see also[19]), whose continuous spacetime limit is the Dirac equation in $(2+1)$– dimensional spacetime. Here, we extend these definitions to allow for spacetime dependent local unitaries, and introduce a dynamics that, in the continuum limit, corresponds to the Dirac equation in a curved $(2+1)$– dimensional spacetime.

The construction, we feel, is interesting. Indeed, given a lattice made of equilateral triangles, we begin by distorting the metric just via a coordinate transformation, following the initial step of the derivation of the Dirac equation in ordinary curved spacetime. But then we realize that the coordinate transformation can be absorbed by a suitable choice of the three gamma matrices that are associated to the three directions provided by the triangles— a possibility offered by the fact that these three directions are, of course, linearly-dependent in the plane. Recall that the role of the gamma matrices is to prescribe a basis of the spin, in which spin up goes one way, and spin down goes the opposite way. In the QW, the local unitaries implement precisely the corresponding changes of base. Thus, the gamma matrices determine the local unitaries in the QW. This, therefore, unravels an equivalence, in the continuum limit, between changing the actual geometry of the lattice, or keeping it fixed but changing the local unitaries in a suitable manner. The final step is to allow the local unitaries to be spacetime dependent and take the continuum limit, thereby recovering the Dirac equation in curved spacetime.

Notice that having three directions in two-dimensional space, as in the honeycomb or triangular lattices, is what provides that extra degree of freedom allowing for the transfer of the geometric distortions into the local unitaries— the square lattice is too rigid in this respect.

Related works. It is already well known that QW can simulate the Dirac equation[3,4,8,20–23], the Klein-Gordon equation[24–26] and the Schrödinger equation[27,28] and that they are a minimal setting in which to simulate particles in some inhomogeneous background field[29–33], with the difficult topic of interactions initiated in[34,35]. Eventually, the systematic study of the impact inhomogeneous local unitaries also gave rise to QW models of particles propagating in curved spacetime. This line of research was initiated by a QW simulations of the curved Dirac equation in $(1+1)$–dimensions, for synchronous coordinates[30,36], and later extended by[37] to any spacetime metrics, and generalized to further spatial and spin dimensions in[38,39]. A related work, from a slightly different perspective, can be found in[40]. All of these models were on the square lattice: to the best our knowledge no one had modeled fermionic transport over non-square lattices. The present paper shows that over the honeycomb and triangular lattices the problem becomes considerably simpler, and the solution elegant.

In a recent work[41], quantum transport over curved spacetime has been compared to electronic transport in deformed graphene, where a pseudo-magnetic field emulates an effective curvature in the tight-binding Hamiltonian (see also[42]). Back to the quantum computing side, the Grover search has been expressed as a QW over the honeycomb lattice[43] (see also[44] for continuous time approach). Reference[45] evaluates the use graphene nanoribbons as a substrate to build quantum gates.

Plan. The paper is organized as follows. First, we remind the reader of the basic concepts and notations surrounding the Dirac equation in a curved spacetime, in $(3+1)$ and $(2+1)$– dimensions. In Methods we revisit our earlier Dirac QW on a honeycomb and on a triangular lattice, and why it worked. Also we show how a simple, homogeneous coordinate transformation impacts the continuum limit of the Dirac QW. In the end of this section, it is shown the duality, i.e. how the coordinate transformation can be absorbed into a choice of local unitaries. Finally, we present the main results: a QW that reproduces the Dirac equation with curvature in the continuum limit, both for the honeycomb and for the triangular lattices. We use $\hbar = c = 1$ units.

Dirac Equation in Curved Spacetime: a Recap

In this Section we recall the basic properties of the Dirac equation in curved spacetime. We refer the reader to[46–48] for a review. We start by describing the case of a $(3+1)$– dimensional spacetime with coordinates x^μ, $\mu=0, \ldots 4$, where x^0 is the time coordinate, and metric tensor $g_{\mu\nu}(x)$ in these coordinates. At each point x, it is possible to introduce a set of four vectors $\{e_\mu{}^a(x)/a,\ \mu = 0,\ \ldots 4\}$, referred to as the tetrad or vierbein, that locally diagonalizes the metric tensor i.e.,

$$g_{\mu\nu}(x) = e_\mu{}^a(x) e_\nu{}^b(x) \eta_{ab}. \tag{1}$$

(here and thereafter, summation over repeated indices is assumed), where $\eta_{ab} = \mathrm{Diag}(1, -1, -1, -1)$. Notice that, given a vierbein, one can obtain a new one, which would also satisfy Eq. (1), by performing an arbitrary Lorentz transformation. The inverse of the vierbein is denoted $e^{\mu}{}_{a}$ (interchanged indices), satisfying

$$e^{\mu}{}_{a}(x)e_{\nu}{}^{a}(x) = \delta^{\mu}_{\nu}, \quad e_{\mu}{}^{a}(x)e^{\mu}{}_{b}(x) = \delta^{a}_{b}. \tag{2}$$

Using (1) and (2), one has

$$g_{\mu\nu}(x)e^{\mu}{}_{a}(x)\, e^{\nu}{}_{b}(x) = \eta_{ab}. \tag{3}$$

Thus, tetrads can be understood as normalized tangent vectors that relate the original coordinates to a local inertial frame. We use the common convention that inertial coordinates are designated by latin indices, and original coordinates by greek indices. Latin indices are lowered and raised by η_{ab}, greek indices by $g_{\mu\nu}$. In the local inertial frame, one is legitimated to use the Dirac γ– matrices, i.e. matrices satisfying the Clifford algebra $\{\gamma^{a}, \gamma^{b}\} = 2\eta^{ab}\mathbb{I}$. From these, one defines $\sigma^{ab} = \frac{i}{2}[\gamma^{a}, \gamma^{b}]$.

Given a Dirac field $\psi(x)$, the action of a local Lorentz transformation $\Lambda^{a}{}_{b}(x)$ can be written as

$$\psi \to U_{\Lambda}\psi, \tag{4}$$

where

$$U_{\Lambda}(x) = e^{-\frac{i}{4}\theta_{ab}(x)\sigma^{ab}}, \tag{5}$$

and $\theta_{ab}(x)$ are the parameters of the transformation, defined by $\Lambda^{a}{}_{b}(x) = \delta^{a}_{b} + \theta^{a}{}_{b}(x)$. One can prove that this operator acts on Dirac gamma matrices as follows:

$$U_{\Lambda}{}^{-1}\gamma^{a}U_{\Lambda} = \Lambda^{a}{}_{b}\gamma^{b}. \tag{6}$$

With the above notations, the Dirac equation in curved space

$$i\gamma^{a}e^{\mu}{}_{a}(x)\mathcal{D}_{\mu}\,\psi - m\,\psi = 0, \tag{7}$$

where m is the particle mass, is invariant under a local Lorentz transformation provided the generalized derivative that we use is

$$\mathcal{D}_{\mu} = \partial_{\mu} + \Gamma_{\mu}, \tag{8}$$

where Γ_{μ} transforms according to

$$\Gamma_{\nu} \to \Gamma'_{\nu} = U_{\Lambda}\Gamma_{\nu}U_{\Lambda}^{-1} - \partial_{\nu}(U_{\Lambda})U_{\Lambda}^{-1}. \tag{9}$$

The correction Γ_{μ} to the derivative can then be obtained as[47]

$$\Gamma_{\mu}(x) = -\frac{i}{4}\omega_{ab\mu}(x)\sigma^{ab}, \tag{10}$$

where $\omega_{ab\mu}(x)$ is the so-called spin connection, and can be expressed in terms of the tetrads and the affine connection as

$$\omega^{a}{}_{b\nu} = e_{\mu}{}^{a}\partial_{\nu}e^{\mu}{}_{b} + e_{\mu}{}^{a}e^{\sigma}{}_{b}\Gamma^{\mu}_{\sigma\nu}. \tag{11}$$

From Eq. (7) one can define a four-vector current

$$j^{\mu} = \sqrt{g}e^{\mu}{}_{a}\overline{\psi}\gamma^{a}\psi, \tag{12}$$

where g is the (absolute value of) the determinant of the metric, so that it is conserved:

$$\partial_{\mu}j^{\mu} = 0. \tag{13}$$

This justifies the normalization condition

$$\int j^{0}\,dv = \int \sqrt{g}e^{0}{}_{0}\psi^{\dagger}\psi dv = 1, \tag{14}$$

with dv the volume element in space.

$(2+1)$– *dimensions*. When the space dimension is lower than 3, the γ–matrices become 2×2. Then, the Dirac Eq. (7) can be simplified to give

$$i\gamma^{a}\left[e^{\mu}{}_{a}\partial_{\mu}\psi + \frac{1}{2\sqrt{g}}\partial_{\mu}(e^{\mu}{}_{a}\sqrt{g})\psi\right] - m\psi = 0. \tag{15}$$

We will now express this equation in Hamiltonian form. We name the greek indices $\mu = t, x, y$, and the latin indices $a = 0, 1, 2$. By performing a local Lorentz transformation, it is possible to arrive to a form of the tetrad such that $e^t{}_a = 0$ for $a = 1, 2$. Then, by introducing the change of wavefunction given by[49]:

$$\chi = g^{1/4}(e^t{}_0)^{1/2}\psi \tag{16}$$

and multiplying Eq. (15) by $\beta \equiv \gamma^0$, one gets

$$i\partial_t\chi + \frac{i}{2}\{B^s, \partial_s\}\chi - \frac{m}{e^t{}_0}\beta\chi = 0, \tag{17}$$

where $s = 1, 2$, and we have introduced the notation $B^s = \alpha^a \frac{e^s{}_a}{e^t{}_0}$, with the usual Dirac α–matrices $\alpha^a \equiv \beta\gamma^a$. In particular, one can make the choice $\gamma^0 = \sigma^z$, $\gamma^1 = i\sigma^y$ and $\gamma^2 = -i\sigma^x$. Then α^0 becomes the identity matrix, $\alpha^1 = \sigma^x$ and $\alpha^2 = \sigma^y$, with σ^i $(i = 1, 2, 3)$ the Pauli matrices.

According to Eqs (14) and (16), the normalization condition becomes simply

$$\int \chi^\dagger \chi dv = 1. \tag{18}$$

Methods

Dirac QW. A possible representation of the Dirac equation in flat spacetime is obtained from Eq. (17) by using the canonical tetrads $e^\mu{}_a = \delta^\mu_a$ and the choice of Dirac α–matrices made at the end of the last section:

$$i\partial_t\psi(t) = H_D\psi(t) \quad \text{with} \quad H_D = p_x\sigma^x + p_y\sigma^y + m\sigma^z. \tag{19}$$

where p_i is the i^{th} component of the momentum operator.

It is now very well-known that one can define a QW on the lattice that converges, in the limit of both the lattice spacing and the time step going to zero, towards the solutions of (19). This is done by defining a Hilbert space $\mathcal{H} = \mathcal{H}_x \otimes \mathcal{H}_y \otimes \mathcal{H}_c$, where $\mathcal{H}_x \otimes \mathcal{H}_y$ stands for the space degrees of freedom, as spanned by the basis states $x = \varepsilon j$, $y = \varepsilon k$ with $j, k \in \mathbb{Z}$, whereas $\mathcal{H}_c = \text{Span}\{|c\rangle / c \in \{-1, 1\}\}$ describes the internal 'coin' (spin) degree of freedom. Over $\mathcal{H}_x \otimes \mathcal{H}_y$, the p_i will now denote the quasimomentum operators defined by

$$\begin{aligned} \exp(-i\varepsilon p_x)|x, y\rangle &= |x + \varepsilon, y\rangle \\ \exp(-i\varepsilon p_y)|x, y\rangle &= |x, y + \varepsilon\rangle. \end{aligned} \tag{20}$$

The Dirac QW will evolve a state $\psi(t)$ into

$$\begin{aligned} \psi(t + \varepsilon) &= \exp(-im\varepsilon\sigma^z)\exp(-i\varepsilon p_x\sigma^x)\exp(-i\varepsilon p_y\sigma^y) \\ &\approx \exp(-i\varepsilon H_D)\psi(t) \end{aligned} \tag{21}$$

using the Trotter-Kato formula. It follows that one recovers the Dirac Eq. (19) in the continuum limit when ε goes to zero, where the p_i become the true momentum operators $p_i = -i\partial_i$.

Recently[18] we showed that Dirac dynamics can be implemented by a QW, not only over square lattices, but also over the honeycomb and triangular lattices (see also[19]). The honeycomb lattice QW is easier to introduce. It defines three directions u_i, $i = 0, 1, 2$ having relative angles of 120°, let u_i^j denote their coordinates. The idea is to introduce three unitary 2×2–matrices τ^i with eigenvalues ± 1 such that H_D can be written as

$$H_D = \pi_i\tau^i + m\sigma^z, \tag{22}$$

where $\pi_i \equiv u_i^j p_j$ represents the quasimomentum operator along the u_i direction. Then, the corresponding QW can again be defined by a Lie-Trotter expansion of Eq. (21), with H_D defined in (22). The triangular lattice QW makes use of a similar setup, although the translations are generated by rotations of the triangles themselves, bringing apart the internal components of the field ψ, which is assumed to 'live' in the edges of the triangles, one component ($\psi^\uparrow$ or $\psi^\downarrow$) on each side.

Coordinate transformation on the dirac equation. The construction of the Dirac equation in curved spacetime relies on the equivalence principle, which means that one can introduce a local transformation of coordinates at a given point, so that one recovers the flat equation in the neighborhood of that point. The curved Dirac equation is then that which stems from applying reverse the local transformation, upon the flat Dirac equation. Our line of thought follows that step, i.e., starting from the flat case Dirac QW, perform an arbitrary change of coordinates so as to obtain the curved Dirac QW. Let us begin with just an homogeneous change of coordinates on the Dirac equation.

First notice that Eq. (3) can be writen as $e^T g e = \eta$, where e and g are just the representation of the tetrads and metric in matricial form, and ^{T} denotes the matrix transpose. Now, under a global change of coordinates Γ such that $x' = \Gamma x$, the metric g and the vierbein transform as

$$\begin{aligned} g \mapsto g' &= (\Gamma^T)^{-1} g \Gamma^{-1} \\ e \mapsto e' &= \Gamma e \end{aligned} \tag{23}$$

This transformation fulfills the tetrads-metric relation,

$$e'^{T} g' e' = e^{T} \Gamma^{T} (\Gamma^{T})^{-1} g \Gamma^{-1} \Gamma e = e^{T} g e = \eta. \tag{24}$$

Next we start from a QW that reproduces the flat equation, and introduce a deformation (described by the transformation Γ) that will end up with a more generic metric g'. We can make a simple choice, given by the canonical tetrads ${e^{\mu}}_{a} = {\delta}_{a}^{\mu}$ for the initial coordinates, and then transform them according to Eq. (23). Since we are considering a deformation of the spatial sites of the lattice, the time components will be left unchanged, and the matrix Γ will take the form

$$\Gamma = \begin{pmatrix} 1 & 0 & 0 \\ 0 & \lambda_{11} & \lambda_{12} \\ 0 & \lambda_{21} & \lambda_{22} \end{pmatrix}. \tag{25}$$

where each λ_{ij} are position independent, although they are allowed to depend on time.

Under this restriction, we can reduce the problem to a transformation on a bidimensional space, where ${e^{t}}_{0} = 1$, which implies that Eq. (17) adopts the simpler form

$$i\partial_t \chi + \frac{i}{2}\{B^s, \partial_s\}\chi - m\beta\chi = 0. \tag{26}$$

Let us consider how this transformation will affect the QW defined on a triangular lattice, as introduced in Sect. III (see[18]). Such transformation will imply modifying the vectors u_i, yielding the new vectors

$$u_i^{'} = \begin{pmatrix} \lambda_{11} & \lambda_{12} \\ \lambda_{21} & \lambda_{22} \end{pmatrix} u_i \equiv \Lambda u_i. \tag{27}$$

Introducing these vectors in our algorithms and calculating the continuum limit, we arrive at the following equation

$$i\partial_t \psi = \Big[(\lambda_{11}\sigma^x + \lambda_{12}\sigma^y)p_x + (\lambda_{21}\sigma^x + \lambda_{22}\sigma^y)p_y\Big]\psi + m\sigma^z\psi, \tag{28}$$

which describes the Dirac equation on a flat geometry. A comparison with Eq. (17) gives

$$B^x = \lambda_{11}\sigma^x + \lambda_{12}\sigma^y \tag{29}$$

$$B^y = \lambda_{21}\sigma^x + \lambda_{22}\sigma^y. \tag{30}$$

This procedure can be used for a homogeneous transformation, such as the one defined above. In the next section, we introduce an alternative, which consists in redefining the τ^i matrices. As we shall see, this redefinition also allows for an inhomogeneous (i.e., space-time dependent) $\Lambda(t, x, y)$ transformation, thereby resulting in a Dirac equation in curved space.

Curved dirac equation from a non-homogeneous QW. We now generalize the ideas developed in the previous Sect. with the purpose to obtain, in the continuum limit, the Dirac equation on a curved spacetime, for a given metrics with a triangular tetrad, as discussed in Sect. II. We start by looking at the set of matrices $B^s = \alpha^a \frac{{e^s}_a}{{e^t}_0}$, as a linear transformation over the set of usual Pauli matrices, in the same spirit as Eqs (29) and (30). This leads us to define the transformation $\Lambda(t, x, y)$, with matrix elements

$$\Lambda^s_a \equiv \frac{{e^s}_a}{{e^t}_0} \tag{31}$$

(we have omitted the time and space dependence for convenience). Then, the above mentioned transformation reads

$$B^s = \Lambda^s_a \alpha^a. \tag{32}$$

We now make use of the property that relates the τ^i matrices, defined in Eq. (22), with the Pauli matrices: $u_i^k \tau^i = \sigma^k$ (see[18]). In this way, we arrive to

$$B^s = \Lambda^s_k u_i^k \tau^i. \tag{33}$$

The above equation can be understood as a transformation performed on the u_i vectors, c.f. Eq. (27), as the origin of the curved spacetime equation.

Instead of introducing a distortion $\Lambda(t, x, y)$ on the lattice via the modification of the u_i vectors, the unitary matrices τ^i can be transformed to produce the same effect. In other words, we seek for a set of matrices $\beta^i(t, x, y)$ that fulfill the following conditions:

- (C1) We impose that

$$\Lambda_k^j(t, x, y)u_i^k\tau^i = u_i^j\beta^i(t, x, y). \tag{34}$$

- (C2) Each of them has $\{-1, 1\}$ as eigenvalues, i.e. at any time step and at any point (x, y) of the lattice there exist three unitaries $U_i(t, x, y)$ such that

$$\beta^i(t, x, y) = U_i^\dagger(t, x, y)\sigma^z U_i(t, x, y). \tag{35}$$

Notice that condition (C1) implies that the coordinate transformation dictated by $\Lambda_k^j(t, x, y)$ is transferred to the unitary operations, which become new spacetime dependent $\beta^i(t, x, y)$, instead of the original τ^i. Additionally, condition (C2) will allow us to rewrite the QW evolution in terms of the usual state-dependent translation operators. Let us apply these ideas to the honeycomb and the triangular lattice.

To alleviate the notations, in what follows we will omit the spacetime dependence both in these matrices and in the $U_i(t, x, y)$, and write simply β^i and U_i. The above conditions allow to calculate the β^i matrices, which can be written as a combination of Pauli matrices, i.e. $\beta^i = \vec{n}^i \cdot \vec{\sigma}$, where each $\vec{n}^i$ must be a real, unit vector $\vec{n}^i = (\sin\theta_i \cos\phi_i,\ \sin\theta_i \sin\phi_i,\ \cos\theta_i)$ for some angles θ_i and ϕ_i (that are time and position dependent).

In this way

$$\beta_i = U_i^\dagger\sigma_z U_i = \begin{pmatrix} \cos\theta_i & e^{-i\phi_i}\sin\theta_i \\ e^{i\phi_i}\sin\theta_i & -\cos\theta_i \end{pmatrix}, \tag{36}$$

and each U_i can be obtained by diagonalization of the corresponding β^i. With an appropriate choice of phases, we finally write them as

$$U_i = \begin{pmatrix} e^{\frac{i\phi_i}{2}}\cos\frac{\theta_i}{2} & e^{-\frac{i\phi_i}{2}}\sin\frac{\theta_i}{2} \\ -e^{\frac{i\phi_i}{2}}\sin\frac{\theta_i}{2} & e^{-\frac{i\phi_i}{2}}\cos\frac{\theta_i}{2}, \end{pmatrix}. \tag{37}$$

Before we proceed to examine the induced QW on the honeycomb and triangular lattices together with their limits, let us discuss what the situation would have been in the square lattice, had we implement the above procedure. In this case, the original Dirac matrices can be chosen to be the Pauli matrices, and the two unit vectors u_i can be taken to be the canonical ones, so that the requirement of Eq. (34) simply becomes

$$\Lambda_k^j\sigma^k = \beta^j. \tag{38}$$

But then, since condition (C2) implies that $\det(\beta^j) = -1$ for each j, we need that

$$\sum_k (\Lambda_k^j)^2 = 1. \tag{39}$$

Thus the square lattice only allows for a limited form of "duality", i.e. only those transformations satisfying condition (39) can be absorbed into the unitaries, whereas the honeycomb and triangular lattices allow for arbitrary transformations.

Results

Honeycomb QW. In this section we define the QW over the honeycomb, following a similar procedure as in[18]. After the ideas developed in Methods, we define the following Hamiltonian to be used in the QW:

$$\mathcal{H} = \frac{1}{2}u_i^j(\beta^i p_j + p_j\beta^i) + \widetilde{m}\sigma^z \tag{40}$$

with $\widetilde{m} = m/e^t{}_0$. Expanding the Hamiltonian, we arrive to:

$$\mathcal{H} = -iu_i^j U_i^\dagger\sigma_z\partial_j U_i - \frac{i}{2}u_i^j\left[(\partial_j U_i^\dagger)\sigma_z U_i - U_i^\dagger\sigma_z(\partial_j U_i)\right] + \widetilde{m}\sigma^z \tag{41}$$

After substitution of Eq. (37), one obtains

$$(\partial_j U_i^\dagger)\sigma_z U_i - U_i^\dagger\sigma_z(\partial_j U_i) = -i\cos\theta_i\partial_j\phi_j\mathbb{I}, \tag{42}$$

with $\mathbb{I}$ the identity matrix. Notice that, unlike in the flat space situation, there is no possible choice of the phases in the U_is that makes Eq. (42) vanish for all values of i. One may wonder whether there is a reason behind this, for example the existence of some topological or gauge invariant that forbids all these quantities to be simultaneously zero. This issue might deserve further investigation in the future. In any case, the additional term in Eq. (42) that arises from the choice given by Eq. (37) contributes only as a space-time dependent phase, which is easy to handle both from the theoretical and from the experimental point of view. We finally arrive to:

$$\mathcal{H} = \sum_i (U_i^\dagger \sigma_z \pi_i U_i + \gamma_i \mathbb{I}) + \widetilde{m}\sigma^z \tag{43}$$

where $\gamma_i = -\frac{i}{2}\cos\theta_i \pi_i \phi_i$. In order to define the QW, we make use of the Lie-Trotter product formula to decompose the evolution of the wavefunction $\psi(t+\varepsilon) = e^{-i\varepsilon\mathcal{H}}\psi(t)$ as a product of unitary matrices

$$e^{-i\varepsilon\left[\sum_i (U_i^\dagger \sigma_z \pi_i U_i + \gamma_i) + \widetilde{m}\sigma^z\right]} \approx e^{-i\widetilde{m}\varepsilon\sigma^z} \prod_i e^{-i\varepsilon U_i^\dagger \sigma_z \pi_i U_i} e^{-i\varepsilon\gamma_i}. \tag{44}$$

Applying condition (C1), and introducing the translation operators along the u_i direction as $T_i = e^{-i\varepsilon\sigma^z\pi_i}$, the QW on a honeycomb can be defined as:

$$\psi(t+\varepsilon) = e^{-i\widetilde{m}\varepsilon\sigma^z} \prod_i U^\dagger{}_i T_i U_i e^{-i\varepsilon\gamma_i}\psi(t) \tag{45}$$

By construction, in the continuous limit, we arrive to the Dirac equation in $2+1$ curved space-time, under the form

$$i\partial_t\psi = \frac{1}{2}\left[u_i^j\beta^i(t,x,y)p_j + u_i^j p_j \beta^i(t,x,y)\right]\psi + \widetilde{m}\sigma^z\psi. \tag{46}$$

As expected, this equation can be nicely rewritten under the form Eq. (17), if we define $B^j(t,x,y) \equiv u_i^j\beta^i(t,x,y)$.

Triangular QW. Let us describe first the dynamics corresponding to the massless case. Again, we follow the same procedure as in[18]. The triangles have equilateral sides labeled by $k=0,1,2$. The two-dimensional spinors live on the edges shared by adjacent triangles. We denote them by $\psi(t,v,k) = \begin{pmatrix}\psi^\uparrow(t,v,k)\\ \psi^\downarrow(t,v,k)\end{pmatrix}$, with v a triangle and k a side. Therefore, the position at the lattice will be labeled by (v,k). The evolution of the Triangular QW is defined as the composition of three operators. The first operator is the application of the 2×2 unitary matrix $U_i(t,v,k)$, defined in Methods, to each two-dimensional spinor on every edge shared by two neighboring triangles. The second operator, R, simply rotates every triangle anti-clockwise. The third operator is just the application of the unitary matrix $U_i^\dagger(t,v,k+1)$ again at each edge shared by two neighboring triangles, where the addition $k+1$ is understood modulo 2. Altogether, the Triangular QW evolution is given by:

$$\begin{aligned}\psi(t+\varepsilon/3,v,k) &= U_i^\dagger(t,v,k)[P^\uparrow U_i(t,v,k-1)e^{-i\varepsilon\gamma_i}\psi(t,v,k-1)\\ &\quad \oplus P^\downarrow U_i(t,e(v,k),k-1)e^{-i\varepsilon\gamma_i}\psi(t,e(v,k),k-1)] \equiv W_i(t)\psi(t)\end{aligned} \tag{47}$$

where $P^\uparrow$ and $P^\downarrow$ are the projectors over the upper and lower component of the spinor, respectively, and $e(t,v,k)$ is the neighbor of triangle v alongside k at fixed time t. We define one timestep of the evolution by the composition of the three operators W_i, and include the mass term, as follows

$$\psi(t+\varepsilon) = e^{-i\widetilde{m}\varepsilon\sigma^z}(W_2W_1W_0)\psi(t) \tag{48}$$

By expanding this equation up to first order in ε, after a tedious but straightforward computation, one arrives to the following equation in the continuum limit:

$$\begin{aligned}\partial_t\psi &= \left(U_0^\dagger\sigma^z U_0 - \frac{1}{2}U_1^\dagger\sigma^z U_1 - \frac{1}{2}U_2^\dagger\sigma^z U_2\right)\partial_x\psi + \frac{\sqrt{3}}{2}(U_1^\dagger\sigma^z U_1 - U_2^\dagger\sigma^z U_2)\partial_y\psi\\ &\quad + \partial_x\left(U_0^\dagger\sigma^z U_0 - \frac{1}{2}U_1^\dagger\sigma^z U_1 - \frac{1}{2}U_2^\dagger\sigma^z U_2\right)\psi + \frac{\sqrt{3}}{2}\partial_y(U_1^\dagger\sigma^z U_1 - U_2^\dagger\sigma^z U_2)\psi\\ &\quad - i\widetilde{m}\sigma^z\psi\end{aligned} \tag{49}$$

where the above terms appear from an expansion at order $O(\varepsilon)$. Notice that, if we define $B^x \equiv \left(\beta^0 - \frac{1}{2}\beta^1 - \frac{1}{2}\beta^2\right)$, and $B^y \equiv \frac{\sqrt{3}}{2}(\beta^1 - \beta^2)$, Eq. (49) adopts the desired form of (17).

Numerical simulations. In order to illustrate how the above scheme can be used to describe the dynamics of a particular system, we have computed the behaviour of a massless fermion in a $(2+1)$- dimensional spacetime black hole, whose metric in Lemaître coordinates is given by:

$$ds^2 = \left(1 - \frac{r_s}{r}\right)dt^2 - \frac{d\rho^2}{1-\frac{r_s}{r}} - r^2 d\theta^2, \tag{50}$$

where $r = \left(\frac{3(\rho-t)}{2}\right)^{\frac{2}{3}} r_s^{\frac{1}{3}}$, and r_s is the Schwarzschild radius. To simplify the simulations and the plots, we have not considered the angular motion, so that the variation in θ is zero. This allows us to describe the QW probability density in the plane (t,x), where x plays the role of ρ. The deformation $\Lambda(t,x)$ to induce the former metric reads:

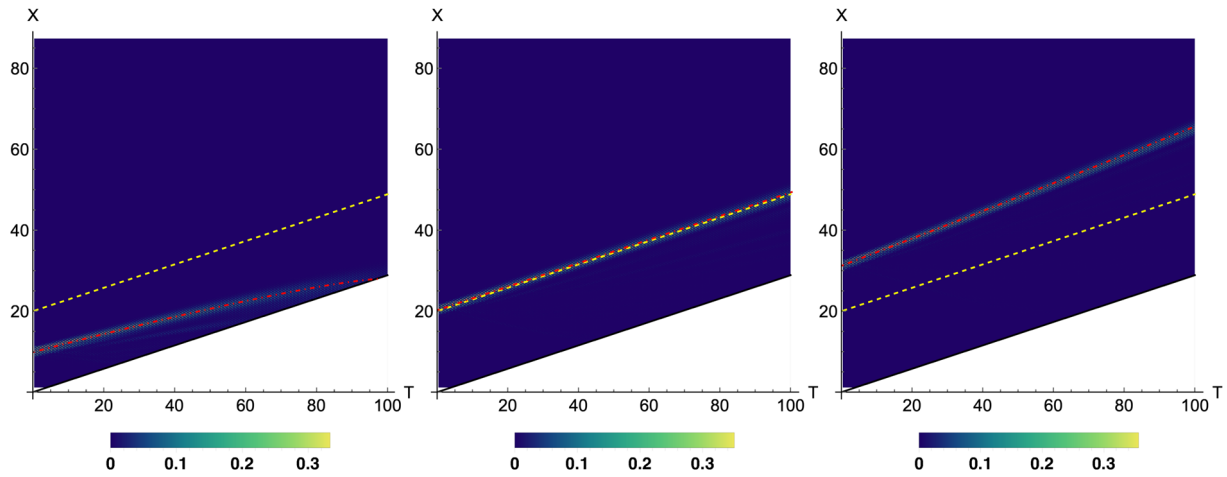

Figure 1. Probability density of a QW in the plane (t, x), compared with the classical geodesic (dot dashed red line). Dashed yellow line refers to the black hole horizon. Coordinates T and X are given by $T = \frac{\sqrt{3}}{6}\varepsilon t$, where the factor $\frac{\sqrt{3}}{6}$ is a necessary rescaling of the time coordinate[18], and $X = \varepsilon x$ with $\varepsilon = \frac{1}{3}$. The number of time steps is $t = 300$. The initial condition is $\psi(0, v, 1) = g(v - v_0)(1, 1)^T$ where $g(v)$ is a Gaussian function with $\sigma = 3$. See the text for an explanation of the different panels.

$$\Lambda(t, x) = \begin{pmatrix} \frac{\sqrt{r(t, x)}}{r_s} & 0 \\ 0 & \frac{1}{r(t, x)} \end{pmatrix}. \tag{51}$$

In Fig. 1 we can observe the dynamics of the walker in the projected plane (t, x). Depending on the initial position of the walker, the trajectories in the spacetime vary. The event horizon is given by $r_h = \frac{\sqrt{3}}{6}\varepsilon t + \frac{2}{3}r_s$. Therefore, when the particle is initialized inside the horizon with $x_{v_0} = 9.94$ (left panel), the QW ends up in the singularity. On the other hand, if the QW starts exacly at the horizon (central panel), the probability distribution will follow the horizon trajectory. Finally, if the initial state lies outside the horizon with $x_{v_0} = 31.31$ (right panel), it propagates away from the singularity. These results are in agreement with[30], in which they study a QW with the same metric in $(1 + 1)$- dimensional spacetime.

Discussion

We introduced a Quantum Walk (QW) over the honeycomb and the triangular lattice. In both cases, our starting point was the possibility to rewrite the targeted Hamiltonian as a sum of momentum operators along the three relevant directions of the lattice, each weighted by a suitably chosen gamma matrix. This procedure has been introduced in[18] — our targeted Hamiltonian was then that of the Dirac equation, which we recovered in the continuum limit. In the present work, we realized that due to the linear dependence of the three preferred directions of the honeycomb and the triangular lattices, one could also obtain the Hamiltonian of the Dirac equation under an arbitrary change of coordinates. We emphasized that applying the same procedure, but for the square lattice, only allows for a very limited set of changes of coordinates.

Then, by making the gamma matrices to be spacetime dependent, we obtained the Curved Dirac equation in an arbitrary background metric. Overall, the QW hereby constructed over the honeycomb and the triangular lattices thus recovers, in the continuum limit, the Dirac equation in curved $(2 + 1)$– dimensional spacetime. We believe that the duality between changes of metric, and changes of gamma matrices weighting non linearly-independent momentum operators, is profound and may lead to further developments.

References

1. Ambainis, A., Childs, A. M., Reichardt, B. W., Špalek, R. & Zhang, S. Any and-or formula of size n can be evaluated in time $n^{1/2}$+o(1) on a quantum computer. *SIAM J. on Comput.* **39**, 2513–2530 (2010).
2. Wang, G. Efficient quantum algorithms for analyzing large sparse electrical networks. *Quantum Info. Comput.* **17**, 987–1026 (2017).
3. Bialynicki-Birula, I. Weyl, Dirac, and Maxwell equations on a lattice as unitary cellular automata. *Phys. Rev. D.* **49**, 6920–6927 (1994).
4. Meyer, D. A. From quantum cellular automata to quantum lattice gases. *J. Stat. Phys* **85**, 551–574 (1996).
5. Feynman, R. P. Simulating physics with computers. *Int. J. Theor. Phys.* **21**, 467–488 (1982).
6. Genske, M. *et al.* Electric quantum walks with individual atoms. *Phys. review letters* **110**, 190601 (2013).
7. Sansoni, L. *et al.* Two-particle bosonic-fermionic quantum walk via integrated photonics. *Phys. Rev. Lett.* **108**, 010502, https://doi.org/10.1103/PhysRevLett.108.010502 (2012).
8. Arrighi, P., Forets, M. & Nesme, V. The Dirac equation as a Quantum Walk: higher-dimensions, convergence. *Journal of Physics A: Mathematical and Theoretical*, **47**, 46 Pre-print arXiv:1307.3524 (2013).
9. Arrighi, P., Facchini, S. & Forets, M. Discrete lorentz covariance for quantum walks and quantum cellular automata. *New J. Phys.* **16**, 093007 (2014).

10. Bisio, A., D Ariano, G. M. & Perinotti, P. Quantum walks, weyl equation and the lorentz group. *Foundations Phys.* **47**, 1065–1076 (2017).
11. Neto, A. C., Guinea, F., Peres, N. M., Novoselov, K. S. & Geim, A. K. The electronic properties of graphene. *Rev. modern physics* **81**, 109 (2009).
12. Ye, L. *et al*. Massive dirac fermions in a ferromagnetic kagome metal. *Nat.* **555**, 638 (2018).
13. Bougroura, H., Aissaoui, H., Chancellor, N. & Kendon, V. Quantum-walk transport properties on graphene structures. *Phys. Rev. A* **94**, 1–11, https://doi.org/10.1103/PhysRevA.94.062331 arXiv:1611.02991v1 (2016).
14. Kitagawa, T., Rudner, M. S., Berg, E. & Demler, E. Exploring topological phases with quantum walks. *Phys. Rev. A - At. Mol. Opt. Phys.* **82**, https://doi.org/10.1103/PhysRevA.82.033429 1003.1729 (2010).
15. Regge, T. General relativity without coordinates. *Il Nuovo Cimento (1955–1965)* **19**, 558–571, https://doi.org/10.1007/BF02733251 (1961).
16. Rovelli, C. Loop quantum gravity. *Living Rev. Relativ.* **1**, 1, https://doi.org/10.12942/lrr-1998-1 (1998).
17. Ambjorn, J., Jurkiewicz, J. & Loll, R. The universe from scratch. *Contemp. Phys.* **47**, 103–117, https://doi.org/10.1080/00107510600603344 (2006).
18. Arrighi, P., Di Molfetta, G., Márquez-Martín, I. & Pérez, A. Dirac equation as a quantum walk over the honeycomb and triangular lattices. *Phys. Rev. A* **97**, 062111, https://doi.org/10.1103/PhysRevA.97.062111 (2018).
19. Jay, G., Debbasch, F. & Wang, J. B. Dirac quantum walks on triangular and honeycomb lattices. *Phys. Rev. A* **99**, 032113 (2019).
20. Succi, S. & Benzi, R. Lattice boltzmann equation for quantum mechanics. *Phys. D: Nonlinear Phenom.* **69**, 327–332 (1993).
21. Dellar, P. J., Lapitski, D., Palpacelli, S. & Succi, S. Isotropy of three-dimensional quantum lattice boltzmann schemes. *Phys. Rev. E* **83**, 046706, https://doi.org/10.1103/PhysRevE.83.046706 (2011).
22. Bisio, A., D'Ariano, G. M. & Tosini, A. Quantum field as a quantum cellular automaton i: the dirac free evolution in one dimension. *arXiv preprint arXiv:1212.*2839 (2012).
23. Chandrashekar, C. Two-component dirac-like hamiltonian for generating quantum walk on one-, two-and three-dimensional lattices. *Sci. reports* **3**, 2829 (2013).
24. Chandrashekar, C., Banerjee, S. & Srikanth, R. Relationship between quantum walks and relativistic quantum mechanics. *Phys. Rev. A.* **81**, 62340 (2010).
25. Arrighi, P. & Facchini, S. Decoupled quantum walks, models of the klein-gordon and wave equations. *EPL Europhysics Lett.* **104**, 60004 (2013).
26. di Molfetta, G. & Debbasch, F. Discrete-time quantum walks: Continuous limit and symmetries. *J. Math. Phys.* **53**, 123302–123302 (2012).
27. Strauch, F. W. Relativistic quantum walks. *Phys. Rev. A* **73**, 054302 (2006).
28. Love, P. & Boghosian, B. From Dirac to Diffusion: decoherence in Quantum Lattice gases. *Quantum Inf. Process.* **4**, 335–354 (2005).
29. Cedzich, C. *et al*. Propagation of quantum walks in electric fields. *Phys. review letters* **111**, 160601 (2013).
30. Di Molfetta, G., Brachet, M. & Debbasch, F. Quantum walks in artificial electric and gravitational fields. *Phys. A: Stat. Mech. its Appl.* **397**, 157–168 (2014).
31. Márquez-Martín, I., Di Molfetta, G. & Pérez, A. Fermion confinement via quantum walks in (2 + 1)-dimensional and (3 + 1)-dimensional space-time. *Phys. Rev. A* **95**, 042112, https://doi.org/10.1103/PhysRevA.95.042112 (2017).
32. Di Molfetta, G. & Pérez, A. Quantum walks as simulators of neutrino oscillations in a vacuum and matter. *New J. Phys.* **18**, 103038, https://doi.org/10.1088/1367-2630/18/10/103038 (2016).
33. Arnault, P., Di Molfetta, G., Brachet, M. & Debbasch, F. Quantum walks and non-abelian discrete gauge theory. *Phys. Rev. A* **94**, 012335, https://doi.org/10.1103/PhysRevA.94.012335 (2016).
34. Meyer, D. A. Quantum lattice gases and their invariants. *Int. J. Mod. Phys. C* **8**, 717–735 (1997).
35. Ahlbrecht, A. *et al*. Molecular binding in interacting quantum walks. *New J. Phys.* **14**, 073050 (2012).
36. Di Molfetta, G., Brachet, M. & Debbasch, F. Quantum walks as massless dirac fermions in curved space-time. *Phys. Rev. A* **88**, 042301 (2013).
37. Arrighi, P., Facchini, S. & Forets, M. Quantum walking in curved spacetime. *Quantum Inf. Process.* **15**, 3467–3486 (2016).
38. Arnault, P. & Debbasch, F. Quantum walks and gravitational waves. *Annals Phys.* **383**, 645–661, https://doi.org/10.1016/j.aop.2017.04.003 (2017).
39. Arrighi, P. & Facchini, F. Quantum walking in curved spacetime: (3+1) dimensions, and beyond. *Quantum Inf. Comput.* 17, 0810–0824 ArXiv:1609.00305 (2017).
40. Mallick, A., Mandal, S., Karan, A. & Chandrashekar, C. M. Simulating dirac hamiltonian in curved space-time by split-step quantum walk, https://doi.org/10.1088/2399-6528/aafe2f. 1712.03911v3.
41. Stegmann, T. & Szpak, N. Current flow paths in deformed graphene: from quantum transport to classical trajectories in curved space. *New J. Phys.* **18**, 053016 (2016).
42. Kerner, R., Naumis, G. G. & Gómez-Arias, W. A. Bending and flexural phonon scattering: Generalized dirac equation for an electron moving in curved graphene. *Phys. B: Condens. Matter* **407**, 2002–2008 (2012).
43. Abal, G., Donangelo, R., Marquezino, F. L. & Portugal, R. Spatial search on a honeycomb network. *Math. Struct. Comput. Sci.* **20**, 999–1009, https://doi.org/10.1017/S0960129510000332 1001.1139 (2010).
44. Foulger, I., Gnutzmann, S. & Tanner, G. Quantum walks and quantum search on graphene lattices. *Phys. Rev. A - At. Mol. Opt. Phys.* **91**, 1–15, arXiv:1312.3852v1, https://doi.org/10.1103/PhysRevA.91.062323 (2015).
45. Karafyllidis, I. G. Quantum walks on graphene nanoribbons using quantum gates as coins. *J. Comput. Sci.* **11**, 326–330 (2015).
46. Lawrie, I. D. *Unified grand tour of theoretical physics*, 2nd edn (Taylor & Francis, New York, 2001).
47. Koke, C., Noh, C. & Angelakis, D. G. Dirac equation in 2-dimensional curved spacetime, particle creation, and coupled waveguide arrays. *Annals Phys.* **374**, 162–178, https://doi.org/10.1016/j.aop.2016.08.013 (2016).
48. Yepez, J. Einstein's vierbein field theory of curved space. 1106.2037v1 (2011).
49. De Oliveira, C. & Tiomno, J. Representations of dirac equation in general relativity. *Il Nuovo Cimento* **24**, 672–687 (1962).

Acknowledgements

We acknowledge the very enlightening discussion on general covariance with Luca Fabbri. This work has been funded by the INFINITI and the CNRS PEPs Spain-France PIC2017FR6, the STICAmSud project 16STIC05 FoQCoSS and the Spanish Ministerio de Economía, Industria y Competitividad, MINECO-FEDER project FPA2017-84543-P, SEV-2014-0398 and Generalitat Valenciana grant GVPROMETEOII2014-087. We acknowledge support from CSIC Research Platform PTI-001.

Author Contributions

P.A., G.D.M., I.M.M. and A.P. contribute equally to the results of this paper. All authors reviewed the manuscript.

Additional Information

Competing Interests: The authors declare no competing interests.

6 Perspectives and Conclusions

Summary

6.1 Tetrahedral QW

A natural question, after developing the 2D QW over the honeycomb and triangular lattices, and showing that one can recover the Dirac equation in the continuum, is the question whether it is possible to extend this result to three dimensional space. In order to discretize the 3D space, simplicial complexes will be used. Therefore, the objective is defining a quantum walk based model over a tetrahedral space. The work is in progress, however we can already provide an outline of the solution.

There is no way to fill the Euclidean space using regular tetrahedrons, for which all four faces are equilateral triangles [124]. However, we can construct a 3D lattice by dividing a cube in six tetrahedrons, as represented in Fig.(6.1). There are more possible approaches to fill the 3D, for further explanation we refer to [124]. This one is probably the simplest. The tetrahedron used, albeit non-reglular, is unique in sizes. Using this construction, we can fill the 3D space by replicating the cube and gluing them together.

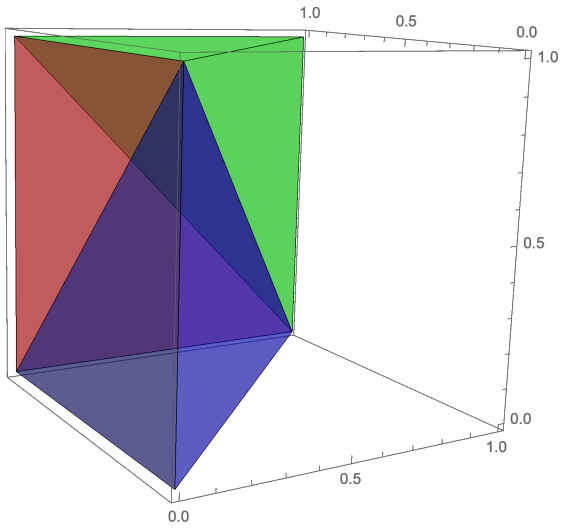

Figure 6.1: Half cube constructed by three irregular tetrahedrons

It can be very useful to define the dual graph of the 3D tetrahedral lattice, in order to make simple the definition of the QW. In Fig.(6.2), we can visualize the dual graph, in which the points refer to tetrahedrons, whereas the cables refer to the connections between them. The cables are distinguished by colored and black ones. The colored cables connect a tetrahedron with another one living on a different cube. The colors (red, blue and green) indicate different vector directions. The black lines connect tetrahedrons living in the same cube.

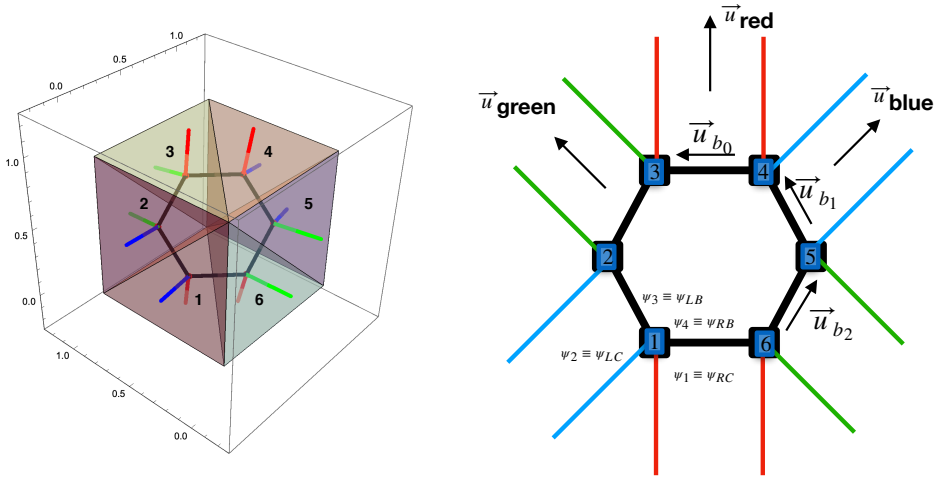

(a) (b)

Figure 6.2: (a) Cube constructed by the composition of 6 tetrahedrons. (b) Dual graph, which represents a cube. Every point represents a tetrahedra, the cables refer to the connection between tetrahedrons, as it is represented in (a)

Then, we define a $\mathbf{C}^4$ spinor at the center of every tetrahedron,

$$\psi(\vec{x},t) = \begin{pmatrix} \psi_1(\vec{x},t) \\ \psi_2(\vec{x},t) \\ \psi_3(\vec{x},t) \\ \psi_4(\vec{x},t) \end{pmatrix} \equiv \begin{pmatrix} \psi_{RC}(\vec{x},t) \\ \psi_{LC}(\vec{x},t) \\ \psi_{LB}(\vec{x},t) \\ \psi_{RB}(\vec{x},t) \end{pmatrix}. \tag{6.1}$$

where LC, RC, LB and RB refer to: Left-Colored,Right-Colored, Left-Black and Right-Black, respectively. The use of this notation is due to the position in which the spinor components are placed in the dual graph, Fig.(6.2). However, this does not mean that the spinor amplitudes are living on the interface between tetrahedrons: it is just a manner of labeling the spinor amplitudes, in order to make easier the the QW using the dual graph. The evolution will be a composition of six rotation coins[1] and also six different *swap-translation* operators, at every tetrahedron in the same cube.

The particularity of this QW over the tetrahedral space is that, in one cube, the system is not translational invariant, and we have to keep track of the position of the spinor in order to define the translation operator.

First, let us write the six different directions in which the spinor components can move: $\vec{u}_{\text{red}}$, $\vec{u}_{\text{blue}}$, $\vec{u}_{\text{green}}$, $\vec{u}_{b_1}$, $\vec{u}_{b_2}$, $\vec{u}_{b_3}$. They are showed in Fig.(6.2) using the

[1]Still to be precised

dual graph. Notice that, due to the fact that the cube is made by two symmetric prisms, the direction vectors are symmetric on the opposite side of the graph.

$$u_0 = (-\frac{1}{4}, \frac{1}{4}, 0) \quad u_1 = (0, \frac{1}{4}, \frac{1}{4}) \quad u_2 = (\frac{1}{4}, 0, \frac{1}{4})$$
$$u_{\text{blue}} = (\frac{1}{2}, \frac{1}{4}, -\frac{1}{4}) \quad u_{\text{red}} = (-\frac{1}{4}, -\frac{1}{4}, -\frac{1}{2}) \quad u_{\text{red}} = (\frac{1}{4}, \frac{1}{2}, -\frac{1}{4}). \tag{6.2}$$

As mentioned above, we need to define, at every tetrahedron, an unitary coin $\mathbf{R}_i$, where $i = 1...6$. As the goal is recovering, in the continuum, the Dirac equation, the coins play an important role. At the moment, we have not found a proper set of coins which allows us to find the right continuous limit.

The *swap-translation* operator means that, apart of doing the usual spin conditional translation, we perform a swap at the same time. For instance, let us define, at a given time step, the components of the spinor at the tetrahedron-1.

$$\psi(\vec{x}_{T_1}, t+1) = \begin{pmatrix} (U_3\psi(\vec{x}_{T_1} - \vec{u}_{\text{red}}, t))_{RB} \\ (U_5\psi(\vec{x}_{T_1} - \vec{u}_{\text{blue}}, t))_{LB} \\ (U_2\psi(\vec{x}_{T_1} + \vec{u}_{b_1}, t))_{LC} \\ (U_6\psi(\vec{x}_{T_1} - \vec{u}_{b_0}, t))_{RC} \end{pmatrix}. \tag{6.3}$$

where $\vec{x}_{T_1}$ refers to the position of the tetrahedron-1. Therefore, we take the spinor components from the adjacent tetrahedrons with respect to the one we are situated, see Fig.(6.2). However, we do not connect the same spinor components. The first spinor component (RC) in tetrahedron-1 at time step $t+1$, is taken from the forth component (LB) of the spinor at the tetrahedron-3, at time step t (after applying the coin). On the other hand, the same occurs between the second component (LC), of the spinor in the tetrahedron-1, at time step $t+1$, and the third component (LB) of the spinor in the tetrahedron-5, at time step t.

This correspondence between spinor components $RC \leftrightarrow RB$ and $RL \leftrightarrow LB$, is established at every translation operator in the six different tetrahedrons. The reason to define the translation operator with this swap, is because we want the spinor amplitudes to explore every tetrahedron, in the case of choosing identity matrices as coins. Otherwise, it would not be possible to explore the six different tetrahedrons defined in the cube.

The rest of the translation operators are defined as:

$$\psi(\vec{x}_{T_2}, t+1) = \begin{pmatrix} (U_4\psi(\vec{x}_{T_2} - \vec{u}_{\text{blue}}, t))_{RB} \\ (U_6\psi(\vec{x}_{T_2} + \vec{u}_{\text{green}}, t))_{LB} \\ (U_3\psi(\vec{x}_{T_2} + \vec{u}_{b_2}, t))_{LC} \\ (U_1\psi(\vec{x}_{T_2} - \vec{u}_{b_1}, t))_{RC} \end{pmatrix}. \tag{6.4}$$

$$\psi(\vec{x}_{T_3}, t+1) = \begin{pmatrix} (U_5\psi(\vec{x}_{T_3} + \vec{u}_{\text{green}}, t))_{RB} \\ (U_1\psi(\vec{x}_{T_3} + \vec{u}_{\text{red}}, t))_{LB} \\ (U_4\psi(\vec{x}_{T_3} - \vec{u}_{b_0}, t))_{LC} \\ (U_2\psi(\vec{x}_{T_3} - \vec{u}_{b_2}, t))_{RC} \end{pmatrix}. \tag{6.5}$$

$$\psi(\vec{x}_{T_4}, t+1) = \begin{pmatrix} (U_6\psi(\vec{x}_{T_4} + \vec{u}_{\text{red}}, t))_{RB} \\ (U_2\psi(\vec{x}_{T_4} + \vec{u}_{\text{blue}}, t))_{LB} \\ (U_5\psi(\vec{x}_{T_4} - \vec{u}_{b_1}, t))_{LC} \\ (U_3\psi(\vec{x}_{T_4} + \vec{u}_{b_0}, t))_{RC} \end{pmatrix}. \tag{6.6}$$

$$\psi(\vec{x}_{T_5}, t+1) = \begin{pmatrix} (U_1\psi(\vec{x}_{T_5} + \vec{u}_{\text{blue}}, t))_{RB} \\ (U_3\psi(\vec{x}_{T_5} - \vec{u}_{\text{green}}, t))_{LB} \\ (U_6\psi(\vec{x}_{T_5} - \vec{u}_{b_2}, t))_{LC} \\ (U_4\psi(\vec{x}_{T_5} + \vec{u}_{b_1}, t))_{RC} \end{pmatrix}. \tag{6.7}$$

$$\psi(\vec{x}_{T_6}, t+1) = \begin{pmatrix} (U_2\psi(\vec{x}_{T_6} - \vec{u}_{\text{green}}, t))_{RB} \\ (U_4\psi(\vec{x}_{T_6} - \vec{u}_{\text{red}}, t))_{LB} \\ (U_1\psi(\vec{x}_{T_6} + \vec{u}_{b_0}, t))_{LC} \\ (U_5\psi(\vec{x}_{T_6} + \vec{u}_{b_2}, t))_{RC} \end{pmatrix}. \tag{6.8}$$

Looking at the former recursion function, we can realize that the translation operators in the tetrahedrons T_1, T_2 and T_3 are just the conjugates of the translation operators in T_4, T_5 and T_6. This is because of the already mentioned symmetry between the two prism that construct the cube.

We have shown how to define a QW-based model over a discretized tetrahedral 3D space, however there are still opened questions. The main question is whether there is a existing continuous limit that reproduces the Dirac equation in $(3+1)$-dimensional space.

As this is the first model defined over the tetrahedral lattice, we believe that this QW, with a nontrivial topology, could have different and exotic features with respect to the QWs defined over cubic spaces. How does the probability distribution evolve? Is there any advantage in Grover search algorithms? Is it possible to apply the duality principle in 3D, Sect.(5.5)?

On the other hand, inspired by the attempts of quantum gravity theories, where the space is triangulated by tetrahedrons, this QW model can, perhaps, give some insight in the fermionic transport over those spaces.

6.2 Conclusions

In this thesis we have studied several models using DTQW schemes. We have pointed out in the introduction that DTQW are a useful tool for developing quantum algorithms, however we focus on another important area that is growing in the recent years: *quantum simulation*.

In Chapter (2), we recall the concept of quantum simulation. It is introduced

the, well-known, continuous limit of QWs, and it is shown how in the continuum limit, the QW describes a family of differential equations, by choosing the appropriate coin parameters.

Based on a brane-world model proposed by Ruvakov [114], we define both a 2D and a 3D quantum walk. In this brane-world model, particles live in a $N + 1 + 1_s$ space-time, where N refers to the ordinary spatial dimensions, and 1_s refers to the extra dimension. The only manner to access the extra dimension is by having a large amount of energy, which may not be accessible in current experiments.

In this way, we can define a QW with an inhomogeneous coin, which is position-dependent, in 2D and 3D spatial dimensions, in which one of these spatial dimension plays the role of the "extra" one. Hence, by tuning a coin parameter, the energy regime can be selected. For certain parameters, we cannot access to the extra dimension: as a consequence, the walker becomes confined in 1D (2D), in the case of the 2D (3D) QW. On the other hand, if the walker can access to the extra dimension (high energy regime), it behaves like a free quantum walk.

Normally, localization in QWs is achieved via random or periodic coins, however in this model, the walker becomes localized by the action of a coin which changes in space in a regular, nonperiodic manner. On other hand, another remarkable feature is that, in the case in which the walker is confined, the state is topologically protected, which could be useful for experimental implementations or quantum algorithms.

In Chapter (3), we introduced gauge invariance for 1D and 2D QWs coupled to external electromagnetic fields. Introducing gauge invariance in lattice theories is not trivial, since there are plenty of ways to do it, for which the same continuous limit is achieved.

We compare this gauge invariance with previous models, pointing out that, our proposal to implement the invariance in the DTQW, has the advantage that the discrete derivatives which are introduced are similar to the discrete derivatives used in lattice gauge theories.

In Chapter (4), we answer the open-question about whether it is possible to recover the behavior of relativistic fermions, in the continuum, by changing the geometry in which the quantum walk is defined, to triangular and honeycomb lattices. There are previous works which consider QWs over such structures, for spatial search algorithms, graphene properties, localization processes, etc. However, none of them was known to have a well-known physics equation in the continuum limit.

We in turn define a QW over the honeycomb and triangular lattices, proving that it is possible to recover the Dirac equation in the continuous limit. This result shows that these simulation results need not to rely on a grid.

On the other hand, graphene materials are potential candidates for experimental realization of quantum simulators. The fact that we define QWs over the honeycomb lattices, could be beneficial for future implementation of quantum

simulation schemes, based on QW models using these materials.

Finally, in Chapter (5), we extend the model introduced in the previous chapter. Inspired by the theory of deformation in solid materials, we wonder whether it is possible to deform the lattice in such a way that, in the continuum, we recover the Dirac equation in a $2+1$ curved space time.

By a method we introduce, called *duality*, we impose a deformation on the lattice, and then we encode this transformation into local space-time dependent coins. In such a way, we can simulate, in the continuum, the curved Dirac equation, whereas the lattice remains unaltered.

There is a special interest in simulating the effects of gravity on the dynamics of fermions. In addition, there are also some studies on using curved graphene, to simulate fermions on a curved space-time. Obviously, the deformations that can be made to the material are limited. Our work can open the possibility to simulate an arbitrary background metric, e.g using undeformed graphene, by implementing local coins operators at every discrete point.

6.3 Perspectives

QWs have the ability to simulate specific quantum systems. Most of the results involve one particle, although there are studies in which two particles are involved. Apart from being capable of simulating quantum theories, QWs are attractive because they can illustrate physical theories in a simple and elegant manner, through unitary operators on a discrete lattice. In our opinion, the next step in the field of quantum simulators based on QWs protocols, is the study of interacting multi particle models, that would allow to make a connection with theories like Quantum Field Theory [12, 113].

On the other hand, it is necessary to implement these QWs models in labs. Physical implementations of QWs are getting better, year after year [142, 138]. We believe that in the next few years, there will be experiments involving multiparticle models, which are hard to simulate using classic computers since the increment of complexity grows exponentially with the number of particles.

Analog quantum simulation (AQS) has been developed further than digital quantum simulation (DQS), in the last years, because DQS needs error correction algorithms which significantly increase the cost of the computation. Recently, there is a large number of big companies working on building new prototypes of quantum computers, such Google, IBM, Microsoft etc, based on quantum circuits schemes. This industry is increasing considerably[2], and there is even a recent study in which they claim to achieve quantum supremacy by using a 53 qubits quantum computer [16]

Probably in the next years we will have reliable quantum computers based on hundreds of qubits, which may overcome some classical computations. That is

[2]IBM just announces a quantum computer of 53 qubits

why we think that another approach that needs consideration for implementing QWs is the use of quantum circuits. There are already some studies which implement QWs in quantum circuits [57, 24, 35, 55], although still further research in this topic is necessary, such as implementing inhomogeneous coin operators, non-rectangular lattices, or implementing experimental test in current quantum computers.

Publications and Scientific Communications

Publications

•I. Márquez-Martín, G. Di Molfetta and A.Pérez. Fermion confinement via quantum walks in (2+1)-dimensional and (3+1)-dimensional space-time. Phys. Rev. A 95, 042112, https://journals.aps.org/pra/abstract/10.1103/PhysRevA.95.042112
•I. Márquez-Martín, P.Arnault, G. Di Molfetta and A.Pérez. Electromagnetic lattice gauge invariance in two-dimensional discrete-time quantum walks. Phys. Rev. A 98, 032333, https://journals.aps.org/pra/abstract/10.1103/PhysRevA.98.032333
•P. Arrighi, G. D. Molfetta, I. Márquez-Martín, and A. Pérez. The Dirac equation as a quantum walk over the honeycomb and triangular lattices. Phys. Rev. A 97, 062111 https://journals.aps.org/pra/abstract/10.1103/PhysRevA.97.062111
•P. Arrighi, G. D. Molfetta, I. Márquez-Martín, and A. Pérez. From curved spacetime to spacetime-dependent local unitaries over the honeycomb and triangular Quantum Walks. Scientific Reports volume 9, Article number: 10904 (2019), https://www.nature.com/articles/s41598-019-47535-4

Communications

•Winter School, "Complex Networks: From Classical to Quantum, Theory and Experimental Implementation" from the 3rd to the 7th of April, 2017 Obergurgl (Austria). http://quantum-networks.org/obergurgl2017. *Poster session*.
•Conference, "New Trends in Complex Quantum Systems Dynamics" 8-12 May 2017 Cartagena (Spain) http://www.cqs.upct.es. Poster session.
•Workshop, "Quantum simulation models workshop" 12 Jun 2017 Marseille (France) https://mqwsw.sciencesconf.org. *Talk*.
•Conference, "Quantum Simulation (ICQSIM)" at Ecole Normale Supérieure, Paris, from the 13th to the 17th of November, 2017. https://icqsim2017.sciencesconf.org. *Poster session*
•Workshop, “8th Workshop of Quantum Simulation and Quantum Walks 2018” Perth, from the 14th to the 16th of December, 2018. *Poster session*.

•School, "Thematic research programme: Operator algebras, groups and applications to quantum information" 6-10 May, 2019. ICMAT, Madrid (Spain).
•Conference, "5th conference on quantum information in Spain" 28-31 May, 2019 Barcelona (Spain). *Poster session*.
•Workshop, "9na Jornada de Lógica, Computación e Información Cuántica" 24 October, 2019 Buenos Aires (Argentina). *Talk*.

Bibliography

[1] G. Abal, R. Donangelo, M. Forets, et al. "Spatial quantum search in a triangular network". In: *Mathematical Structures in Computer Science* 22.3 (2012), pp. 521–531. ISSN: 09601295. DOI: 10.1017/S0960129511000600 (cit. on pp. 59–62, 67).

[2] G. Abal, R. Donangelo, F. L. Marquezino, et al. "Spatial search on a honeycomb network". In: *Mathematical Structures in Computer Science* 20.6 (2010), pp. 999–1009. ISSN: 09601295. DOI: 10.1017/S0960129510000332 (cit. on pp. 59–61).

[3] G. S. Agarwal and P. K. Pathak. "Quantum random walk of the field in an externally driven cavity". In: *Physical Review A - Atomic, Molecular, and Optical Physics* 72.3 (2005), pp. 1–6. ISSN: 10502947. DOI: 10.1103/PhysRevA.72.033815 (cit. on p. 30).

[4] A. Ambainis, E. Bach, A. Nayak, et al. "One-dimensional quantum walks". In: *Conference Proceedings of the Annual ACM Symposium on Theory of Computing*. 2001 (cit. on p. 24).

[5] Andris Ambainis. "Quantum Walk Algorithm for Element Distinctness". In: *Proceedings of the 45th Annual IEEE Symposium on Foundations of Computer Science*. FOCS '04. Washington, DC, USA: IEEE Computer Society, 2004, pp. 22–31. ISBN: 0-7695-2228-9. DOI: 10.1109/FOCS.2004.54. URL: https://doi.org/10.1109/FOCS.2004.54 (cit. on p. 17).

[6] Andris Ambainis, Julia Kempe, and Alexander Rivosh. "Coins Make Quantum Walks Faster". In: *Proceedings of the Sixteenth Annual ACM-SIAM Symposium on Discrete Algorithms*. SODA '05. Philadelphia, PA, USA: Society for Industrial and Applied Mathematics, 2005, pp. 1099–1108. ISBN: 0-89871-585-7. URL: http://dl.acm.org/citation.cfm?id=1070432.1070590 (cit. on p. 60).

[7] P. W. Anderson. "Absence of Diffusion in Certain Random Lattices". In: *Phys. Rev.* 109 (1956) (cit. on p. 33).

[8] M. Ansari. "Dirac equation in a 5-dimensional Kaluza-Klein theory". In: *Indian Journal of Pure and Applied Mathematics* 41.6 (2010), pp. 715–736. ISSN: 00195588. DOI: 10.1007/s13226-010-0041-x (cit. on p. 34).

[9] Pablo Arnault and Fabrice Debbasch. "Quantum walks and discrete gauge theories". In: *Physical Review A - Atomic, Molecular, and Optical Physics* 93.5 (2016), pp. 1–6. ISSN: 10941622. DOI: 10.1103/PhysRevA.93.052301. arXiv: 1508.00038 (cit. on pp. 33, 47, 49).

[10] Pablo Arnault and Fabrice Debbasch. "Quantum walks and gravitational waves". In: *Annals of Physics* 383 (2017), pp. 645–661. ISSN: 1096035X. DOI: 10.1016/j.aop.2017.04.003. URL: http://dx.doi.org/10.1016/j.aop.2017.04.003 (cit. on p. 74).

[11] Pablo Arnault, Giuseppe Di Molfetta, Marc Brachet, et al. "Quantum walks and non-Abelian discrete gauge theory". In: *Physical Review A* 94.1 (2016), pp. 1–6. ISSN: 24699934. DOI: 10.1103/PhysRevA.94.012335 (cit. on p. 33).

[12] Pablo Arrighi, Cédric Bény, and Terry Farrelly. "A quantum cellular automaton for one-dimensional QED". In: (2019), pp. 1–14. arXiv: 1903.07007. URL: http://arxiv.org/abs/1903.07007 (cit. on pp. 30, 101).

[13] Pablo Arrighi and Stefano Facchini. "Quantum walking in curved spacetime: $(3+1)$ dimensions, and beyond". In: *Quantum Information and Computation* 17.9-10 (2017), pp. 810–824. ISSN: 15337146. arXiv: arXiv:1609.00305v2 (cit. on p. 74).

[14] Pablo Arrighi, Stefano Facchini, and Marcelo Forets. "Quantum walking in curved spacetime". In: *Quantum Information Processing* 15.8 (2016), pp. 3467–3486. ISSN: 15700755. DOI: 10.1007/s11128-016-1335-7 (cit. on p. 74).

[15] Pablo Arrighi, Giuseppe Di Molfetta, and Stefano Facchini. "Quantum walking in curved spacetime: discrete metric". In: *Quantum* (2018). DOI: 10.22331/q-2018-08-22-84 (cit. on p. 74).

[16] Frank Arute, Kunal Arya, Ryan Babbush, et al. "Quantum supremacy using a programmable superconducting processor". In: *Nature* 574.7779 (2019), pp. 505–510. ISSN: 1476-4687. DOI: 10.1038/s41586-019-1666-5. URL: https://doi.org/10.1038/s41586-019-1666-5 (cit. on p. 101).

[17] J K Asbóth. "Symmetries, topological phases, and bound states in the one-dimensional quantum walk". In: *Phys. Rev. B* 86.19 (Nov. 2012), p. 195414. DOI: 10.1103/PhysRevB.86.195414. URL: https://link.aps.org/doi/10.1103/PhysRevB.86.195414 (cit. on p. 63).

[18] János K Asbóth and Hideaki Obuse. "Bulk-boundary correspondence for chiral symmetric quantum walks". In: *Phys. Rev. B* 88.12 (Sept. 2013), p. 121406. DOI: 10.1103/PhysRevB.88.121406. URL: https://link.aps.org/doi/10.1103/PhysRevB.88.121406 (cit. on p. 63).

[19] János K. Asbóth, László Oroszlány, and András Pályi. *A Short Course on Topological Insulators*. 2016. ISBN: 978-3-319-25605-4. DOI: 10.1007/978-3-319-25607-8. arXiv: 1509.02295 (cit. on p. 42).

[20] Alán Aspuru-Guzik and Philip Walther. “Photonic quantum simulators”. In: *Nature Physics* 8 (Apr. 2012), p. 285. URL: https://doi.org/10.1038/nphys2253%20http://10.0.4.14/nphys2253 (cit. on p. 29).

[21] David Bailin and Alex Love. “Kaluza-Klein theories in twelve dimensions”. In: *Nuclear Physics, Section B* 254.C (1985), pp. 543–554. ISSN: 05503213. DOI: 10.1016/0550-3213(85)90232-9 (cit. on p. 34).

[22] Radhakrishnan Balu, Daniel Castillo, and George Siopsis. “Physical realization of topological quantum walks on IBM-Q and beyond”. In: *Quantum Science and Technology* 3.3 (2018). ISSN: 20589565. DOI: 10.1088/2058-9565/aab823 (cit. on p. 31).

[23] Radhakrishnan Balu, Daniel Castillo, and George Siopsis. “Physical realization of topological quantum walks on {IBM}-Q and beyond”. In: *Quantum Science and Technology* 3.3 (Apr. 2018), p. 35001. DOI: 10.1088/2058-9565/aab823. URL: https://doi.org/10.1088%7B%5C%%7D2F2058-9565%7B%5C%%7D2Faab823 (cit. on p. 63).

[24] Radhakrishnan Balu, Daniel Castillo, and George Siopsis. “Physical realization of topological quantum walks on IBM-Q and beyond”. In: *Quantum Science and Technology* 3.3 (2018). ISSN: 20589565. DOI: 10.1088/2058-9565/aab823 (cit. on p. 102).

[25] H C Berg. *Random Walks in Biology*. Princeton paperbacks. Princeton University Press, 1993. ISBN: 9780691000640. URL: https://books.google.es/books?id=DjdgXGLoJY8C (cit. on p. 19).

[26] Scott D. Berry and Jingbo B. Wang. “Two-particle quantum walks: Entanglement and graph isomorphism testing”. In: *Physical Review A - Atomic, Molecular, and Optical Physics* 83.4 (2011), pp. 1–12. ISSN: 10502947. DOI: 10.1103/PhysRevA.83.042317 (cit. on p. 30).

[27] Immanuel Bloch, Jean Dalibard, and Wilhelm Zwerger. “Many-body physics with ultracold gases”. In: *Reviews of Modern Physics* 80.3 (2008), pp. 885–964. ISSN: 00346861. DOI: 10.1103/RevModPhys.80.885 (cit. on p. 29).

[28] Hamza Bougroura, Habib Aissaoui, Nicholas Chancellor, et al. “Quantum-walk transport properties on graphene structures”. In: *Physical Review A* 94.6 (2016), pp. 1–11. ISSN: 24699934. DOI: 10.1103/PhysRevA.94.062331. arXiv: arXiv:1611.02991v1 (cit. on pp. 59, 65).

[29] D. Bouwmeester, I. Marzoli, G. P. Karman, et al. “Optical Galton board”. In: *Physical Review A* 61.1 (1999), pp. 1–9. ISSN: 1050-2947. DOI: 10.1103/physreva.61.013410 (cit. on p. 30).

[30] L. Brey and H. A. Fertig. “Electronic states of graphene nanoribbons studied with the Dirac equation”. In: *Physical Review B - Condensed Matter and Materials Physics* 73.23 (2006), pp. 2–6. ISSN: 10980121. DOI: 10.1103/PhysRevB.73.235411 (cit. on p. 65).

[31] C. Cedzich, T. Geib, A. H. Werner, et al. "Quantum walks in external gauge fields". In: *Journal of Mathematical Physics* 60.1 (2019). ISSN: 00222488. DOI: 10.1063/1.5054894 (cit. on p. 49).

[32] C Cedzich, F A Grünbaum, C Stahl, et al. "Bulk-edge correspondence of one-dimensional quantum walks". In: *Journal of Physics A: Mathematical and Theoretical* 49.21 (Apr. 2016), 21LT01. DOI: 10.1088/1751-8113/49/21/21lt01. URL: https://doi.org/10.1088%7B%5C%%7D2F1751-8113%7B%5C%%7D2F49%7B%5C%%7D2F21%7B%5C%%7D2F21lt01 (cit. on p. 63).

[33] Ll. G. Chambers, Carl M. Bender, and Steven A. Orszag. "Advanced Mathematical Methods for Scientists and Engineers". In: *The Mathematical Gazette* (1979). ISSN: 00255572. DOI: 10.2307/3616036 (cit. on p. 26).

[34] C. M. Chandrashekar. "Implementing the one-dimensional quantum (Hadamard) walk using a Bose-Einstein condensate". In: *Physical Review A - Atomic, Molecular, and Optical Physics* 74.3 (2006), pp. 1–7. ISSN: 10502947. DOI: 10.1103/PhysRevA.74.032307 (cit. on p. 30).

[35] Chen-Fu Chiang, Daniel Nagaj, and Pawel Wocjan. "Efficient Circuits for Quantum Walks". In: (2009), pp. 1–15. arXiv: 0903.3465. URL: http://arxiv.org/abs/0903.3465 (cit. on p. 102).

[36] Andrew M. Childs. "Universal computation by quantum walk". In: *Physical Review Letters* 102.18 (2009), pp. 1–4. ISSN: 00319007. DOI: 10.1103/PhysRevLett.102.180501. arXiv: 0806.1972 (cit. on p. 17).

[37] J. Ignacio Cirac and Frank Verstraete. "Renormalization and tensor product states in spin chains and lattices". In: *Journal of Physics A: Mathematical and Theoretical* 42.50 (2009). ISSN: 17518113. DOI: 10.1088/1751-8113/42/50/504004 (cit. on p. 28).

[38] John Clarke and Frank K Wilhelm. "Superconducting quantum bits". In: *Nature* 453 (June 2008), p. 1031. URL: https://doi.org/10.1038/nature07128%20http://10.0.4.14/nature07128 (cit. on p. 29).

[39] Robin Côté, Alexander Russell, Edward E. Eyler, et al. "Quantum random walk with Rydberg atoms in an optical lattice". In: *New Journal of Physics* 8 (2006). ISSN: 13672630. DOI: 10.1088/1367-2630/8/8/156 (cit. on p. 30).

[40] Andrea Crespi, Roberto Osellame, Roberta Ramponi, et al. "Anderson localization of entangled photons in an integrated quantum walk". In: *Nature Photonics* 7 (Mar. 2013), p. 322. URL: https://doi.org/10.1038/nphoton.2013.26%20http://10.0.4.14/nphoton.2013.26%20https://www.nature.com/articles/nphoton.2013.26%7B%5C#%7Dsupplementary-information (cit. on p. 34).

[41] Jean Dalibard, Fabrice Gerbier, Gediminas Juzeliunas, et al. “Colloquium: Artificial gauge potentials for neutral atoms”. In: *Reviews of Modern Physics* 83.4 (2011), pp. 1523–1543. ISSN: 00346861. DOI: 10.1103/RevModPhys.83.1523 (cit. on p. 29).

[42] Giacomo Mauro D’Ariano, Marco Erba, and Paolo Perinotti. “Isotropic quantum walks on lattices and the Weyl equation”. In: *Physical Review A* (2017). ISSN: 24699934. DOI: 10.1103/PhysRevA.96.062101 (cit. on p. 18).

[43] Fabrice Debbasch. “Action principles for quantum automata and Lorentz invariance of discrete time quantum walks”. In: *Annals of Physics* 405 (2019), pp. 340–364. ISSN: 1096035X. DOI: 10.1016/j.aop.2019.03.005. URL: https://doi.org/10.1016/j.aop.2019.03.005 (cit. on p. 50).

[44] J. D. Debus, M. Mendoza, and H. J. Herrmann. “Shifted Landau levels in curved graphene sheets”. In: *Journal of Physics Condensed Matter* 30.41 (2018). ISSN: 1361648X. DOI: 10.1088/1361-648X/aadecd (cit. on p. 74).

[45] G. Di Molfetta and F. Debbasch. “Discrete-time quantum walks: Continuous limit symmetries”. In: *Journal of Mathematical Physics* 53.12 (2012). ISSN: 00222488. DOI: 10.1063/1.4764876 (cit. on p. 31).

[46] Giuseppe Di Molfetta and Pablo Arrighi. “A quantum walk with both a continuous-time and a continuous-spacetime limit”. In: (2019), pp. 1–8. arXiv: 1906.04483. URL: http://arxiv.org/abs/1906.04483 (cit. on p. 31).

[47] Giuseppe Di Molfetta, M. Brachet, and Fabrice Debbasch. “Quantum walks as massless Dirac fermions in curved space-time”. In: *Physical Review A - Atomic, Molecular, and Optical Physics* 88.4 (2013), pp. 1–5. ISSN: 10502947. DOI: 10.1103/PhysRevA.88.042301 (cit. on pp. 33, 74).

[48] Giuseppe Di Molfetta, Marc Brachet, and Fabrice Debbasch. “Quantum walks in artificial electric and gravitational fields”. In: *Physica A: Statistical Mechanics and its Applications* 397 (2014), pp. 157–168. ISSN: 03784371. DOI: 10.1016/j.physa.2013.11.036. URL: http://dx.doi.org/10.1016/j.physa.2013.11.036 (cit. on pp. 47, 49).

[49] Tiegang Di, Mark Hillery, and M. Suhail Zubairy. “Cavity QED-based quantum walk”. In: *Physical Review A - Atomic, Molecular, and Optical Physics* 70.3 (2004), pp. 3–7. ISSN: 10502947. DOI: 10.1103/PhysRevA.70.032304 (cit. on p. 30).

[50] W. Dür, R. Raussendorf, V. M. Kendon, et al. “Quantum walks in optical lattices”. In: *Physical Review A - Atomic, Molecular, and Optical Physics* 66.5 (2002), p. 8. ISSN: 10941622. DOI: 10.1103/PhysRevA.66.052319 (cit. on p. 30).

[51] K. Eckert, J. Mompart, G. Birkl, et al. “One- and two-dimensional quantum walks in arrays of optical traps”. In: *Physical Review A - Atomic, Molecular, and Optical Physics* 72.1 (2005), pp. 1–9. ISSN: 10502947. DOI: 10.1103/PhysRevA.72.012327 (cit. on p. 30).

[52] a. Einstein. “Über die von der molekularkinetischen Theorie der Wärme geforderte Bewegung von in ruhenden Flüssigkeiten suspendierten”. In: *Ann. d. Phys.* 322.8 (1905), pp. 549–560. DOI: 10.1002/andp.19053220806. URL: http://onlinelibrary.wiley.com/doi/10.1002/andp.19053220806/abstract (cit. on p. 19).

[53] Vladimir Fal’ko. “Quantum information on chicken wire”. In: *Nature Physics* 3 (Mar. 2007), p. 151. URL: https://doi.org/10.1038/nphys556%20http://10.0.4.14/nphys556 (cit. on p. 65).

[54] Richard P Feynman. “Simulating Physics with Quantum Computers”. In: *Inernational Journal of Theoretical Physics* 21.6/7 (1982), pp. 467–488 (cit. on p. 28).

[55] François Fillion-Gourdeau, Steve MacLean, and Raymond Laflamme. “Algorithm for the solution of the Dirac equation on digital quantum computers”. In: *Physical Review A* 95.4 (2017), pp. 1–17. ISSN: 24699934. DOI: 10.1103/PhysRevA.95.042343. arXiv: 1611.05484 (cit. on p. 102).

[56] Kyriakos Flouris, Sauro Succi, and Hans J. Herrmann. “Quantized Alternate Current on Curved Graphene”. In: *Condensed Matter* 4.2 (2019), p. 39. DOI: 10.3390/condmat4020039 (cit. on p. 74).

[57] S. Fujiwara, H. Osaki, I. M. Buluta, et al. “Scalable networks for discrete quantum random walks”. In: *Physical Review A - Atomic, Molecular, and Optical Physics* 72.3 (2005), pp. 1–4. ISSN: 10502947. DOI: 10.1103/PhysRevA.72.032329 (cit. on pp. 31, 102).

[58] Antonio Gallerati. “Graphene properties from curved space Dirac equation”. In: *European Physical Journal Plus* 134.5 (2019). ISSN: 21905444. DOI: 10.1140/epjp/i2019-12610-6. arXiv: arXiv:1808.01187v3 (cit. on p. 74).

[59] I. M. Georgescu, S. Ashhab, and Franco Nori. “Quantum simulation”. In: *Reviews of Modern Physics* 86.1 (2014), pp. 153–185. ISSN: 15390756. DOI: 10.1103/RevModPhys.86.153 (cit. on p. 29).

[60] D. R. Grempel, Shmuel Fishman, and R. E. Prange. “Localization in an incommensurate potential: An exactly solvable model”. In: *Physical Review Letters* 49.11 (1982), pp. 833–836. ISSN: 00319007. DOI: 10.1103/PhysRevLett.49.833 (cit. on p. 34).

[61] Geoffrey Grimmett, Svante Janson, and Petra F. Scudo. "Weak limits for quantum random walks". In: *Physical Review E - Statistical, Nonlinear, and Soft Matter Physics* 69.2 2 (2004), pp. 1–6. ISSN: 1063651X. DOI: 10.1103/PhysRevE.69.026119 (cit. on p. 27).

[62] Stéphane Guillet, Mathieu Roget, Pablo Arrighi, et al. "The Grover search as a naturally occurring phenomenon". In: (2019), pp. 1–5. arXiv: 1908.11213. URL: http://arxiv.org/abs/1908.11213 (cit. on pp. 68, 83).

[63] F D M Haldane. "Model for a QHE without Landau levels". In: *Physical review letters* 61.18 (1988), pp. 2015–2018 (cit. on p. 65).

[64] Michael J. Hartmann. "Quantum simulation with interacting photons". In: *Journal of Optics (United Kingdom)* 18.10 (2016). ISSN: 20408986. DOI: 10.1088/2040-8978/18/10/104005 (cit. on p. 29).

[65] Yusuke Higuchi, Norio Konno, Iwao Sato, et al. "Spectral and asymptotic properties of Grover walks on crystal lattices". In: *Journal of Functional Analysis* 267.11 (2014), pp. 4197–4235. ISSN: 0022-1236. DOI: 10.1016/j.jfa.2014.09.003. URL: http://dx.doi.org/10.1016/j.jfa.2014.09.003 (cit. on pp. 62, 63).

[66] Norio Inui, Yoshinao Konishi, and Norio Konno. "Localization of two-dimensional quantum walks". In: *Physical Review A - Atomic, Molecular, and Optical Physics* 69.5 A (2004), pp. 1–9. ISSN: 10502947. DOI: 10.1103/PhysRevA.69.052323 (cit. on p. 34).

[67] Gareth Jay, Fabrice Debbasch, and J. B. Wang. "Dirac quantum walks on triangular and honeycomb lattices". In: *Physical Review A* 99.3 (2019), pp. 1–11. ISSN: 24699934. DOI: 10.1103/PhysRevA.99.032113 (cit. on pp. 50, 68).

[68] Alain Joye and Marco Merkli. "Dynamical Localization of Quantum Walks in Random Environments". In: *Journal of Statistical Physics* 140.6 (2010), pp. 1025–1053. ISSN: 00224715. DOI: 10.1007/s10955-010-0047-0 (cit. on p. 34).

[69] Ioannis G. Karafyllidis. "Quantum walks on graphene nanoribbons using quantum gates as coins". In: *Journal of Computational Science* 11 (2015), pp. 326–330. ISSN: 18777503. DOI: 10.1016/j.jocs.2015.05.006 (cit. on pp. 59, 65).

[70] J. P. Keating, N. Linden, J. C F Matthews, et al. "Localization and its consequences for quantum walk algorithms and quantum communication". In: *Physical Review A - Atomic, Molecular, and Optical Physics* 76.1 (2007), pp. 1–5. ISSN: 10502947. DOI: 10.1103/PhysRevA.76.012315. arXiv: 0606205 [quant-ph] (cit. on p. 34).

[71] Vivien M Kendon. “A random walk approach to quantum algorithms.” In: *Philosophical transactions. Series A, Mathematical, physical, and engineering sciences* 364.October (2006), pp. 3407–3422. ISSN: 1364-503X. DOI: 10.1098/rsta.2006.1901. arXiv: 0609035 [quant-ph] (cit. on p. 19).

[72] Lutz Kilian and Mark P. Taylor. “Why is it difficult to beat the random walk forecast of exchange rates?” In: *Journal of International Economics* (2003). ISSN: 00221996. DOI: 10.1016/S0022-1996(02)00060-0 (cit. on p. 19).

[73] Takuya Kitagawa, Mark S. Rudner, Erez Berg, et al. “Exploring topological phases with quantum walks”. In: *Physical Review A - Atomic, Molecular, and Optical Physics* 82.3 (2010), pp. 1–12. ISSN: 10502947. DOI: 10.1103/PhysRevA.82.033429. arXiv: 1003.1729 (cit. on pp. 59, 60, 63, 65).

[74] Oskar Klein. “Quantentheorie und fünfdimensionale Relativitätstheorie”. In: *Zeitschrift für Physik* 37.12 (Dec. 1926), pp. 895–906. ISSN: 0044-3328. DOI: 10.1007/BF01397481. URL: https://doi.org/10.1007/BF01397481 (cit. on p. 34).

[75] Hagen Kleinert. “Nonholonomic mapping principle for classical and quantum mechanics in spaces with curvature and torsion”. In: *General Relativity and Gravitation* 32.5 (2000), pp. 769–839. ISSN: 00017701. DOI: 10.1023/A:1001962922592 (cit. on p. 83).

[76] Peter L. Knight, Eugenio Roldán, and J. E. Sipe. “Optical cavity implementations of the quantum walk”. In: *Optics Communications* 227.1-3 (2003), pp. 147–157. ISSN: 00304018. DOI: 10.1016/j.optcom.2003.09.024 (cit. on p. 30).

[77] Peter L. Knight, Eugenio Roldán, and J. E. Sipe. “Quantum walk on the line as an interference phenomenon”. In: *Physical Review A - Atomic, Molecular, and Optical Physics* 68.2 (2003), p. 4. ISSN: 10941622. DOI: 10.1103/PhysRevA.68.020301 (cit. on p. 30).

[78] B. Kollár, M. Štefaňák, T. Kiss, et al. “Recurrences in three-state quantum walks on a plane”. In: *Physical Review A - Atomic, Molecular, and Optical Physics* 82.1 (2010), pp. 1–7. ISSN: 10502947. DOI: 10.1103/PhysRevA.82.012303 (cit. on pp. 62, 63).

[79] Norio Konno. “Quantum random walks in one dimension”. In: 1.5 (2002), pp. 345–354. arXiv: 0206053 [quant-ph]. URL: http://arxiv.org/abs/quant-ph/0206053 (cit. on p. 27).

[80] E. Kroener. “Continuized Crystal - a Bridge Between Micro- and Macromechanics?” In: *Zeitschrift fur angewandte Mathematik und Mechanik* 66.5 (1986), pp. 284–292. ISSN: 0044-2267 (cit. on p. 83).

[81] Y. Lahini, R. Pugatch, F. Pozzi, et al. "Observation of a localization transition in quasiperiodic photonic lattices". In: *Physical Review Letters* 103.1 (2009), pp. 1–4. ISSN: 00319007. DOI: 10.1103/PhysRevLett.103.013901 (cit. on p. 34).

[82] Maciej Lewenstein, Anna Sanpera, Veronica Ahufinger, et al. "Ultracold atomic gases in optical lattices: mimicking condensed matter physics and beyond". In: *Advances in Physics* 56.2 (2007), pp. 243–379. DOI: 10.1080/00018730701223200. URL: https://doi.org/10.1080/00018730701223200 (cit. on p. 29).

[83] Guocai Liu, Shi Liang Zhu, Shaojian Jiang, et al. "Simulating and detecting the quantum spin Hall effect in the kagome optical lattice". In: *Physical Review A - Atomic, Molecular, and Optical Physics* 82.5 (2010), pp. 1–8. ISSN: 10502947. DOI: 10.1103/PhysRevA.82.053605 (cit. on p. 29).

[84] S. Lloyd. "Universal Quantum Simulators: Correction". In: *Science* 279.5354 (1998), 1113h–1117. ISSN: 00368075. DOI: 10.1126/science.279.5354.1113h. URL: http://www.sciencemag.org/cgi/doi/10.1126/science.279.5354.1113h (cit. on p. 28).

[85] L Lovász. "Random walks on graphs: A survey". In: *Combinatorics Paul Erdos is Eighty* (1993). ISSN: 03044149. DOI: 10.1.1.39.2847 (cit. on p. 19).

[86] Neil B. Lovett, Sally Cooper, Matthew Everitt, et al. "Universal quantum computation using the discrete-time quantum walk". In: *Physical Review A - Atomic, Molecular, and Optical Physics* 81.4 (2010). ISSN: 10502947. DOI: 10.1103/PhysRevA.81.042330. arXiv: 0910.1024 (cit. on p. 17).

[87] Jacob Lubliner. "Plasticity Theory: Revised Edition". In: *Journal of Applied Mechanics* 59.1 (2006), p. 540. ISSN: 00218936. DOI: 10.1115/1.2899459. URL: http://www.getcited.org/pub/102800120 (cit. on p. 81).

[88] Changyuan Lyu, Luyan Yu, and Shengjun Wu. "Localization in quantum walks on a honeycomb network". In: *Physical Review A - Atomic, Molecular, and Optical Physics* 92.5 (2015), pp. 1–10. ISSN: 10941622. DOI: 10.1103/PhysRevA.92.052305 (cit. on pp. 34, 62, 63).

[89] Takuya Machida and Kojimachi Business. "A limit law of the return probability for a quantum walk on a hexagonal lattice". In: 13.7 (2015), pp. 1–12. DOI: 10.1142/S0219749915500549 (cit. on pp. 62, 63).

[90] Yuriy Makhlin, Gerd Scöhn, and Alexander Shnirman. "Josephson-junction qubits with controlled couplings". In: *Nature* 398.6725 (1999), pp. 305–307. ISSN: 1476-4687. DOI: 10.1038/18613. URL: https://doi.org/10.1038/18613 (cit. on p. 29).

[91] K. Manouchehri and J. B. Wang. "Quantum walks in an array of quantum dots". In: *Journal of Physics A: Mathematical and Theoretical* 41.6 (2008). ISSN: 17518113. DOI: 10.1088/1751-8113/41/6/065304 (cit. on p. 31).

[92] K. Manouchehri and J. B. Wang. "Quantum random walks without walking". In: *Physical Review A - Atomic, Molecular, and Optical Physics* 80.6 (2009), pp. 1–4. ISSN: 10502947. DOI: 10.1103/PhysRevA.80.060304 (cit. on p. 30).

[93] P Mark and Mark P Taylor. "econstor the Random Walk Forecast of Exchange Rates ?" In: 3024 (2001) (cit. on p. 19).

[94] Giovanni Modugno. "Anderson localization in Bose-Einstein condensates". In: *Reports on Progress in Physics* 73.10 (2010). ISSN: 00344885. DOI: 10.1088/0034-4885/73/10/102401 (cit. on p. 34).

[95] Miquel Montero. "Invariance in Quantum Walks". In: *Research Advances in Quantum Dynamics*. Ed. by Paul Bracken. Rijeka: IntechOpen, 2016. Chap. 1. DOI: 10.5772/62872. URL: https://doi.org/10.5772/62872 (cit. on p. 50).

[96] I Montvay and G Munster. *Quantum fields on a lattice*. Cambridge Monographs on Mathematical Physics. Cambridge University Press, 1997. ISBN: 9780521599177, 9780511879197. DOI: 10.1017/CBO9780511470783. URL: http://www.cambridge.org/uk/catalogue/catalogue.asp?isbn=0521404320 (cit. on p. 47).

[97] Cristopher Moore and Alexander Russell. "Quantum Walks on the Hypercube". In: *Randomization and Approximation Techniques in Computer Science*. Ed. by José D P Rolim and Salil Vadhan. Berlin, Heidelberg: Springer Berlin Heidelberg, 2002, pp. 164–178. ISBN: 978-3-540-45726-8 (cit. on p. 61).

[98] R Motwani and P Raghavan. "Randomized Algorithms. Cambridge International Series on Parallel Computation". In: *Cambridge University Press.* (1995) (cit. on p. 19).

[99] G. Münster and M. Walzl. "Lattice Gauge Theory - A short Primer". In: (2000). arXiv: 0012005 [hep-lat]. URL: http://arxiv.org/abs/hep-lat/0012005 (cit. on p. 47).

[100] C. Navarrete-Benlloch, A. Pérez, and Eugenio Roldán. "Nonlinear optical Galton board". In: *Physical Review A - Atomic, Molecular, and Optical Physics* 75.6 (2007), pp. 1–7. ISSN: 10502947. DOI: 10.1103/PhysRevA.75.062333. arXiv: 0604084 [quant-ph] (cit. on p. 34).

[101] Ashwin Nayak and Ashvin Vishwanath. "Quantum Walk on the Line". In: *arXiv preprint quant-ph/0010117* (2000), p. 20. ISSN: 0031-9007. DOI: 10.1103/PhysRevLett.91.130602. arXiv: 0010117 [quant-ph]. URL: http://arxiv.org/abs/quant-ph/0010117 (cit. on pp. 24, 27).

[102] Jae Dong Noh and Heiko Rieger. "Random Walks on Complex Networks". In: *Physical Review Letters* 92.11 (2004), pp. 118701–1. ISSN: 00319007. DOI: 10.1103/PhysRevLett.92.118701. arXiv: 0307719v2 [cond-mat] (cit. on p. 19).

[103] K. S. Novoselov, A. K. Geim, S. V. Morozov, et al. "Electric Field Effect in Atomically Thin Carbon Films Supplementary". In: *Science* 5.1 (2004), pp. 1–12. ISSN: 00092509. DOI: 10.1126/science.aab1343. arXiv: arXiv:1402.6991v1. URL: http://www.ncbi.nlm.nih.gov/pubmed/16871208%7B%5C%%7D0Ahttp://link.aip.org/link/JVTBD9/v31/i1/p011802/s1%7B%5C&%7DAgg=doi%7B%5C%%7D0Ahttp://www.ncbi.nlm.nih.gov/pubmed/15672141%7B%5C%%7D0Ahttp://www.ncbi.nlm.nih.gov/pubmed/16333865%7B%5C%%7D0Ahttp://www.ncbi.nlm.nih.gov/pubmed/15269792%7B%5C%%7D0Ahttp://www. (cit. on p. 65).

[104] K. S. Novoselov, A. K. Geim, S. V. Morozov, et al. "Two-dimensional gas of massless Dirac fermions in graphene". In: *Nature* 438.7065 (2005), pp. 197–200. ISSN: 00280836. DOI: 10.1038/nature04233 (cit. on pp. 60, 65).

[105] Hideaki Obuse and Norio Kawakami. "Topological phases and delocalization of quantum walks in random environments". In: *Phys. Rev. B* 84.19 (Nov. 2011), p. 195139. DOI: 10.1103/PhysRevB.84.195139. URL: https://link.aps.org/doi/10.1103/PhysRevB.84.195139 (cit. on p. 63).

[106] M. Oliva-Leyva and Gerardo G. Naumis. "Generalizing the Fermi velocity of strained graphene from uniform to nonuniform strain". In: *Physics Letters, Section A: General, Atomic and Solid State Physics* 379.40-41 (2015), pp. 2645–2651. ISSN: 03759601. DOI: 10.1016/j.physleta.2015.05.039. URL: http://dx.doi.org/10.1016/j.physleta.2015.05.039 (cit. on p. 74).

[107] C G de Oliveira and J Tiomno. "Representations of Dirac equation in general relativity". In: *Il Nuovo Cimento (1955-1965)* 24.4 (May 1962), pp. 672–687. ISSN: 1827-6121. DOI: 10.1007/BF02816716. URL: https://doi.org/10.1007/BF02816716 (cit. on p. 80).

[108] Jiannis K Pachos. "Manifestations of topological effects in graphene". In: *Contemporary Physics* 50.2 (2009), pp. 375–389. DOI: 10.1080/00107510802650507. URL: https://doi.org/10.1080/00107510802650507 (cit. on p. 65).

[109] Deepak Pandey, Nandan Satapathy, M S Meena, et al. "Quantum walk of light in frequency space and its controlled dephasing". In: 042322.May (2011), pp. 1–7. DOI: 10.1103/PhysRevA.84.042322 (cit. on p. 30).

[110] R G Parr. "Density Functional Theory". In: *Annual Review of Physical Chemistry* 34.1 (1983), pp. 631–656. DOI: 10.1146/annurev.pc.34.100183.003215. URL: https://doi.org/10.1146/annurev.pc.34.100183.003215 (cit. on p. 28).

[111] Alberto Peruzzo, Mirko Lobino, Jonathan C F Matthews, et al. "Quantum Walks of Correlated Photons". In: *Science* 329.5998 (2010), pp. 1500–1503. ISSN: 0036-8075. DOI: 10.1126/science.1193515. URL: https://science.sciencemag.org/content/329/5998/1500 (cit. on p. 30).

[112] L. A. Pipes and Mary L. Boas. "Mathematical Methods in the Physical Sciences." In: *The American Mathematical Monthly* (1967). ISSN: 00029890. DOI: 10.2307/2315314 (cit. on p. 20).

[113] John Preskill. "Simulating quantum field theory with a quantum computer". In: (2019), p. 024. ISSN: 18248039. DOI: 10.22323/1.334.0024. arXiv: 1811.10085 (cit. on p. 101).

[114] V. A. Rubakov and M. E. Shaposhnikov. "Do we live inside a domain wall?" In: *Physics Letters B* 125.2-3 (1983), pp. 136–138. ISSN: 03702693. DOI: 10.1016/0370-2693(83)91253-4 (cit. on pp. 17, 34, 100).

[115] R. Saito, M. Fujita, G. Dresselhaus, et al. "Electronic structure of chiral graphene tubules". In: *Applied Physics Letters* 60.18 (1992), pp. 2204–2206. ISSN: 00036951. DOI: 10.1063/1.107080 (cit. on pp. 60, 65).

[116] Barry C. Sanders, Stephen D. Bartlett, Ben Tregenna, et al. "Quantum quincunx in cavity quantum electrodynamics". In: *Physical Review A - Atomic, Molecular, and Optical Physics* 67.4 (2003), p. 4. ISSN: 10941622. DOI: 10.1103/PhysRevA.67.042305 (cit. on p. 30).

[117] Linda Sansoni, Fabio Sciarrino, Giuseppe Vallone, et al. "Two-particle bosonic-fermionic quantum walk via integrated photonics". In: *Physical Review Letters* 108.1 (2012), pp. 1–5. ISSN: 00319007. DOI: 10.1103/PhysRevLett.108.010502 (cit. on p. 30).

[118] A Schreiber, K N Cassemiro, V Potoček, et al. "Decoherence and disorder in quantum walks: from ballistic spread to localization." In: *Physical review letters* 106.18 (2011), p. 180403. ISSN: 1079-7114. DOI: 10.1103/PhysRevLett.106.180403. URL: http://www.ncbi.nlm.nih.gov/pubmed/21635071 (cit. on p. 34).

[119] Tal Schwartz, Guy Bartal, Shmuel Fishman, et al. "Transport and Anderson localization in disordered two-dimensional photonic lattices". In: *Nature* 446.7131 (2007), pp. 52–55. ISSN: 14764687. DOI: 10.1038/nature05623 (cit. on p. 34).

[120] Shun-Qing Shen, Wen-Yu Shan, and Hai-Zhou Lu. "Topological insulator and the Dirac equation". In: *SPIN* 1.1 (2010), pp. 33–44. DOI: 10.1142/S2010324711000057. arXiv: 1009.5502. URL: http://arxiv.org/abs/1009.5502%7B%5C%%7D0Ahttp://dx.doi.org/10.1142/S2010324711000057 (cit. on p. 42).

[121] Neil Shenvi, Julia Kempe, and K. Birgitta Whaley. "Quantum random-walk search algorithm". In: *Physical Review A - Atomic, Molecular, and Optical Physics* 67.5 (2003), p. 11. ISSN: 10941622. DOI: 10.1103/PhysRevA.67.052307. arXiv: 0210064 [quant-ph] (cit. on p. 17).

[122] M. Shifman. “Large extra dimensions: Becoming acquainted with an alternative paradigm”. In: *International Journal of Modern Physics A* 25.2-3 (2010), pp. 199–225. ISSN: 0217751X. DOI: 10.1142/S0217751X10048548 (cit. on p. 34).

[123] Yutaka Shikano and Hosho Katsura. “Localization and fractality in inhomogeneous quantum walks with self-duality”. In: *Physical Review E - Statistical, Nonlinear, and Soft Matter Physics* 82.3 (2010), pp. 1–7. ISSN: 15393755. DOI: 10.1103/PhysRevE.82.031122 (cit. on p. 34).

[124] D. M Y Sommerville. “Space-filling Tetrahedra in Euclidean Space”. In: *Proceedings of the Edinburgh Mathematical Society* 41.April (1922), pp. 49–57. ISSN: 14643839. DOI: 10.1017/S0013091500003576 (cit. on p. 95).

[125] J. Struck, C. Ölschläger, R. Le Targat, et al. “Quantum Simulation of Frustrated Classical Magnetism in Triangular Optical Lattices”. In: 333.August (2011), pp. 996–1000 (cit. on p. 29).

[126] B. C. Travaglione and G. J. Milburn. “Implementing the quantum random walk”. In: *Physical Review A - Atomic, Molecular, and Optical Physics* 65.3 (2002), p. 5. ISSN: 10941622. DOI: 10.1103/PhysRevA.65.032310 (cit. on p. 31).

[127] Avatar Tulsi. “Faster quantum-walk algorithm for the two-dimensional spatial search”. In: *Physical Review A - Atomic, Molecular, and Optical Physics* 78.1 (2008), pp. 1–6. ISSN: 10502947. DOI: 10.1103/PhysRevA.78.012310 (cit. on p. 60).

[128] Albertod D. Verga. “Edge states in a two-dimensional quantum walk with disorder”. In: *European Physical Journal B* 90.3 (2017), pp. 1–9. ISSN: 14346036. DOI: 10.1140/epjb/e2017-70433-1 (cit. on p. 36).

[129] F Verstraete, V Murg, and J I Cirac. “Matrix product states, projected entangled pair states, and variational renormalization group methods for quantum spin systems”. In: *Advances in Physics* 57.2 (2008), pp. 143–224. DOI: 10.1080/14789940801912366. URL: https://doi.org/10.1080/14789940801912366 (cit. on p. 28).

[130] G Wendin. “Quantum information processing with superconducting circuits: a review”. In: (2010), pp. 1–1. DOI: 10.1109/CLEOE-IQEC.2007.4386783 (cit. on p. 29).

[131] C. T. White and T. N. Todorov. “Carbon nanotubes as long ballistic conductors”. In: *Nature* 393.6682 (1998), pp. 240–241. ISSN: 00280836. DOI: 10.1038/30420 (cit. on p. 65).

[132] P. A. Whitlock and S. A. Vitiello. "Quantum Monte Carlo simulations of solid 4 He". In: *Lecture Notes in Computer Science (including subseries Lecture Notes in Artificial Intelligence and Lecture Notes in Bioinformatics)* 3743 LNCS.1 (2006), pp. 40–52. ISSN: 03029743. DOI: 10.1007/11666806_4 (cit. on p. 28).

[133] Diederik S Wiersma, Paolo Bartolini, Ad Lagendijk, et al. "Localization of light in a disordered medium". In: *Nature* 390.December (1997), pp. 671–673. ISSN: 00280836. DOI: 10.1038/37757. URL: http://dx.doi.org/10.1038/37757 (cit. on p. 34).

[134] Kenneth G Wilson. "Confinement of quarks". In: *Phys. Rev. D* 10.8 (Oct. 1974), pp. 2445–2459. DOI: 10.1103/PhysRevD.10.2445. URL: https://link.aps.org/doi/10.1103/PhysRevD.10.2445 (cit. on p. 47).

[135] Edward Witten. "Search for a realistic Kaluza-Klein theory". In: *Nuclear Physics, Section B* 186.3 (1981), pp. 412–428. ISSN: 05503213. DOI: 10.1016/0550-3213(81)90021-3 (cit. on p. 34).

[136] Jizhou Wu, Wei-Wei Zhang, and Barry C. Sanders. "Topological quantum walks: theory and experiments". In: (2019), pp. 1–5. arXiv: 1905.11856. URL: http://arxiv.org/abs/1905.11856 (cit. on p. 63).

[137] N. Zagury Y. Aharonov, L. Davidovich. "Quantum random walks". In: *Physical Review A* 48.2 (1993), pp. 1687–1690. ISSN: 1050-2947. DOI: 10.1103/PhysRevA.48.1687. arXiv: 1207.4535v1 (cit. on p. 30).

[138] Zhiguang Yan, Yu Ran Zhang, Ming Gong, et al. "Strongly correlated quantum walks with a 12-qubit superconducting processor". In: *Science* 756.May (2019), pp. 753–756. ISSN: 10959203. DOI: 10.1126/science.aaw1611 (cit. on p. 101).

[139] Yue Yin, D E Katsanos, and S N Evangelou. "Quantum walks on a random environment". In: August 2007 (2008), pp. 1–7. DOI: 10.1103/PhysRevA.77.022302 (cit. on p. 34).

[140] J. Q. You and Franco Nori. "Atomic physics and quantum optics using superconducting circuits". In: *Nature* 474.7353 (2011), pp. 589–597. ISSN: 00280836. DOI: 10.1038/nature10122. URL: http://dx.doi.org/10.1038/nature10122 (cit. on p. 29).

[141] Zhi Zhao, Jiangfeng Du, Hui Li, et al. "Implement Quantum Random Walks with Linear Optics Elements". In: (), pp. –2. arXiv: 0212149v1 [arXiv:quant-ph] (cit. on p. 30).

[142] Jia-Qi Zhou, Ling Cai, Qi-Ping Su, et al. "Protocol of a quantum walk in circuit QED". In: *Physical Review A* 100.1 (2019), pp. 1–6. ISSN: 2469-9926. DOI: 10.1103/physreva.100.012343 (cit. on p. 101).